NTNU – Trondheim
Norwegian University of
Science and Technology

Centrifugal Compressor Load Sharing with the use of MPC

Thomas Ferstad Øvervåg

Master of Science in Engineering Cybernetics (2)
Submission date: March 2013
Supervisor: Jan Tommy Gravdahl, ITK
Co-supervisor: Nur Uddin, ITK

Norwegian University of Science and Technology
Department of Engineering Cybernetics

Abstract

The work presented in this thesis examines the possibilities of having compressors running in an optimal manner which can result in energy savings. This research looks at how a compressor operates and the problems which can occur when connecting several machines, both in series and parallel. It is mainly focused on using Model Predictive Control (MPC), as a setup for controlling each compressor to a fixed operating point on the characteristic with relation to mass flow and pressure. Constraints are set on the controller outputs to help minimize the area of operation. Several types of efficiency are investigated in detail and this has helped to create a continuous efficiency island definition. These continuous curves are assumed to be equal to the characteristic plotted from tests and measurements in the lab. The continuous efficiency definition enables the possibility of calculating an operating point for each compressor. This is done using a Quadric Programming setup, which is calculated explicitly beforehand. Together with this and the implementation of MPC, the result is a load sharing scheme used here on two compressors connected in parallel. The control inputs to the plant being the impeller rotational speeds and the outflow from the throttle valve, while the measurements are in the form of plenum pressure and mass flow from each machine.

Sammendrag

Arbeidet som presenteres i denne avhandlingen undersoker mulighetene for kontroll av kompressorer ved en mer optimal maate, som kan fre til energibesparing. Denne forskningen ser paa hvordan en kompressor fungerer og de problemer som kan oppstaa, naar flere maskiner kobles baade i serie og parallell. Simuleringer er gjort i MATLAB og SIMULINK, og i hovedsak med en ulineaer parallell kompressormodell. Det er i hovedsak fokusert paa bruk av Model Prediktiv Regulering (MPC) for styring av hver kompressor til et fast arbeidspunkt i karakteristiskken, med relasjon til massestromning og trykk. Begrensninger er satt paa kontrollerens utganger for aa redusere driftsomraadet. Flere typer av virkningsgrad er undersokt, og dette har bidratt til utviklingen av kontinuerlige virkningsgradskurver i kompressorkartet. Disse kontinuerlige kurvene antas her lik de karakteristiske plottene fra tester og maalinger i laboratoriet. En kontinuerlig definisjon av virkningsgrad gir en mulighet for beregning av et optimalt arbeidspunkt for hver kompressor i parallellkoblingen. Dette utfoeres ved hjelp av en Kvadratisk Programmeringsalgoritme, som beregnes eksplisitt foer simulering. Sammen med denne og implementeringen av MPC, er resultatet en lastfordelingsalgoritme ment for parallellkoblede sentrifugal kompressorer. Paadraget til anlegget blir rotasjonshastigheten til kompressorhjulene samt paadrag til strupeventilen, mens maalingene er i form av trykk i plenumkammeret og massestromning fra hver maskin som resulterer i en total utstromning fra strupeventilen.

Preface

This thesis is submitted in partial fulfillment of the requirements for the master's degree in Engineering Cybernetics at the Norwegian University of Science and Technology (NTNU).

I would like to thank my main supervisor Professor Jan Tommy Gravdahl which has been very helpful in helping me understand the compressor dynamics, and my co-advisor has been Nur Uddin at the Department of Engineering Cybernetics. I would also like to thank Professor Tor Arne Johansen and Professor Lars Imsland which have contributed in discussions and the making of this thesis. Discussion have been about Model Predictive Control (MPC) and the setup of the control scheme.

My special thanks goes to my friends at NTNU which consisted of D. Kwame Kufoalor and Svein Napsholm, which have helped me a lot through the studies and have been my co-workers through the run.

I would also like to thank my parents, Turid Ferstad Oevervaag and Odd Oevervaag for their fantastic support and the encouragements in completing this master's degree and the fulfillment of this project.

"No amount of experimentation can ever prove me right; a single experiment can prove me wrong."

Albert Einstein

Thomas Ferstad Oevervaag
Trondheim, March 2013

Contents

List of Figures

List of Tables

Abbreviations

NGL	**N**atural **G**as **L**iquids
PI	**P**roportional and **I**ntegral controller
PID	**P**roportional, **I**ntegral and **D**erivative controller
LQR	**L**inear **Q**uadratic **R**egulator
MPC	**M**odel **P**redictive **C**ontroller
NMPC	**N**onlinear **M**odel **P**redictive **C**ontroller
eMPC	**e**xplicit **M**odel **P**redictive **C**ontroller
QP	**Q**uadratic **P**rogramming
BHP	**B**rake **H**orsepower

Chapter 1

Introduction

1.1 Motivation

Natural gas mainly consists of methane, but can also contain ethane, propane, butane and pentane, NaturalGas.org (2012). It is colorless, shapeless and odorless, but it has one very specific good characteristic property. It is combustible, which makes it deliver a high load of energy when lit. Besides from this it also contains very few harmful side products.

There have been an increasing demand for energy in the past and and it will also continue in the future, it is because of this that natural gas is used. This source of energy can for example be used to heat our homes, cook our food, and generate our electricity.

When exploring for gas, it often begins with a geological survey. The surface of the earth is analyzed and through looking at the structure, one can find signs of where it might be petroleum and gas deposits. After these areas are found, a geophysicist perform detailed tests about the potential reservoir. This then helps to describe underground formations containing gas or petroleum. Examples of equipment used by geophysicists are e.g. a seismograph and magnetometers.

Seismic methods are used for detection of the different formations underground. This is because the seismic waves that are sent out reacts differently with different types of materials underground. The first seismograph used to detect fossil fuel was first applied in 1921.

After the surveys and logging of the data is finished, the next job is extraction. Either if the natural gas is located onshore or under water, one has to drill deep into the earths surface. The first offshore drilling rig was put into action in 1869, but was only designed to stay in shallow water.

When the extraction is finished the next step will be production. This is the process of transforming crude oil and gas into a usable product. As mentioned before, natural gas consists of much more than methane which the consumer uses. The natural gas is refined which implies removing products like water, hydrogen sulfide, sand and other gases. Propane and butane is removed to be sold separately.

Processing plants are used to extract the natural gas from the other bi products. To do this the liquids must be separated from the rest. According to NaturalGas.org (2012), there are two main methods for removing natural gas liquids, (NGL). The absorption method and cryogenic expander process, but these will not be mentioned further here.

When the natural gas has finished the purifying process, it has to be transported to the consumer. This is done using miles and miles of pipe, and an example of this is the CNG Transmission Corporation in the U.S. with 10,000 miles of pipeline, 68 compressor stations, 3,362 production wells and 1,510 storage wells. Ferber et al. (1999).

Compressor stations are needed to keep pressure in the pipe at a desired level. An overview of North American compressor stations and interstate pipelines can be seen in Figure 1.1. A centrifugal compressor used in the pipeline can e.g. be run by a turbine that uses up some of the gas in the pipe system, or one can use electric motors. According to Ferber et al. (1999), operating costs of transmission pipelines can be significant because of compressor station fuel costs. This is the main issue in this thesis, to minimize the fuel cost of each compressor station along the transmission line. One have to decide which compressors must be run and which ones to shut off. Another problem is finding the optimal suction pressure.

The control scheme must decide which area of operation would be the best, and how many compressors are needed to uphold the flow and pressure demand at the delivery points. Since these machines might require a lot of energy, a cost would have to be included in the scheme to account for compressor startup and shutdown.

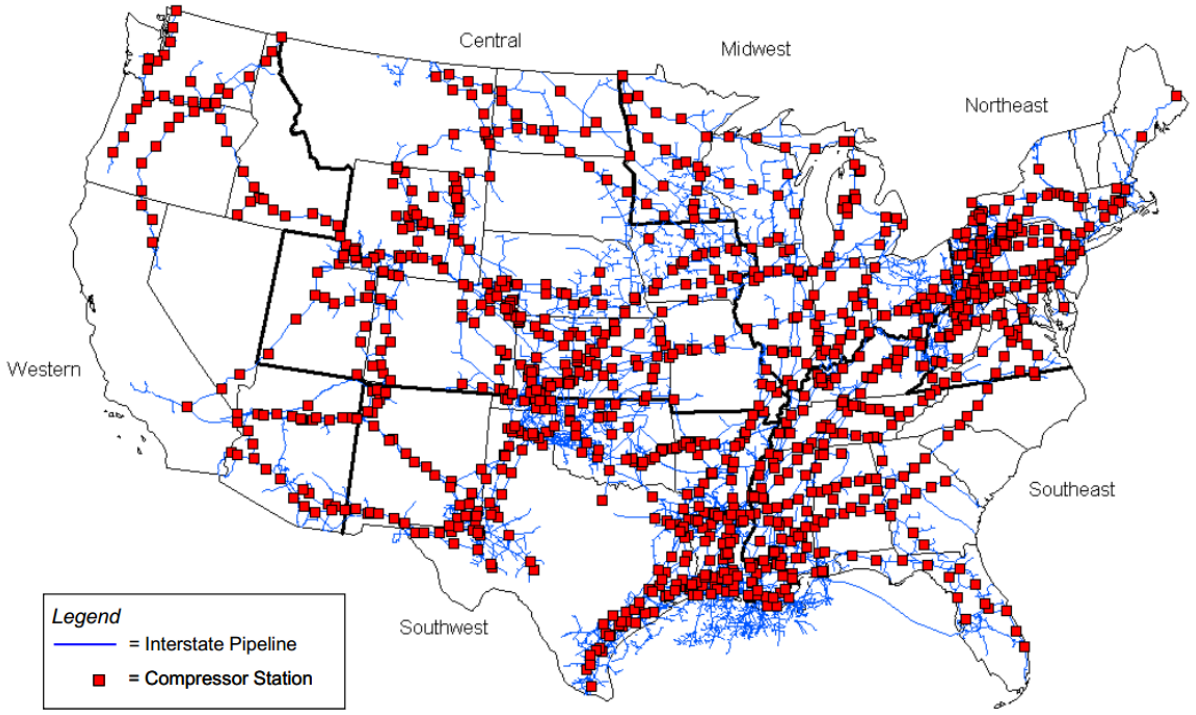

FIGURE 1.1: Compressor station overview with interstate pipeline network in North America, Tobin (2007)

1.2 Gas compressors

When gas is transported through the interstate pipelines and over continents, gas compressors are used to increase pressure in the pipeline. To do this, different types of compressors can be used to transport the gas from one location to another. These are e.g. positive displacement machines or as mentioned earlier, centrifugal compressors. These machines have different advantages and disadvantages.

Positive displacement machines works by holding a volume of the gas closed, and then reducing the volume, thereby creating a higher pressure. The high pressure gas is released through a throttle valve and flows through the pipeline. This process can be seen in Figure 1.2.

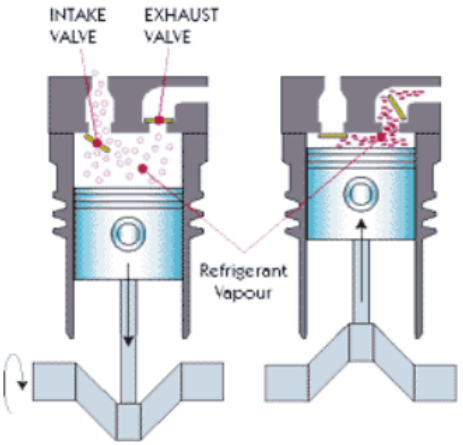

FIGURE 1.2: Reciprocating compressor, PilotLight (2013)

Centrifugal machines on the other hand exert a centrifugal force on the gas, thereby increasing the pressure. This is done by the rotary impeller which transforms kinetic energy to pressure and is also shown in Figure 1.3. This type of compressor is according to Menon (2005) more commonly used in industry, since they have better flexibility and lower installation and maintenance costs. Unfortunately the positive displacement compressors have a higher efficiency rate than centrifugal types, but then again the centrifugal machine can handle larger volumes in a small area.

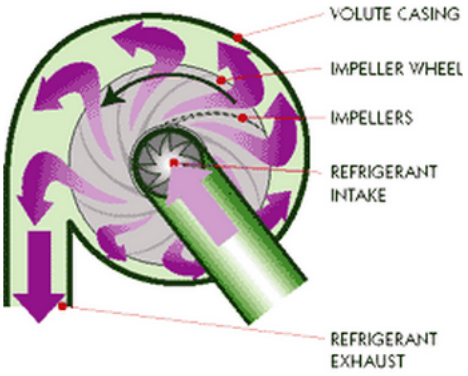

FIGURE 1.3: Centrifugal compressor, PilotLight (2013)

1.3 Constraints on the system

If we look at the transportation system as a whole unit including the pipes, compressors and the rest of the equipment, one can state the overall system constraints. These can e.g. be maximum and minimum throughput of gas, allowable pressure in the pipe and temperature constraints in the discharge of the compressor. These constraints can be dependent on each other in several ways. Two basic points in the system are the

temperature which is dependent on the compression rate, an example can be shown from Menon (2005). If one for example is to achieve a compression ratio of r, and this is exceeding the compression ratio of one compressor, several compressors would have to be installed in series. Then it is useful to look at equation

$$\left(\frac{T_2}{T_1}\right) = \left(\frac{P_2}{P_1}\right)^{\frac{\gamma-1}{\gamma}} \tag{1.1}$$

Where P_1 and P_2 are the suction and discharge pressures of the compressor, measured here in pounds per square inch absolute (psia). The temperatures T_1 and T_2 are then the suction and actual discharge temperatures in Kelvin, with γ being the dimensionless ratio of specific heats of gas. T_2 would here be used as a constraint and to see if this would reach the maximum allowed temperature in the pipeline. If then T_2 become higher than the maximum allowable discharge temperature, another stage must be considered. To calculate how many compressors to use the equation

$$r = (r_t)^{\frac{1}{n}} \tag{1.2}$$

is to be considered. Where r_t is total compression ratio of the system and n is the number of compressors in series. According to Menon (2005) identical compressors connected in series with the compression ratio being the same in each machine, means that the power requirements will be minimized.

1.4 Model predictive control

Probably the simplest way to control a centrifugal compressor used in industry is with a proportional, derivative and integral control, (PID). This does not take into consideration surge constraints and other properties of the system. A way of setting up a compressor unit, is to include a recycle or blow out valve controlled by a PI controller. This is used to stabilize the system and get it out of the surge zone, and is further presented in Oevervaag (2012).

It is from these conclusions that Model Predictive Control (MPC) come into play. This methodology explicitly handles constraints and optimizes the system control response. MPC uses a linear model of the process to predict future system behavior, then the goal is to compute optimal inputs for the process using a cost function, with the possibility of taking disturbances into consideration.

With the exception of the points listed above, MPC is also thought of to handle multi variable systems containing nonlinear dynamics. This will be looked at in this thesis, with a linearized model of the compressor system.

From these arguments, this seems like a good start for investigating if MPC can be used for controlling a single compressor system or also compressors coupled in series and parallel. On the other hand some problems can arise when taking into consideration the computational time of the MPC, giving inputs to the process. This could in theory be handled with the use of explicit Model Predictive Control (e)MPC. The main idea behind explicit MPC is to solve the optimization problem off-line, for all states $x(t)$, Magni et al. (2009). This implies that MPC can be used for fast sampling applications also. For a compression system on the other hand the optimization problem might change for different operating points, which implies that in this thesis (e)MPC will not be considered in detail.

1.5 Organization of report

Firstly this thesis gives a description of why compressors are so important in a gas transportation network, and some info are given about their desired area of operation. Further in Chapter 2 the compressor characteristic is explained, together with surge and rotating stall. These points make out important areas of research and they can produce problems when operating compressors. The chapters 2 and 3 are mostly taken from Oevervaag (2012). In Chapter 3 the non-dimensional model of Greitzer is explained, and the dimensional model from Gravdahl and Egeland (1999). The dimensional model is used in Chapter 4, and is extended to include two compressors connected in parallel with a common plenum volume and one outlet. A set point is chosen in the stable region of the compressor map and simulated in SIMULINK.

Chapter 5 mainly consists of an introduction to the Linear Quadric Regulator, the constrained LQR stated as MPC. Also a short description of NMPC and EMPC is given. A description of efficiency and optimization is given in Chapter 6, together with a definition of the QP formulation used for finding the optimal working point of each compressor. The load sharing formulation is given in Chapter 7. Here an introduction is given describing the previous work on load sharing. The final simulations are presented in Chapter 8 and this includes results from both the single compressor system and the parallel coupled system. The simulations performed in SIMULINK are performed with and without the MPC connected.

At the end of this thesis in Chapters 9 and 10 the results, conclusion and a listing of further work is presented. Following this thesis are the scripts and diagrams used for simulations, these are shown in the Appendices and included on a CD.

1.6 Project set up

The simulations in this thesis are performed using MATLAB R2012a software and is run using a 64-bit operating system (win64). The toolboxes consists of SIMULINK version 7.9 (R2012a) and Model Predictive Control Toolbox 4.1.

1.7 Scope of work

As is argued in the previous sections, a conclusion is reached about the problem description and the scope of this thesis. The problems are as follows:

1. Formulate a dynamic model for multiple centrifugal compressors in series and/or parallel configuration. The model should be suitable for load sharing design.

2. Design a load sharing algorithm for the model(s) in 1. and investigate how MPC can be used for this purpose.

3. Simulate the load sharing algorithm for different multiple compressor configurations.

Chapter 2

Background

2.1 How the compressor works

The compressor characteristic curve is what defines the compressor field of operation. It is designed to give an expression for the pressure p_{02} shown in Figure 3.1 which is measured at the outlet of the compressor. This is dependent of both impeller rotational speed and mass flow. To define the pressure rise from a compressor, the frontal and back end stagnation pressure p_{01} and p_{02} are stated which defines

$$\Delta p := p_{02} - p_{01} \tag{2.1}$$

This process is also defined to be isentropic, which means that no heat is added to the flow, and no energy transformations occur due to friction or dissipative effects.

An example of the characteristic curve is shown below in Figure 2.1.

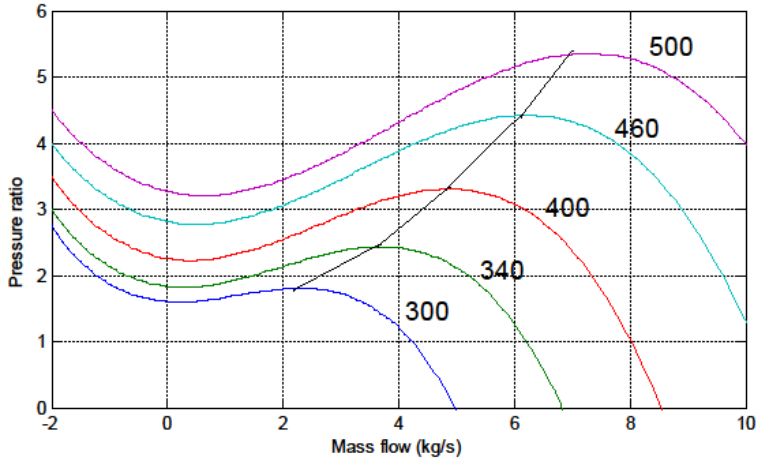

FIGURE 2.1: Compressor speed lines [rps] with the surge line shown and non dimensional pressure ratio

The script for simulating this is written in MATLAB, and given in Oevervaag (2012), together with the equations which are found in Egeland and Gravdahl (2002). As seen here the characteristic curve is made continuous in both mass flow w and rotational speed ω, using polynomial curve fitting. This can be seen from equation (3.15). It can also be done using a third order approximation where $N = 2\pi\omega$ and is defined as the rotational speed in revolutions per sec. The equations are

$$\Psi_c(w, N) = c_0(N) + c_1(N)w + c_2(N)w^2 + c_3(N)w^3 \tag{2.2}$$

and $c_i(N)$ given as

$$c_i(N) = c_{i0} + c_{i1}N + c_{i2}N^2 + c_{i3}N^3 \tag{2.3}$$

where $c_i, i = 0, 1, 2, 3$ are coefficients corresponding to a respective rotational speed. The results of this can be seen in Egeland and Gravdahl (2002).

2.2 Surge

One of the greatest problems with using compressors is a phenomenon called surge. To explain this one can simply say that it is compressed gas flowing the wrong way in the compression system, breaking down the continuous flow pattern. More specific the surge point in a compressor occurs when the compressor back pressure is high and the compressor cannot pump against this high head, causing the flow to separate and reverse its direction, Boyce (2012). Figure 2.1 shows this unstable area on the left side of the surge line.

There are large forces at work when dealing with compressors. One example of this is if one changes the focus to the mechanical part of the machine. In Figure 2.2 it is shown that surge can damage the machine, not just with the highly compressed air, but these forces can also rip loose objects which can be sucked in and then damage the impeller.

FIGURE 2.2: Damaged impeller, performance turbochargers (2013)

According to Gravdahl and Egeland (1999) there are two different types of surge, mild/-classic surge and deep surge. The last one explained above. Classic surge is flow and pressure fluctuating in the compressor system making a limit cycle in the compressor characteristic, as seen in Figure 2.3. A limit cycle can be explained as an isolated periodic orbit. For example when one trajectory traces out a closed curve, the solution of the problem will be realized by a point which follows around the curve. For surge this means that all trajectories starting in the neighborhood of the limit cycle, ultimately tend toward the limit cycle as time $\rightarrow \infty$. Figure 2.3 shows a simulation of surge. Here a stable limit cycle is shown and is plotted as a function of the plenum pressure and mass flow out of the compressor.

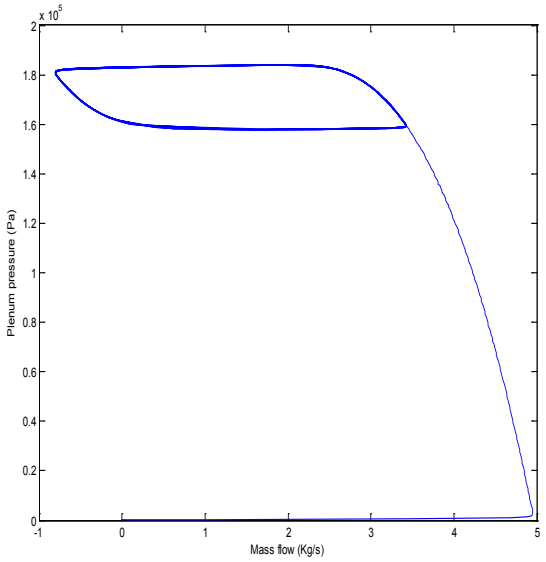

FIGURE 2.3: Compressor surge, with measurements plotted in [Pa] and flow in [kg/s], Oevervaag (2012)

Cite Boyce (2012).

"A decrease in the mass flow rate, an increase in the rotational speed of the impeller, or both can cause the compressor to surge."

Also whether surge is caused by a decrease in flow velocity or an increase in rotational speeds, the blades or the stators can stall. One should note that operating at higher efficiency implies operation closer to surge. It should be noted here that total pressure increase, occur only in the rotational part of the compressor, the blades.

According to Gravdahl and Egeland (1999) and shown in Figure 2.4. The operating point A on the characteristic is a stable working point. If a disturbance in the flow through the system comes into action and do not make the flow go past the surge line, the system will be stable. This is because an increase in pressure will increase the flow out through the throttle valve and thus making the working point stay in the right area.

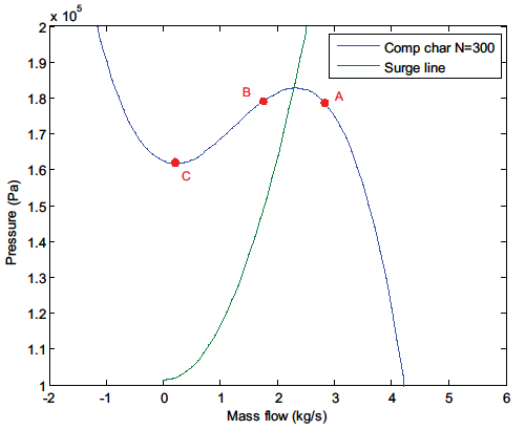

FIGURE 2.4: Compressor characteristic plotted for N=300 revolutions/s. With surge line. Figure based on Gravdahl & Egeland (1999)

On the other hand when the point of operation is on B, the system will be unstable. In this case a reduction of mass flow will also imply a reduction in pressure head and this leads to a further reduction of flow through the throttle valve. Eventually this leads to point C on the characteristic curve because the pressure upstream of the throttle falls below the compressor delivery pressure. After the mass flow has increased the cycle repeats and from this the conclusion is that operating points on the positive slope of the characteristic are unstable while on the negative part of the curve they are stable.

To avoid surge there are two commonly known methods. These will be mentioned later in this report, but for the main overview they are surge avoidance and active surge control.

2.3 Rotating stall

In axial and centrifugal compressors, surge causes irregularities in the flow and as shown above we can more or less understand how the dynamics work. Another problem in especially axial compressors, is rotating stall.

When the normal flow pattern which is steady and axisymmetric is disturbed e.g. change in rotor speed, the problem can sometimes be called rotating stall. This means that flow no longer is uniform and stall cells with reduced flow is developed and with this a fall in pressure rise from the compressor. Stall cells propagate at (20-70%) of the rotor speed, Gravdahl and Egeland (1999). In Figure 2.5 the phenomena is shown more clearly. To quote Gravdahl and Egeland (1999) "Suppose that there is a non-uniformity in the inlet flow such that a locally higher angle of attack is produced on blade B which is enough to stall it. The flow now separates from the suction surface of the blade, producing a flow

blockage between B and C. This blockage causes a diversion of the inlet flow away from B towards A and C, resulting in a increased angle of attack on C, causing it to stall".

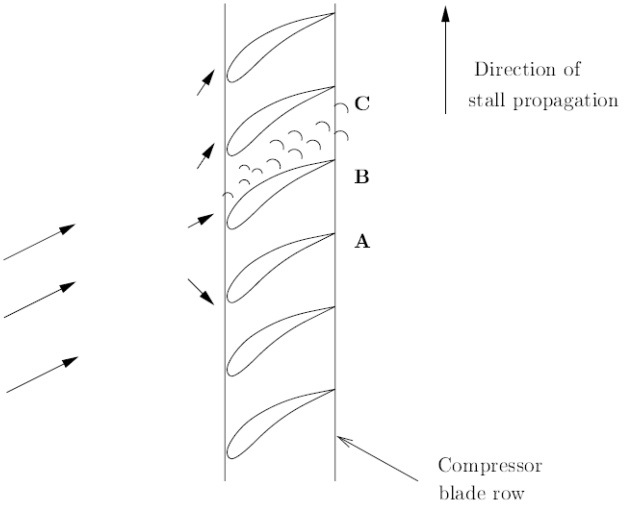

FIGURE 2.5: Inception of rotating stall, Gravdahl & Egeland (1999)

Most of the research has been done on axial compressors. However there are theories about rotating stall in centrifugal compressors. According to Ruprecht et al. (2005) impeller rotating stall could result from flow perturbations at the impeller exit and that would not allow the flow to follow the blading. This might be because of disturbances within the impeller passages or strong interactions between the impeller and the diffuser. One main reason for rotating stall can be the impeller blade geometry or simply the angle of incidence at the impeller leading edge.

2.4 Compressor choke

In the modeling of compressor systems the Mach number plays an important role. Normally the flow can be assumed incompressible for Ma < 0.3, but as stated by White (2008) for the flow in ducts the most important property is if the Mach number is less than or larger than 1. Another concept in dealing with stability and compressor dynamics is the choke point which happens when the mass flow reaches Ma $= 1$. Which is the boundary zone between subsonic and supersonic flow.

$$Ma = \frac{V}{c} \tag{2.4}$$

Equation (2.4) shows how the Mach number is found. V is the speed of flow and c is the speed of sound in the working medium, and for air at a temperature of 15 degrees Celsius the number is about 340 m/s. It is seen that when mass flow reaches the sonic velocity

in the compressor we get what in industry is called stone walling. Better explained as is a limit for the flow in the compressor.

Chapter 3

The Simple Model

3.1 Introduction

Modeling of compression systems have been done for a long time. The one best known is the model of Greitzer (1976), which is used to simulate the whole compression system and most importantly surge and rotating stall. A simplified version of the model is

$$\frac{d\Phi}{d\xi} = B(\Psi_c(\Phi) - \Psi) \tag{3.1}$$

$$\frac{d\Psi}{d\xi} = \frac{1}{B}(\Phi - \Phi_T(\Psi)) \tag{3.2}$$

Which is taken from Gravdahl and Egeland (1999). The variables are here dimensionless, Φ is the compressor mass flow, Ψ_c is the compressor characteristic pressure rise, Ψ is the pressure difference across the duct, Φ_T the throttle mass flow and ξ is non dimensional time. In his paper Greitzer (1976a), he defined surge and rotating stall with a B-parameter. This is defined as

$$\begin{aligned} B &:= \frac{U}{2\omega_H L_c} \\ &= \frac{U}{2a}\sqrt{\frac{V_p}{A_c L_c}} \end{aligned} \tag{3.3}$$

In Greitzer (1976b) this parameter was verified using a three stage axial compressor. To get a surge response the B-parameter get larger than B_{crit} and stall is reached when B $<$ B_{crit}. The variables used here are U which is the mean rotor velocity, ω_H the Helmholtz resonator frequency, L_c is the duct length, V_p the plenum volume, A_c is the area of flow and a is the speed of sound.

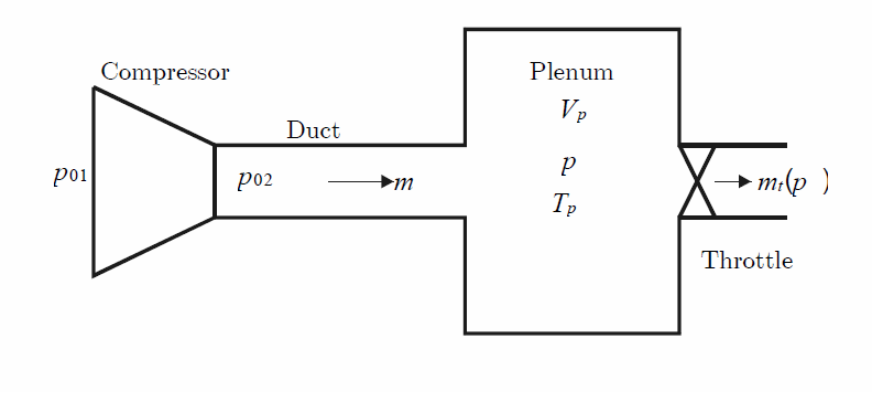

FIGURE 3.1: The compressor, plenum and throttle system, Greitzer (1976)

The model shown in Figure 3.1 is taken from Greitzer (1976). This model consists of a duct plenum system with the compressor in the rear and a throttle valve at the end. This is a plain system with no surge control method applied. Atmospheric pressure is here noted as p_{01}, p_{02} is spoken of as pressure in the duct. The pressure in the plenum is most often given by p_p but is here noted p, further T_p is temperature in plenum and lastly $m_t(p)$ is the mass flow through the throttle valve as a function of the plenum pressure.

3.2 Model

The first model is found in Gravdahl and Egeland (1999). The two first equations (3.4) and (3.5) is the same as in the Greitzer model.

$$\dot{p}_p = \frac{c_p^2}{V_p}(w - w_t) \tag{3.4}$$

$$\dot{w} = \frac{A_1}{L}(p_{02} - p_p) \tag{3.5}$$

$$\dot{\omega} = \frac{1}{J}(\tau_d - \tau_c) \tag{3.6}$$

Here w is the mass flow through the duct and w_t is the exit flow through the valve. Plenum volume is V_p, and the sonic velocity in the plenum is denoted c_p. Further, the A_1 and L constants are respectively the area and length of the duct running from the compressor and into the plenum. Lastly it is worth to mention the impeller and the shaft dynamics shown in Figure 3.2, where ω is the angular velocity of the shaft. The motor drive torque is denoted τ_d, and τ_c is the compressor torque, and finally J is the shaft inertia. The modeling of the shaft dynamics might be useful e.g. in compressor control, but will not be looked further into for now.

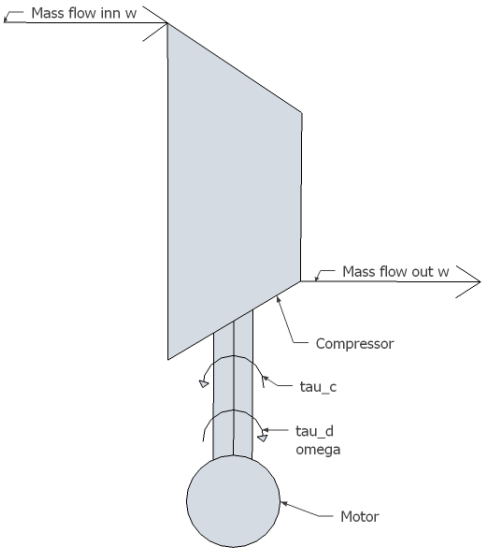

FIGURE 3.2: Compressor shaft dynamics

3.3 Derivation of the model

To model and simulate the ordinary compressor one have to have a basic knowledge of fluid dynamics, and this is what this section is all about. The model of (3.4) and (3.5) will here be discussed and derived.

Starting with the change in pressure in the plenum volume, one can see that it is based on change of mass.

$$\frac{d}{dt}(\rho_p V_p) = w - w_t \tag{3.7}$$

$$\dot{\rho}_p V_p = w - w_t \tag{3.8}$$

While ρ_p is the density of gas in the plenum, mass flow into and out of the plenum changes the value on the left side of equation (3.4). The flow from the throttle valve is

$$w_t = k_t \sqrt{(p_p - p_{01})} \tag{3.9}$$

where k_t is represented as the throttle opening, and p_{01} is atmospheric pressure.

From Egeland and Gravdahl (2002) and the knowledge that the process in the plenum is isentropic

$$\frac{dp_p}{p_p} = \kappa \frac{d\rho_p}{\rho_p} \tag{3.10}$$

$$\dot{p}_p = \kappa R T_p \dot{\rho}_p \tag{3.11}$$

where $\kappa = \frac{c_p}{c_v}$ and R are respectively the ratio of specific heats and mean compressor radius, with c_v being the specific heat at constant volume. It now follows from equations (3.8) and (3.11) that the result becomes

$$\dot{p}_p \frac{V_p}{\kappa R T_p} = w - w_t \tag{3.12}$$

when lastly $\kappa R T_p = c_p^2$ with c_p being the sonic velocity the result is

$$\dot{p}_p = \frac{c_p^2}{V_p}(w - w_t) \tag{3.13}$$

Now continuing to the next differential equation. With the use of the momentum equation the change in mass through the duct is derived. To start the derivation it is worth mentioning that the pressure on the inlet of the duct is equal to p_{02} which is the pressure rise developed in the compressor.

$$p_{02} = \Psi_c(w, \omega) p_{01} \tag{3.14}$$

and here Ψ_c being

$$\Psi_c(w, \omega) = \left(1 + \frac{\mu r_2^2 \omega^2 - \frac{r_1^2}{2}(\omega - \alpha v)^2 - k_f w^2}{c_p T_{01}}\right)^{\frac{\kappa}{\kappa - 1}} \tag{3.15}$$

In some of the models used in the simulations in this report, a constant rotational speed is applied, which leads to the characteristic being only dependent on mass flow. The constant k_f is the fluid friction constant and μ accounts for the rotor blades, while α is always larger than zero and handles the point of zero incidence loss. For an through explanation of the constants in this equation move to Egeland and Gravdahl (2002). In the compressor inlet the fluid velocity is increased and at the diffuser the fluid is slowed down. This develops an increase in the static pressure which is given as

$$p = p_0 - \frac{1}{2} C^2 \tag{3.16}$$

Knowing the momentum equation

$$\frac{d}{dt}(m_d C) = A_1 p_{02}(w, \omega) - A_1 p_p \tag{3.17}$$

and knowing that $m_d = LA_1\rho$ and the ordinary equation for mass flow being

$$w = \rho A_1 C \tag{3.18}$$

the fluid velocity is derived to be

$$C = \frac{w}{\rho A_1} \tag{3.19}$$

this results in

$$\frac{d}{dt}(\frac{LA_1\rho w}{\rho A_1}) = A_1 p_{02}(w, \omega) - A_1 p_p \tag{3.20}$$

$$\frac{d}{dt}(Lw) = A_1 p_{02}(w, \omega) - A_1 p_p \tag{3.21}$$

Finally the equation is derived looking like

$$\dot{w} = \frac{A_1}{L}(p_{02}(w, \omega) - p_p) \tag{3.22}$$

The equation (3.14) is inserted into (3.22) resulting in

$$\dot{w} = \frac{A_1}{L}(\Psi_c(w, \omega)p_{01} - p_p) \tag{3.23}$$

The pressure in the model above stated in equations (3.13) and (3.23) is given in pascal. Now some small changes can be made to get the system and the measurements in bar. Firstly a new variable is defined

$$p_b := \frac{1}{101325} p_p \tag{3.24}$$

with p_b being the plenum pressure in bar and the derivative

$$\dot{p}_b = \frac{1}{101325}\dot{p}_p \tag{3.25}$$

is inserted into equation (3.13) giving

$$101325\dot{p}_b = \frac{c_p^2}{V_p}(w - w_t) \tag{3.26}$$

$$\dot{p}_b = \frac{1}{101325}\frac{c_p^2}{V_p}(w - w_t) \tag{3.27}$$

Now using equation (3.24) and repeating the procedure for equation (3.23)

$$\dot{w} = \frac{A_1}{L}(\Psi_c(w, \omega)p_{01} - 101325p_b) \tag{3.28}$$

Also the new model for the throttle valve is developed to be

$$w_t = k_t\sqrt{(101325p_b - p_{01})} \tag{3.29}$$

Equation (3.26), (3.28) and finally (3.29) are implemented and simulated in the SIMULINK diagram in Appendix A.

3.4 The dimensionless model of Greitzer

The reason to non-dimensionalize a system is to totally or partially remove the units from equations containing physical values. This helps to parameterize problems and can be used in dimensional analysis. The method is best used in analysis of differential equations as will be shown here, but is not restricted to this. Other reasons to nondimensionalize a system can be comparison between sizes of terms in the equations and it allows for identification of for example the dominant terms of differential equations. Looking at the non dominant physical properties some can also be neglected and the total system then may be simplified. Lastly it is worth mentioning that by non-dimensionalization, parameters may be collected in groups and hence reducing the number of single parameters, Louie et al. (1998).

Material from the appendices of Gravdahl and Egeland (1999), and the book Egeland and Gravdahl (2002) have been used here. To do this the model will have to go from equations (3.4) and (3.5) to (3.1) and finally (3.2). This is done step by step and is

shown below. Firstly the non-dimensional time will be introduced, and it is defined by

$$\xi := t\omega_H \tag{3.30}$$

Where ω_H is the Helmholtz frequenzy and is in this situation defined as

$$\omega_H := c_p\sqrt{\frac{A_1}{V_pL}} \tag{3.31}$$

Secondly $\frac{1}{2}\rho U^2$ and ρUA is used to non-dimensionalize pressure and mass flow. With U beeing the mean rotor velocity. Now using this to state ϕ and ϕ_t as the non dimensional flow in the duct and out from the throttle valve:

$$\phi = \frac{w}{\rho U A_1} \tag{3.32}$$

$$\phi_t = \frac{w_t}{\rho U A_1} \tag{3.33}$$

Now inserting this into equation (3.13).

$$\dot{p}_p = \frac{c_p^2}{V_p}(\phi\rho U A_1 - \phi_t \rho U A_1) \tag{3.34}$$

Rearranging

$$\dot{p}_p\frac{1}{\rho U A_1} = \frac{c_p^2}{V_p}(\phi - \phi_t) \tag{3.35}$$

To further compute this to nondimensional pressure difference the Helmholtz frequency equation (3.31) is rearranged to

$$\omega_H^2 = c_p^2\frac{A_1}{V_pL} \tag{3.36}$$

and equation (3.35) is extended with$\frac{L}{L}$ and this gives

$$\dot{p}_p\frac{1}{\rho U} = \frac{c_p^2 A_1}{V_pL}L(\phi - \phi_t) \tag{3.37}$$

inserting (3.36) into (3.37) it is easily seen that

$$\dot{p}_p \frac{1}{\rho U} = \omega_H^2 L(\phi - \phi_t) \tag{3.38}$$

using what is stated in the start of this section, non-dimensional pressure is

$$\frac{d\Psi}{dt} = \frac{1}{\frac{1}{2}\rho U^2} \frac{dp_p}{dt} \tag{3.39}$$

$$\frac{dp_p}{dt} \frac{1}{\rho U} = \omega_H^2 L(\phi - \phi_t) \tag{3.40}$$

inserting equation (3.39) into (3.40) the answer yields

$$\frac{\frac{1}{2}\rho U^2}{\rho U} \frac{d\Psi}{dt} = \omega_H^2 L(\phi - \phi_t) \tag{3.41}$$

lastly stating non-dimensional time on differential form

$$d\xi = \omega_H dt \tag{3.42}$$

and combining with equation (3.41) the system becomes

$$\frac{d\Psi}{d\xi} = \frac{2\omega_H L}{U}(\phi - \phi_t) \tag{3.43}$$

making the final result equal to equation (3.2). The static pressure rise coefficient is defined from Egeland and Gravdahl (2002) to be

$$\Psi := \frac{p_p - p_{01}}{\frac{1}{2}\rho U^2} \tag{3.44}$$

To use the pressure difference a simple change is made by adding and subtracting p_{01} to equation (3.23) and this results in

$$\dot{w} = \frac{A_1}{L}(\Psi_c(w,\omega)p_{01} - p_p + p_{01} - p_{01}) \tag{3.45}$$

Using the time differentiation of equation (3.19) the result yields

$$\frac{1}{\frac{1}{2}\rho U^2}\frac{dw}{dt} = \frac{A_1}{L}\frac{(\Psi_c(w,\omega)-1)p_{01}}{\frac{1}{2}\rho U^2} - \frac{p_p - p_{01}}{\frac{1}{2}\rho U^2} \tag{3.46}$$

further inserting equation (3.32) into (3.46)

$$\frac{\rho A_1 U}{\frac{1}{2}\rho U^2}\frac{d\phi}{dt} = \frac{A_1}{L}(\psi_c(\phi) - \psi) \tag{3.47}$$

turning into non-dimensional time the equation becomes

$$\omega_H \frac{A_1}{\frac{1}{2}U}\frac{d\phi}{d\xi} = \frac{A_1}{L}(\psi_c(\phi) - \psi) \tag{3.48}$$

rearranging

$$\frac{d\phi}{d\xi} = \frac{U}{2\omega_H L}(\psi_c(\phi) - \psi) \tag{3.49}$$

Referring to equation (3.3) and inserting this into (3.49) the total system in equation (3.1) is obtained.

where

$$\Psi_c(\Phi) = \psi_{c0} + H\left(1 + \frac{3}{2}\left(\frac{\Phi}{W} - 1\right) - \frac{1}{2}\left(\frac{\Phi}{W} - 1\right)^3\right) \tag{3.50}$$

with $\psi_{c0} > 0$ being the shut-off value of the compressor characteristic, H the semi height and W the semi with on the characteristic as shown in Figure 3.3. For further explanation of the constants we refer to Gravdahl and Egeland (1999).

This cubic characteristic was used in Moore and Greitzer (1986), with the Y-axis representing non dimensional pressure ratio, and on the X-axis the state is non dimensional flow.

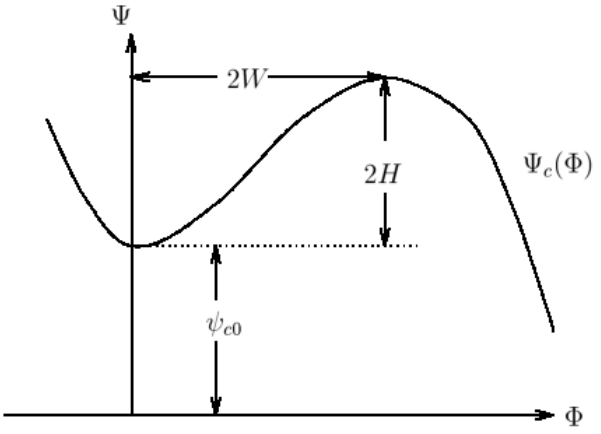

FIGURE 3.3: Cubic axisymmetric compressor characteristic, Gravdahl and Egeland (1999)

3.5 Stability

Here the stability of the Greitzer model is described. Using the system found in Uddin and Gravdahl (2012).

$$\dot{\phi}_1 = \frac{1}{\tilde{I}}(\psi_c - \psi) \tag{3.51}$$

$$\dot{\psi} = \frac{1}{\tilde{C}}(\phi_1 - \phi_2) \tag{3.52}$$

With $\tilde{I} = B^{-1}$ and $\tilde{C} = B$. The non-dimensional compressor mass flow is noted ϕ_1 and the throttle valve $\phi_2 = \gamma_T\sqrt{\psi_p}$, where γ_T is the throttle gain. Mentioned earlier, ψ and ψ_c is the plenum pressure and the compressor pressure rise.

Following the standard rules of linearization the A matrix is computed to be

$$A = \begin{pmatrix} -\frac{1}{B}\frac{\partial\phi_2}{\partial\psi} & \frac{1}{B} \\ -B & B\frac{\partial\psi_c}{\partial\phi_1} \end{pmatrix} \tag{3.53}$$

and now the total system found in Egeland and Gravdahl (2002) is shown to be

$$\frac{d}{d\xi}\begin{pmatrix}\psi \\ \phi_1\end{pmatrix} = \begin{pmatrix} -\frac{1}{Bg_t} & \frac{1}{B} \\ -B & Bg_c \end{pmatrix}\begin{pmatrix}\psi \\ \phi_1\end{pmatrix} \tag{3.54}$$

The two variables g_c and g_t are stated as the slopes of the compressor characteristic and the throttle pressure drop characteristic.

When looking for the eigenvalues of the A matrix the characteristic equation is solved. Starting with

$$det(\lambda I - A) = 0 \tag{3.55}$$

and the expression become

$$\lambda^2 + \left(\frac{1}{Bg_t} - Bg_c\right)\lambda + \left(1 - \frac{g_c}{g_t}\right) = 0 \tag{3.56}$$

and finally

$$\lambda = \frac{-\left(\frac{1}{Bg_t} - Bg_c\right) \pm \sqrt{\left(\frac{1}{Bg_t} - Bg_c\right)^2 - 4\left(1 - \frac{g_c}{g_t}\right)}}{2} \tag{3.57}$$

According to Gravdahl and Egeland (1999) the system is unstable if $\left(1 - \frac{g_c}{g_t}\right) < 0$ or $\left(\frac{1}{Bg_t} - Bg_c\right) < 0$. For the first case the slope of the compressor characteristic is steeper than the slope of the throttle line, and this makes the system statically unstable and this is also referred to as a saddle-point, Khalil (2002). When looking at the second one being less then zero it makes the dynamic instability occur. To be more specific, this point is on the positive rise of the compressor characteristic, almost at the top.

To get the system stable, the condition

$$g_c < \frac{1}{B^2 g_t} \tag{3.58}$$

have to apply, and also

$$g_c < g_t \tag{3.59}$$

must be valid if the compressor is to achieve a stable node or stable focus equilibrium.

Two other examples of equilibrium points is an unstable node and unstable focus. These will take place if $\left(\frac{1}{Bg_t} - Bg_c\right) < 0$ and $\left(1 - \frac{g_c}{g_t}\right) > 0$. All of these are dependent of the Greitzer B parameter. For the instability case one can see that if B becomes sufficiently small $B < \frac{1}{g_t}$, the static instability will occur first. To cite Gravdahl and Egeland (1999) "It is to be emphasized that whether or not the instability is dynamic or static, the *nonlinear* system of (3.1) and (3.2) will go into surge oscillations. "

Chapter 4

Model Extension

4.1 Introduction

To achieve the delivery requirements of the gas network, one might have to increase the pressure range and flow capacity in the compressor station by adding more compressors to the network. In gas pipeline networks, compressors can be set up in both series and parallel. Parallel connections are set up to increase the flow in the network, since a compressor will be a bottleneck in the pipeline. This is shown in Figure 4.2 taken from Menon (2005).

Series connections of compressors on the other hand are set up to increase the overall pressure. They each compress the same gas but at different compression ratios, as can be seen in Figure 4.1. Here it is shown that each compressor has a compression ratio of 1.2, and the suction pressure is 900 pounds per square inch absolute (psia) at the first compressor. The discharge pressure is 1296 psia and this is achieved at two stages. Doing a simple calculation results in a total head of 1.44 psia.

The problem with compressors connected in series, and having multiple stages is the system temperature constraint. The temperature rise from one stage to another can be described from the equation:

$$\left(\frac{T_2}{T_1}\right) = \left(\frac{P_2}{P_1}\right)^{\frac{\gamma-1}{\gamma}} \tag{4.1}$$

where P_1 and P_2 are respectively the suction and the discharge pressure. The temperature rise is (T_2 - T_1) and γ is dimensionless ratio of specific heats of gas. Since high temperatures make the throughput of gas require more energy, which implies a lower efficiency in the pipeline, it is desirable to have the temperature rise as low as possible.

This is solved by cooling the gas between each stage to as low as the inlet temperature. This helps the gas to keep a low as possible temperature at the discharge. Also it is important to notice equation (4.1) and the discharge temperature to be dependent on the pressure ratio. From Menon (2005) it is stated that the preferable compression ratio is 1.5 - 2.0 for centrifugal compressors.

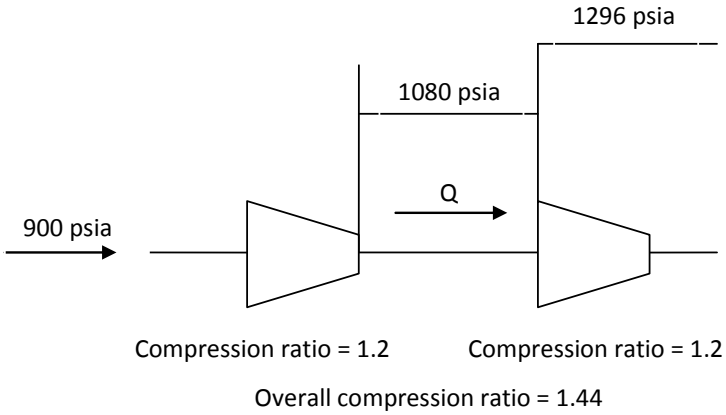

FIGURE 4.1: Compressors in series, Menon (2005)

The Figure 4.3 shows a coupling of three compressors connected in parallel. For the parallel coupling, the load of 900 MMCFD (million standard cubic feet per day) is shared between the units, the pressure ratio of each compressor is 1.4 and the pressure is 1260 at the discharge.

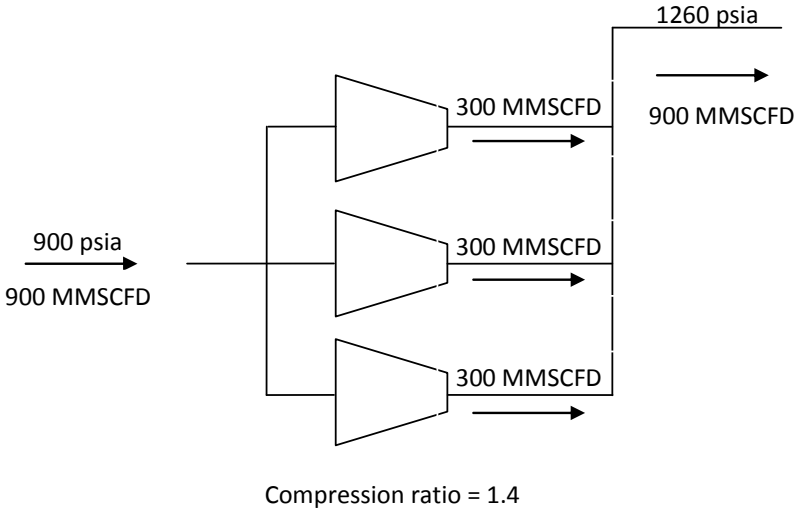

FIGURE 4.2: Compressors in parallel, Menon (2005)

4.2 The parallel Model

As the next step we are to introduce the extended model as a parallel connection. The model is here made dimensional, preferable because it might be easier to follow the dynamics in the system and the relations to the physical plant.

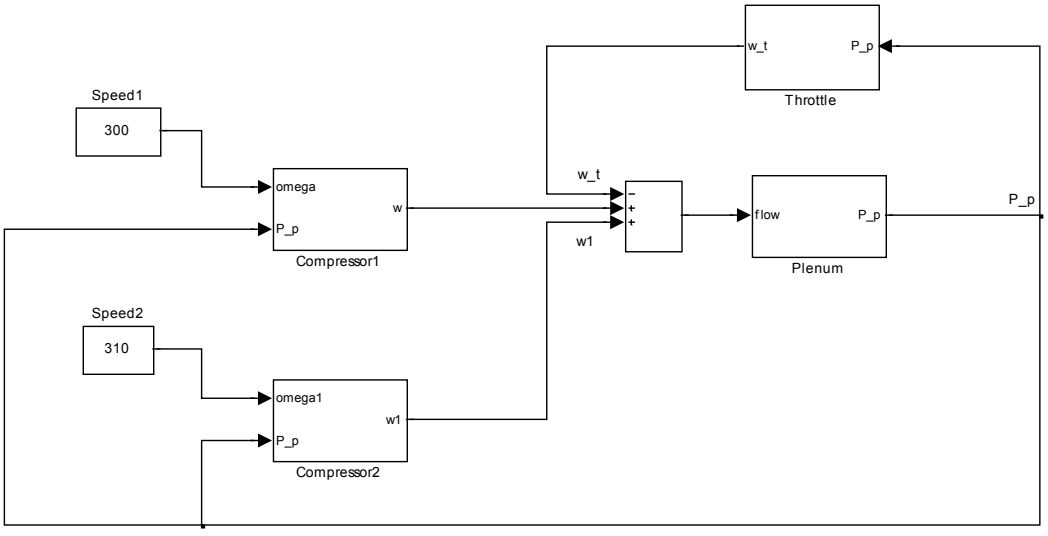

FIGURE 4.3: Parallel coupling of centrifugal compressors in SIMULINK

The extended model is shown in Figure 4.3, and it consists of two compressors coupled in parallel with a common plenum and one throttle valve being the discharge. This model is put together from the equations (3.4) and (3.5) with an extension. For simulation and linearization purposes the Speed1 and Speed2 are set to constant values. A simulation is shown in Figure 8.4, assuming the compressor lies in the stable area. The total system equations is shown below.

$$\dot{p}_p = \frac{c_p^2}{V_p}(w + w_1 - w_t) \tag{4.2}$$

$$\dot{w} = \frac{A_1}{L}(p_{02} - p_p) \tag{4.3}$$

$$\dot{w}_1 = \frac{A_2}{L_2}(p_{03} - p_p) \tag{4.4}$$

Equation (4.2) now shows the equation for the total flow in the system, with two mass flows running into the system (w and w_1), and one flow out from the throttle valve. This again equals the change in pressure in the plenum (V_p). The two differential equations

for mass flow being (4.3) and (4.4). The throttle valve is here modeled as

$$w_t = k_t u_v \sqrt{(101325 p_b - p_{01})}. \tag{4.5}$$

4.3 Stability of the parallel model

In this section MATLAB is used as a tool for the linearization of the nonlinear model represented by the equation (4.2), (4.3) and (4.4). The speed of each compressor are set to constant levels and the throttle valve represented by equation (4.5) is adjusted with a constant gain to get a reasonable output flow. The linearization of the model results in the system equations below, stated as a linear system, Chen (2009):

$$A = \begin{pmatrix} -9 & 0 & -385 & 0 \\ 0 & -9 & -385 & 0 \\ 1 & 1 & -15 & -55 \\ 0 & 0 & 0 & -2 \end{pmatrix}$$

$$B = \begin{pmatrix} 0 & 3 & 0 \\ 0 & 0 & 3 \\ 0 & 0 & 0 \\ 1 & 0 & 0 \end{pmatrix}$$

$$C = \begin{pmatrix} 0 & 0 & 1 & 0 \\ 0 & 0 & 14 & 48 \\ 1 & 0 & 0 & 0 \\ 0 & 1 & 0 & 0 \end{pmatrix}$$

$$D = \begin{pmatrix} 0 & 0 & 0 & 0 \\ 0 & 0 & 0 & 0 \\ 0 & 0 & 0 & 0 \\ 0 & 0 & 0 & 0 \end{pmatrix}$$

From the computed eigenvalues of the system matrix A, it is seen that the equilibrium point for this system is stable. This is on the other hand not a requirement for the linear

prediction model used in MPC, Imsland (2007).

$$
\begin{aligned}
eig(A) = & \\
-12.0074 + 29.4431i & \\
-12.0074 - 29.4431i & \\
-8.5920 & \\
-2.0000 &
\end{aligned}
\tag{4.6}
$$

To further analyze the linear model described above, the rank of the observability and controllability matrix are both 4 and the length of the state space matrix A are also 4. This implies that the system is both controllable and observable, which is a requirement for using model predictive control.

Chapter 5

Model Predictive Control

5.1 A basic formulation

In many control applications, a model of the system is used off-line to help the analysis and control application. In model predictive control, the model is implemented in the control algorithm with the signals being used directly. The usage of nonlinear models has become more common in later days, but then again the problem formulation will not be convex and more computational power will be required. Still, the linear formulation of process models with a convex QP algorithm is more often used, Imsland (2007). The linear formulation is the one which will be most focused on here.

5.2 Linear quadratic control

The linear state space model used here is in discrete form with constant sampling times k and given as

$$x_{k+1} = A_k x_k + B_k u_k \tag{5.1}$$

$$y_k = C_k x_k + D_k d_k \tag{5.2}$$

where the A_k and B_k matrix can be from either a time variant or time invariant system. The equation (5.2) represents the measurements. The x_k and u_k are the state and input vectors, with x_0 stated as the initial condition. The optimal solution of the finite horizon control problem when the desired values are equal to zero, is

$$u_k = -K_k x_k \tag{5.3}$$

with K_k being the feedback gain matrix, and k being in the time horizon from 0 to $n-1$. The u_k is constant between each time sample. The optimal control problem can be formulated as, Foss (2007)

$$J = \frac{1}{2}\sum_{k=0}^{n-1}\{(x_k - x_k^d)^T Q_k (x_k - x_k^d) + (u_k - u_k^d)^T R_k (u_k - u_k^d)\} + \frac{1}{2}(x_n - x_n^d)^T S (x_n - x_n^d) \tag{5.4}$$

The J can be minimized with out constraints, or being subject to constraints. Stating the weight matrices

$$R_k > 0 \tag{5.5}$$

$$S > 0 \tag{5.6}$$

$$Q_k \geq 0 \tag{5.7}$$

which can for instance be diagonal matrices, and they are symmetric.

Moving now to the infinite horizon controller which has a constant feedback gain K, that does not vary with time. The system matrix will then be

$$x_{k+1} = Ax_k + Bu_k \tag{5.8}$$

with x_0 given, and the optimization problem being

$$J = \frac{1}{2}\sum_{k=0}^{\infty} x_k^T Q x_k + u_k^T R u_k \tag{5.9}$$

The solution of the optimization problem and the linear constraints is

$$u_k = -Kx_k \tag{5.10}$$

The feedback gain together with algebraic Riccati equation is described as

$$K = R^{-1}B^T P(I + BR^{-1}B^T P)^{-1}A \tag{5.11}$$

$$P = Q + A^T P(I + BR^{-1}B^T P)^{-1}A \tag{5.12}$$

$$P = P^T \succeq 0 \tag{5.13}$$

It is here assumed that A, B, Q and R do not vary with time, also if on the other hand the reference values x_k^d and u_k^d are non zero as assumed earlier, a feed-forward term is needed.

In the above state equations it was assumed that all states were measured, but which

rarely happen. Therefore it is convenient to add state estimation to the problem formulation. From Foss (2007), the most important difference is that instead of (5.10) the solution becomes

$$u_k = -K\hat{x}_k \tag{5.14}$$

5.3 The constrained formulation

The constrained Linear Quadratic Regulator (LQR) is formulated here as the Model predictive controller. This handles constraints on the inputs and on the states. MPC is effective in the sense that it can operate optimal in the sense of constraints, which often is the most profitably or effective place to be working. The MPC can even be more effective in single loop control systems and can be the logical choice instead of PID where constraints is not considered.

In earlier days it was mostly used in the petrochemical industry, since this could be a relatively slow process. Nowadays the computational power of computers have increased to a factor over 10^6. Therefore we can now use MPC on even more systems. A problem which took about 10 minutes to compute ten years ago, now (2002) only takes 600 microseconds, Maciejowski (2002).

5.4 Cost function

One can think of the problem as a linear programming objective, which consists of a linear cost function and linear constraints. The most common way is to describe the objective function formulation with a Quadratic Programming (QP) formulation.

As seen in Imsland (2007) a finite horizon cost function is used for the MPC,

$$J = \sum_{k=0}^{L-1} x_k^T Q x_k + u_k^T R u_k + x_L^T P x_L \tag{5.15}$$

and the P term is the Riccati matrix defined in (5.12). The QP formulation in this thesis will also be defined as an objective function which is quadratic and the constraints being linear.

This equation (5.15) comes from the infinite horizon cost function

$$J(x_0, \{u_k\}_{k=0,\ldots,\infty}) = \sum_{k=0}^{\infty} x_k^T Q x_k + u_k^T R u_k \tag{5.16}$$

which is used in the LQR formulation. Also here the Q and R are matrices used for tuning, and it is required that the $Q \geq 0$ and $R > 0$ and the state must be detectable through Q. To minimize the infinite horizon cost function (5.16), the optimal future control (5.10) is applied. This is unfortunately only applicable if there are no constraints on the input and the states.

When we take constraints into the picture the optimization problem will be very hard to solve since there are an infinite number of variables to take into consideration. Another way to go to get to the finite horizon cost function which is used for MPC, is to cut off the sum in the function and set

$$J = \sum_{k=0}^{L-1} x_{k+1}^T Q x_{k+1} + u_k^T R u_k \tag{5.17}$$

then setting the L larger than the largest time constant in the process. The problem now will be stability. To solve this and to get closer to an infinite horizon solution, the objective function is divided into two parts.

$$\sum_{k=0}^{\infty} x_k^T Q x_k + u_k^T R u_k = \sum_{k=0}^{L-1} x_k^T Q x_k + u_k^T R u_k + \sum_{k=L}^{\infty} x_k^T Q x_k + u_k^T R u_k \tag{5.18}$$

From Imsland (2007) it is shown that

$$\sum_{k=L}^{\infty} x_k^T Q x_k + u_k^T R u_k = x_L^T P x_L \tag{5.19}$$

which implies

$$\sum_{k=0}^{\infty} x_k^T Q x_k + u_k^T R u_k = \sum_{k=0}^{L-1} x_k^T Q x_k + u_k^T R u_k + x_L^T P x_L \tag{5.20}$$

Then an open-loop optimization is computed at each sample instant with new measurements, but only the first part of the optimal inputs are used in the feedback.

5.5 System constraints

As mentioned earlier, the reason for using a MPC scheme for controlling a process is that it uses constraints in a manner that optimizes the process. An example can be the temperature in the discharge, minimum and maximum pressure in a compression system. Operating close to these constraints will often bring the most profitable operation, which is why we use constraints. The drawback of using constraints is as said earlier, that

constraints on inputs (manipulated variables) and states (controlled variables) implies that we can't use the LQR and optimize on the infinite horizon.

The constraints can be of the equality and inequality types, and interfere on inputs, outputs and states. These can e.g. be stated as

$$u_{min} \leq u \leq u_{max} \tag{5.21}$$

$$y_{min} \leq y = Cx \leq y_{max} \tag{5.22}$$

On the cost function on the other hand the constraints can be formulated as

$$Mx_k + Nc \leq b \tag{5.23}$$

where M and N are matrices and b is a vector of length equal to the number of inequality constraints on the system.

One major problem which can occur is that the objective function with constraints might actually be infeasible. This can happen if there is no possible way the plant can stay within the specified constraints because of a large unexpected disturbance, or e.g. the plant behaves differently than the model. From Maciejowski (2002), it is stated that this problem can be solved by e.g. softening the constraints. If not, the QP solver might stop, and the plant will not get an input signal because the problem will be infeasible. Other methods that can work are if the constraint definition or the horizons are actively managed at each sample, and non-standard solution algorithms are used.

Soft constraints can cross their limits if there are no other options, in relation to hard constraints which can never be exceeded. Of course we have to distinguish between input and output constraints. Input signals can often be limited in the sense that they are connected to actuators which have hard limits. Since it is not possible to stretch these constraints, they are not softened. Output constraints on the other hand can be handled by adding slack variables which are non-zero if the constraints exceed their boundaries.

To keep the constraints within boundaries the deviation is heavily penalized in the objective function.

5.6 Stability

The problem with stability can be solved in several ways. One way is when the predictive controller is designed off-line, with a good model it is easy to check for stability. Then if the controller on the other hand requires any closed loop redesign, the problems start

to arise. This can happen if the prediction horizon is too short. Because the controller cannot see beyond the horizon, it can put the state in a point where it is impossible to reach stabilization.

By using terminal constraints it is easy to ensure stability. This method forces the state to take a specified value at the end of the prediction horizon. On the other hand a general constrained optimization problem can be very difficult to solve and by adding a constraint like this, might not make it feasible.

5.7 Tuning

Tuning of the MPC controller implies getting the desired closed-loop response and at the same time making sure the controller is feasible. The variables used for tuning are the Q and R matrices and the horizon length L. The Q and R matrices are used for getting a more or less aggressive plant behavior and the L decides the computational complexity. A large L, means more time is spent on computing the objective and on the positive we get better performance. When thinking of disturbances in comparison with the horizon length the more will the disturbances affect the future performance.

5.8 Integral action

To remove steady state errors one may want to add integral action to the MPC law. This can be done by introducing it directly into the controller, but then again it has to be accounted for in both the constraints and the cost function, Maciejowski (2002). Also according to Cannon (2012), the closed-loop and stability performance will not be guaranteed if this is not accounted for. If on the other hand a penalty is added on the integrator state and there are no system constraints, the integral action can be introduced without closed-loop stability problems.

Another way of doing this is by adding disturbance states which are affecting the output, e.g.

$$y_k = Cx_k + d_k \tag{5.24}$$

with d_k being a constant and C the measurement matrix. These states can be modeled from slowly-varying disturbances and model errors which are affecting the process. An augmented model is then used as the process model for estimating d_k. With the new

output equation comes a change in the objective function, where this equation needs to be implemented.

5.9 Nonlinear MPC

In comparison to linear MPC which uses linear plant models, nonlinear MPC uses nonlinear models. This approach is used if the plant is affected by severe nonlinearities and if the plant is moved between operating points. By using this theory one can not have convexity in the cost function which is a drawback for on-line optimization. As stated by Maciejowski (2002), simply replacing the linear model with a nonlinear one can give sufficient performance in practice, but then again it can be nearly impossible to analyze. Another method is to re-linearize the nonlinear model when changing between operating points. The update of the plant model can on the other hand be left unchanged if it is near the region of an operating point.

5.10 Explicit MPC

The first multi parametric quadratic program (mp-QP) that appeared in the literature came from Bemporad et al. (2002). This can be explained by citing this paper

> "In the jargon of operations research, programs which depend only on one scalar parameter are referred to as parametric programs, while problems depending on a vector of parameters as multi-parametric programs."

Looking at equation (7) in Bemporad et al. (2002) with the variables explained there, the equation is here stated

$$V(x(t)) = \frac{1}{2}x'(t)Yx(t) + \min_{U} \left\{ \frac{1}{2}U'HU + x'(t)FU, \right. \tag{5.25}$$
$$\left. s.t.\ GU \leq W + Ex(t) \right\}.$$

This is a QP optimization problem and this can be solved off-line, with respect to all the values of the vector $x(t)$ of interest, and make this dependence explicit. From this paper it is stated that equation (5.25) is a mp-QP. To further quote the same paper as above

"Once the multi parametric problem (5.25) has been solved on-line, i.e. the solution $U_t^* = U^*(x(t))$ of (5.25) has been found, the model predictive controller (3) is available explicitly, as the optimal input $u(t)$ consists simply of the first m components of $U^*(x(t))$"

Chapter 6

Optimization

6.1 The efficiency curve

This chapter will describe the optimal running of compressors connected in parallel. At first the Figure 2.1 from Chapter 2 is looked at again. As was explained earlier, this figure shows the pressure ratio as the characteristic function of the compressor when running at different speeds. Now a similar plot is made, but now the focus is on the most effective region of the compressor map. Looking at Figure 6.1 we see here that the figure consists of almost round circles, these might be approximated to ellipses with varying radius. Here it is assumed that the ellipse having the smallest radius is equivalent to the highest efficiency, as seen from the labels of the curves. The most optimal area of operation for this specific compressor would then be with a mass flow of about 40 Lb/Min and a pressure ratio of around 1.45. Normally, these maps are either calculated or generated from a compressor rig test. More on this subject can e.g. be read about in, Boyce (2003). This includes subjects as data acquisition, which is a necessity for constructing performance maps. The compressor data is acquired through pressure measurements and temperature measurement which should be calibrated on-site. Further the flow is measured by e.g. orifice plates in the piping, or venturi tubes which has good accuracy. Power measurements can be done directly at the drive shaft or from measurement of electrical input to the driving motor.

Since these maps are usually generated using the relations between inlet and outlet temperatures, this became a problem for finding a continuous function for the efficiency islands. For this project, we assume the efficiency islands can be approximated to ellipses on the map. This is modeled in Figure 6.2.

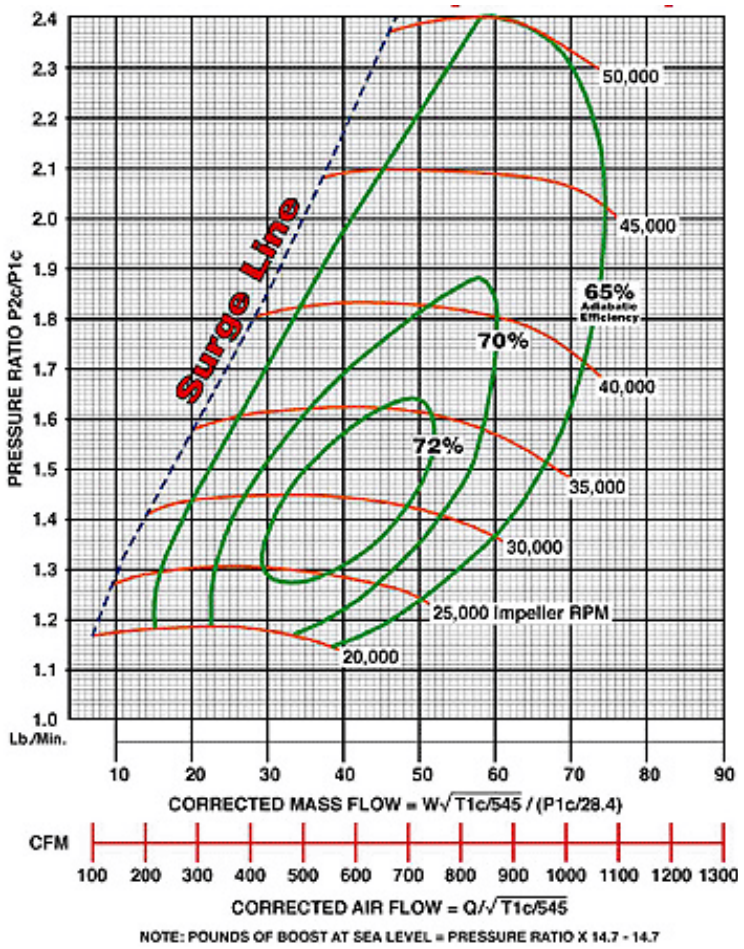

FIGURE 6.1: Real compressor characteristics with efficiency plot, Fahlgren (2013)

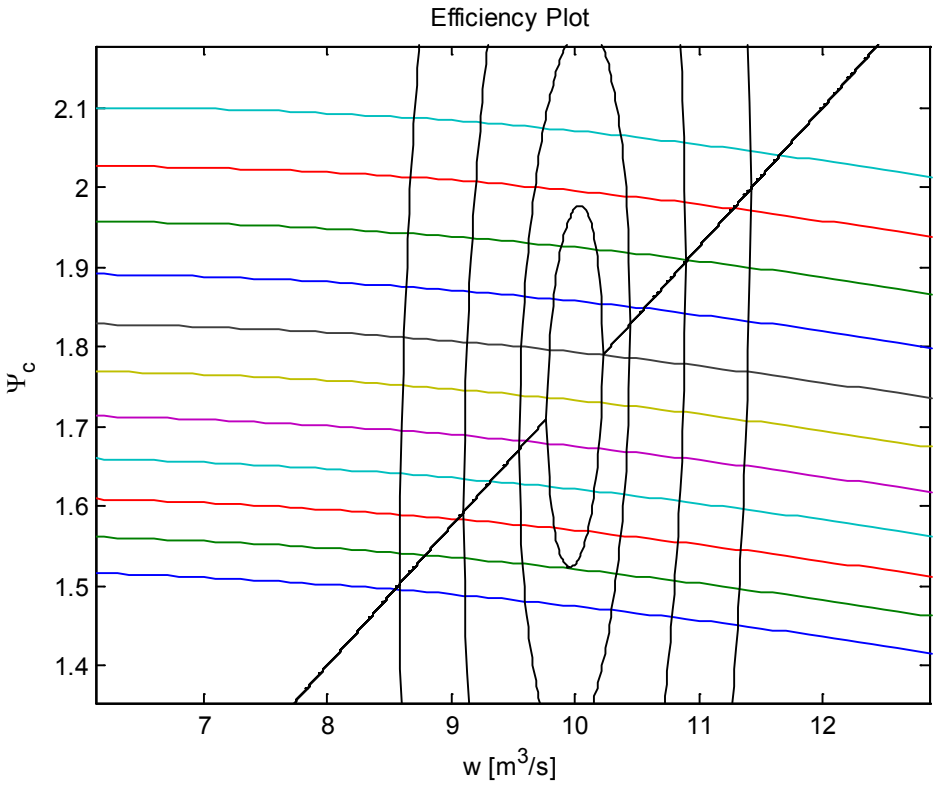

FIGURE 6.2: Compressor characteristics with efficiency plot

6.2 Gas compression

Under ideal conditions the compressor compresses gas at constant entropy, but in reality there is a change in both entropy and enthalpy. The efficiency of a centrifugal compressor is usually interpreted as isentropic rather than polytropic. So it can here be stated that the isentropic efficiency of the compressor is the result of the total changes in enthalpy.

$$\eta_{eff} = \frac{Isentropic\ Work}{Actual\ Work} \tag{6.1}$$

Now, some compression methods are presented to further study the efficiency problem.

6.2.1 Isothermal

In this process the temperature remains constant, but the gas pressure and volume compressed vary from inlet to outlet. This is seen from the ideal gas law

$$P_1 V_1 = P_2 V_2 \tag{6.2}$$

where P_1 and P_2 are the suction and discharge pressure conditions. The two volumes are V_1 and V_2 in the compressed process. The ideal gas law implies that the temperature is constant in the system and therefore requiring minimum losses, but since this is realistically impossible this makes an interesting field of research.

6.2.2 Adiabatic

An adiabatic process that has no losses due to friction is called isentropic, Menon (2005). Since there is no heat transfer to the surroundings from the gas, it can be said that during the adiabatic process the system is thermodynamically isolated. The equation can be described in almost the same way as equation (6.2). Including γ as an exponent to each side, the law becomes

$$P_1 V_1^{\gamma} = P_2 V_2^{\gamma} \tag{6.3}$$

and where γ is denoted as the adiabatic exponent for the gas, usually in ranges from 1.2 - 1.4.

6.2.3 Polytropic

In a polytropic compression system there can be heat transfer, and now the relation between pressure and volume is

$$P_1 V_1^{n} = P_2 V_2^{n} \tag{6.4}$$

with n being the polytropic exponent. This n makes this process again very similar to the adiabatic type of compression process.

6.2.4 Horsepower required

Here the points discussed above are taken into consideration. This section describes the horsepower (HP) formulation. Horsepower is the energy spent per unit time and is dependent upon pressure and flow rate of the gas. The simplest formulation would be to say that energy is the work developed by a force. In this case it would be the differential pressure added to the gas which is then flowing at a velocity. This on the other hand is not complete and a good enough approximation. The compressibility factor and the compression type would also have to be included because of the gas properties which is varying with both pressure and temperature.

The horsepower equation is here defined as

$$HP := \frac{M \times \Delta H}{\eta} \tag{6.5}$$

where
HP = compressor power
M = mass flow rate of gas
η = compressor efficiency
ΔH = compressor head

As seen in equation (6.5) the horsepower required to compress the gas is defined as the mass multiplied with the head of the compressor which is then divided by compressor efficiency. The head is denoted as the amount of energy supplied to the gas from the compressor per unit mass of gas.

Including the efficiency of the drive η_m, which is normally in the range 0.95 to 0.98 the brake horsepower (BHP) is defined as

$$BHP := \frac{HP}{\eta_m} \tag{6.6}$$

which is the required horsepower to run the compressor.

6.3 Optimal working point

Finding the exact optimal point of operation for a compressor can be a challenge, if the optimization is to be done from looking at the compressor map. In this setting on the other hand, a continuous efficiency island definition is very helpful for finding the optimal working area of compressors connected in series and/or parallel. The continuous efficiency characteristic implies that one can choose a desired mass flow, and with this an optimal speed and pressure ratio. These set points for pressure and mass flow will now give the set points for the MPC controller, which will be shown later.

As mentioned earlier the efficiency islands are either calculated or generated from a compressor rig test. These curves can be calculated starting from equation (6.7). The adiabatic efficiency is produced from the theoretical adiabatic temperature rise which is defined as

$$T_a := T_1 \left(\frac{Z_1}{Z_2}\right)\left(\frac{P_2}{P_1}\right)^{\frac{\gamma-1}{\gamma}} - T_1 \tag{6.7}$$

where Z_1 and Z_2 are dimensionless, and defined as compressibility of gas at suction conditions and compressibility of gas at discharge conditions. This is then used in the adiabatic efficiency equation below, which is rewritten from equation (6.1).

$$\eta_{eff} := \frac{T_a}{\Delta T} \tag{6.8}$$

where ΔT is defined as

$$\Delta T := T_2 - T_1 \tag{6.9}$$

Equation (6.8) is used together with temperature measurements to e.g. make the total efficiency island plot. It is important to remember that the gas is assumed to be thermally perfect in association with total temperature and pressure.

Comparing now the island curves of Figure 6.1 and 6.2, it is seen that they can be approximated to have the same shape and characteristic. Therefore in this thesis an assumption is made on the basis of this approximation. It will here be assumed that the approximated characteristic and efficiency islands are to be the same as those in the rig tested efficiency plots. The formulation of the "ellipse" shaped island curves are to be defined as

$$\Upsilon := (p_p - c_1 w)^2 + (w - c_2)^2 \tag{6.10}$$

where p_p and w are as stated before, the plenum pressure and mass flow in the one compressor setup. The curves have their center coordinates represented by c_1 and c_2. The Υ can be compared to the definition of efficiency when running the compressor at a specified operating point, but with values ranging from 0 and up. The lowest number is equivalent to the optimal region of the map. While we see that in Figure 6.1 the smallest ellipse have the highest efficiency, the same can be assumed here for Figure 6.2, that the best possible operating point will be in the "Center of ellipses" as shown in the figure. Equation (6.10) is plotted in Figure 6.2 with values of Υ in the area

$$0.05 \leq \Upsilon \leq 2 \tag{6.11}$$

with 0.05 being the highest efficiency, and 2 the lowest.

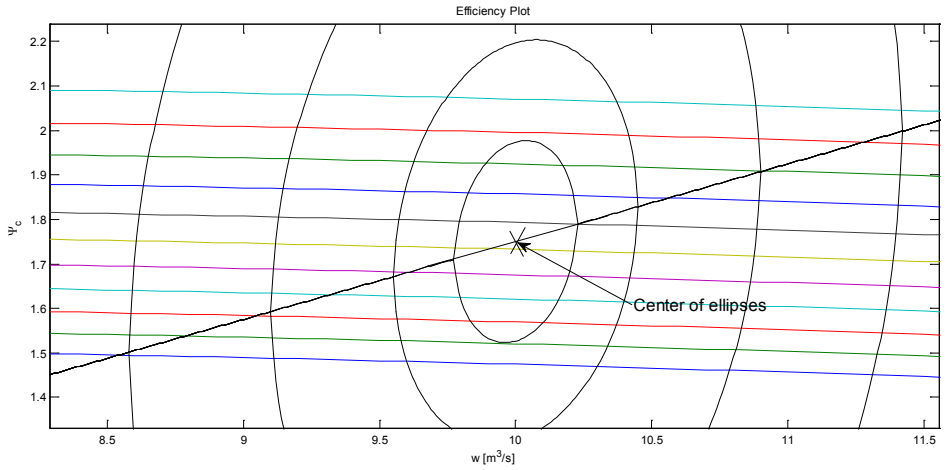

FIGURE 6.3: Compressor characteristics with approximated efficiency ellipses

The Figure 6.3 shows the ellipses in the characteristic plot. In this case the center coordinates are represented by $c_1 = 0.175$ and $c_2 = 10$. These coordinates will then represent the point of optimal mass flow and pressure ratio.

To find the optimal point of operation, equation (6.10) is formulated as a Quadric Programming problem (QP), Nocedal and Wright (2006). This is defined as

$$min\ \Upsilon := \frac{1}{2}x^T Hx + f^T x \tag{6.12}$$

where H is a symmetric and positive definite $n \times n$ matrix, which has the unique solution

$$x^* = -H^{-1}f \tag{6.13}$$

if x do not contain any constraints. Using that $c_1 = 0.175$ and $c_2 = 10$, the H and f matrices are given below in equation (6.14) and (6.20).

$$H = \begin{pmatrix} 2 & -\frac{7}{20} & 0 \\ -\frac{7}{20} & \frac{1649}{800} & 0 \\ 0 & 0 & 200 \end{pmatrix} \tag{6.14}$$

and

$$f = \begin{pmatrix} 0 \\ -20 \\ 0 \end{pmatrix} \tag{6.15}$$

where the state vector x is defined

$$x = \begin{pmatrix} p\_p \\ w \\ 1 \end{pmatrix} \tag{6.16}$$

This Quadric program can be solved by using a QP solver. This is demonstrated below using *quadprog* in MATLAB.

```
syms p_p w;

x = [p_p ;w ;1];

H=[2 -2*0.175 0 ;-2*0.175 2*(1+0.175^2) 0 ;0 0 200];

f = [0 ;-20 ;0];

F = 0.5* x' *H *x + f' *x;


opts = optimset('Algorithm','active-set','Display','off');

lb = zeros(3,1); % Lower bounds
ub = [3 15]; % Upper bounds


[x,fval,exitflag,output,lambda] = ...
    quadprog(H,f,[],[],[],[],lb,ub,[],opts);

p_p = x(1);
w = x(2);
```

The variable p_p will give out the optimal pressure ratio and w represents the optimal flow. For the flow and pressure to be set to a different level, the upper and lower bounds would have to be changed accordingly to fit the demand. For one compressor and knowing which set point is used for desired mass flow (w), the only variable available to solve the equation for is the pressure ratio (Ψ_c), here also described by p_p.

Extending to two parallel coupled compressors gives a different type of objective function. This gives rise to the load sharing problem which will be considered in detail. The ideal setup for the load sharing would probably be if both compressors had the same characteristic with equal efficiency island definition. If the total mass flow from each machine combined is 20 $[m^3/s]$, which will split the flow between the machines at equal rates using the control system. Pressure ratio is at 1.75 [bar], since from looking at the compressor map this set point would result in the compressors running at optimal

conditions. For equal characteristic on the map the cost function for the QP problem would be equal to using equation (6.12) and multiplying this by a factor of two.

The cost function describing two parallel coupled centrifugal machines will in this setup be described as

$$\Upsilon_p := (p_p - c_1 w)^2 + (w - c_2)^2 + (p_p - c_3 w_1)^2 + (w_1 - c_4)^2 \tag{6.17}$$

Here the pressure ratio will have to be the same in each machine, but the flow will vary for each desired set point. So in this case there are three state variables to optimize on. Using the same QP formulation as described in equation (6.12) and specifying $c_1 = c_3 = 0.175$ and $c_2 = c_4 = 10$. This gives the state vector

$$x = \begin{pmatrix} p\_p \\ w \\ w1 \\ 1 \end{pmatrix} \tag{6.18}$$

The new state matrix will in this case be

$$H = \begin{pmatrix} 4 & -\frac{7}{20} & -\frac{7}{20} & 0 \\ -\frac{7}{20} & \frac{1649}{800} & 0 & 0 \\ -\frac{7}{20} & 0 & \frac{1649}{800} & 0 \\ 0 & 0 & 0 & 200 \end{pmatrix} \tag{6.19}$$

and

$$f = \begin{pmatrix} 0 \\ -20 \\ -20 \\ 0 \end{pmatrix} \tag{6.20}$$

The MATLAB script is given in Appendix B. In this script the input will be total mass flow out from both compressors, which will be equally shared if the characteristics are the same.

In the script below the efficiency curves are changed to be unequal each other for each compressor. These characteristics are shown in Figure 8.32 and Figure 8.33. With the desired flow being 25 $[m^3/s]$, which is set as an equality constraint.

```
syms Pp w w1;


opts = optimset('Algorithm','active-set','Display','off');

lb = zeros(3,1); % Lower bounds
ub = [3 15 15]; % Upper bounds

c1=0.175;
c2=10;
c3=0.13;
c4=13;

H = [4 -2*c1 -2*c3 0; -2*c1 2*(1+c1^2) 0 0;...
    -2*c3 0 2*(1+c3^2) 0; 0 0 0 2*(c2^2+c4^2)];
f = [0;-2*c2;-2*c4;0];

Aeq = [0 1 1 0];
beq = [25];


[x,fval,exitflag,output,lambda] = ...
    quadprog(H,f,[],[],Aeq,beq,lb,ub,[],opts);


Pref=x(1);
Wref=x(2);
W1ref=x(3);


x'*[4 -2*c1 -2*c3 0; -2*c1 2*(1+c1^2) 0 0;...
    -2*c3 0 2*(1+c3^2) 0; 0 0 0 2*(c2^2+c4^2)]*x


x'*[0;-2*c2;-2*c4;0]
```

As the optimal pressure ratio is found, this can be used in the compressor characteristic function

$$\Psi_c(w,\omega) = \left(1 + \frac{\mu r_2^2\omega^2 - \frac{r_1^2}{2}(\omega - \alpha w)^2 - k_f w^2}{c_p T_{01}}\right)^{\frac{\kappa}{\kappa-1}} \tag{6.21}$$

Where $\Psi_c(w,\omega)$ is equal to the pressure ratio, Gravdahl and Egeland (1999). While knowing the optimal pressure ratio and mass flow, equation (6.21) can be solved to find the desired impeller rotational speed. For the compressors connected in parallel, the characteristic is calculated for each mass flow and the two set points for speed is found since this will be the only unknown variable.

In this thesis the focus is only to try to develop a load sharing strategy. This problem set up therefore does not take account of startup and shutdown of compressors. This can on the other hand be read about in Boyce (2003). Here different factors are considered when constructing a startup and shutdown control system. This can of course be a problem for the final result, because much power and time consuming procedures is needed to make this happen. The machines used for transporting gas over long distances can be quite large, and energy is required for using the starting and stopping procedures.

Chapter 7

Load sharing

The load sharing topic will in this section be explained in more detail, and ways to define load sharing will be looked at.

7.1 Definition

Load sharing can be defined as an optimal running of each compressor station in a gas pipeline network. This means that if each station is run in an optimal manner in relation to the flow and the suction and discharge pressure, one can save much energy. The minimization objective will be to minimize the fuel amount which is consumed by the gas turbine drives.

Another formulation of the load sharing problem can be to focus more on each compressor station and from there move deeper into the single unit system. Compressors running in parallel are known to have several nonconforming abilities such as areas of efficiency.

According to Nisenfeld and Cho (1978), the most serious problem is balancing the load between the machines. As is stated, the authors have seen nearly 40 different parallel compressor systems, but are yet to see any compressors in parallel which have the same characteristic and which have equal surge and stonewall areas. This also implies that the most efficient compressor will take more of the load and the other might operate with its recycle valve open.

7.2 Previous work on load sharing

In Blotenberg et al. (1984) methods are worked out for controlling three propane compressors in parallel with each compressor having three stage groups. The compressors are run with a constant speed and are controlled by opening and closing throttle valves in the pipe inlet. This procedure presented includes startup and anti-surge control, and last but not least load sharing control. Each compressor has its own anti-surge recycle system with equivalent piping system. A dynamic control line responds to sudden changes in the point of operation and an additional anti-surge safety line is used in front of the surge limit. This must be included since variations in performance curves of each compressor means that the surge limits are different in each unit.

The load sharing procedure states that all compressors must be run at duty points which are at equal distance to the respective surge limits as shown in the Figure 7.1 below.

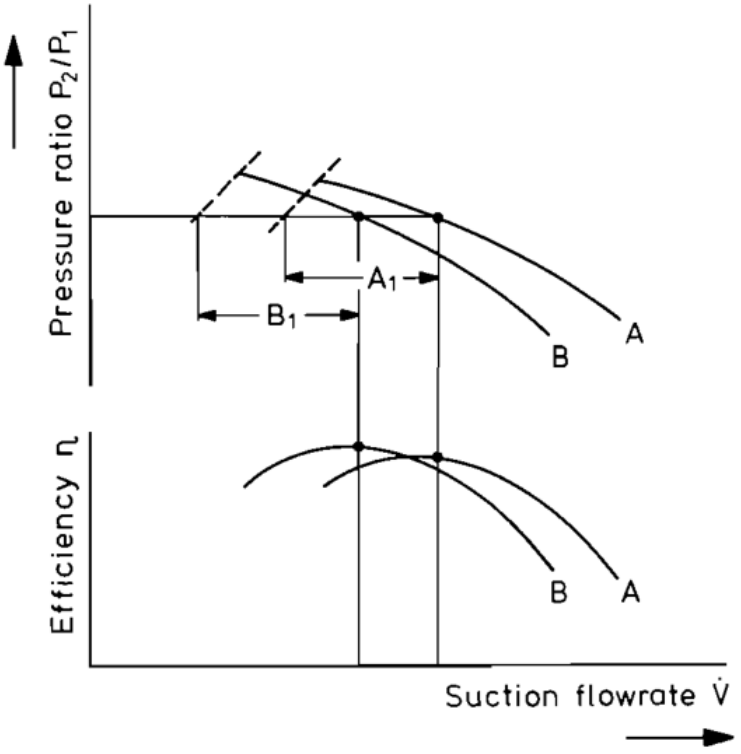

FIGURE 7.1: Standard Load Sharing described in Blotenberg et al. (1984)

The figure shows compressor characteristics for machine A and B and their equivalent distance to each surge margin A_1 and B_1 which are to be equal. This ensures that all compressors are to be operated at their peak efficiency while inside the range of the entire operating range. This method is used because of the risk of having a compressor working too near the surge limit. If this line is crossed the compressor starts recycling and a huge amount of energy is lost in this process.

Implementation of pressure controllers which give input to throttle valves, controls the pressure in the suction piping. This is again controlled by the load sharing controller in a way that upholds the equal distance between the surge limit and duty point in several stages. This implies that the valves are moved in opposite directions of each other and this makes an optimal utilization of the machine performance. Now in the case of a disturbance reducing the flow, the compressors will reach the control line the same time.

In Ferber et al. (1999) an model predictive algorithm is produced, which is meant to optimize a gas pipeline network (TL-400). The pipeline is modeled using a steady state optimizer which focuses on the compressor curves and uses the pipeline constraints, while taking into consideration all the supply and delivery points. This is done by first using an optimizer to make a calculation of the fuel minimization problem, by determining the possible hydraulic operating area of the entire plant while also taking into consideration the starting and stopping of compressors. It is also stated here that running each compressor close to their maximum efficiency is hard to do, since this point might be difficult to find and may still not optimize the entire gas pipeline.

In this load sharing scheme the controller uses the suction and discharge pressure as set points to the process. These two, together with a set point for flow is sent down to each compressor station and their respectively local controllers. The results in this paper imply a more cost effective operation of the entire plant. The control strategy is summarized below as

1. Maintain the pipeline at an optimal pressure profile (normal mode)
2. Gracefully handle the (daily) change in nominations (transition mode) and
3. Automatically handle operations in the event of a compressor going down (event mode).

To see a more detailed description of these points, see the paper of Ferber et al. (1999).

A different formulation of model predictive control of compressor installations is described in the paper of Smeulers et al. (1999). This research focuses on turbo compressors connected in parallel which are meant to boost pressure in gas distribution networks. Using a non linear computer model of the compressor station, the possibility of implementing MPC with two compressors connected in parallel is looked at.

As is mentioned in Chapter 5 the MPC scheme usually uses linear models of the non-linear plant, but for a compressor station this is not sufficient. In this paper a method called successive linearization is used, this is applied since the parameters of the model have to be updated every time step for the actual work point. Together with this, a

Kalman filter is used for the tuning procedure, which corrects the state parameters of the process model.

The setup of the two compressors is shown in Figure 7.2.

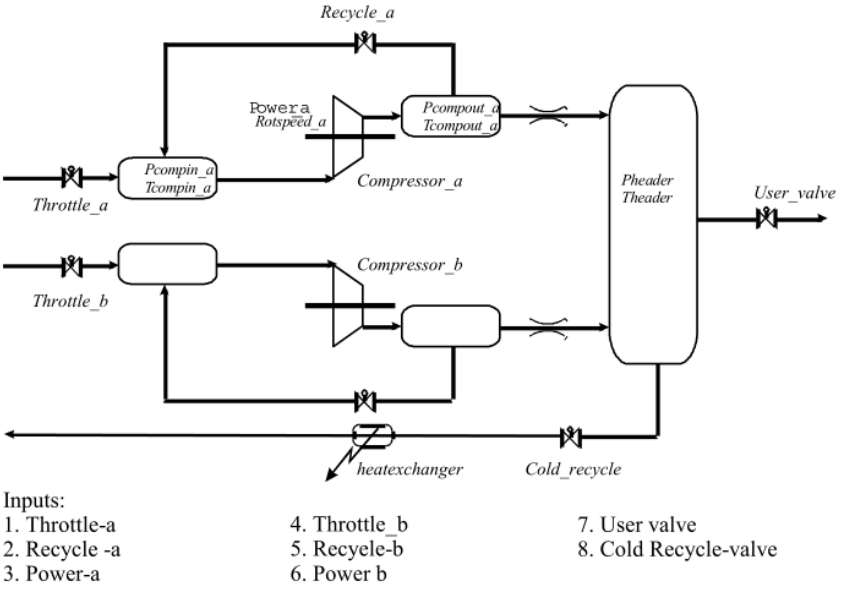

FIGURE 7.2: Compressor station used for the MPC study in Smeulers et al. (1999)

The constraints in the system are set up to be dependent upon speed, surge, temperature, pressure and power. A surge constraint is set up on the compressor characteristic for each compressor, which is also dependent on maximum and minimum rotational speeds. Temperature in the plenum is to be kept as low as possible and this is also set as a constraint. The header is constrained by a minimum and maximum pressure level and lastly move constraints are set on power supply to the compressors and the control valves positions.

As stated earlier the optimization and prediction uses linear models because of the time it takes to get a response is often less in these cases. So due to successive linearization the coefficients are recalculated at every time step. The controller is tuned for optimal performance and the prediction and control horizons are 30 and 8 time steps.

The load sharing problem is here translated to load balancing, with a maximum and equal distance to the surge line. A constraint is then set to less or equal to 1, for the variable $dSurge$ which is

$$dSurge = \frac{actual\_mass\ flow}{mass\ flow\ at\ surge\ for\ the\ same\ rotational\ speed} \tag{7.1}$$

The results of this paper show that it is possible to implement a model predictive controller on this configuration with a Kalman filter capable of compensating for model

mismatches. The MPC can influence controlled inputs and outputs, and constraint handling together with dynamic optimization which is set to benefit the performance of the station.

7.3 Load sharing scheme

To define a smaller area of operation the compressor characteristic in Figure 7.3 is used. This now shows the upper and lower limits for the speed of each compressor. The impeller velocity is in this case bounded from 280 [rps] up to and including 315 [rps]. This range is chosen since the linearization is performed with the impellers running at 300 rounds/s and this then seemed like a profound choice, which also constrain the MPC.

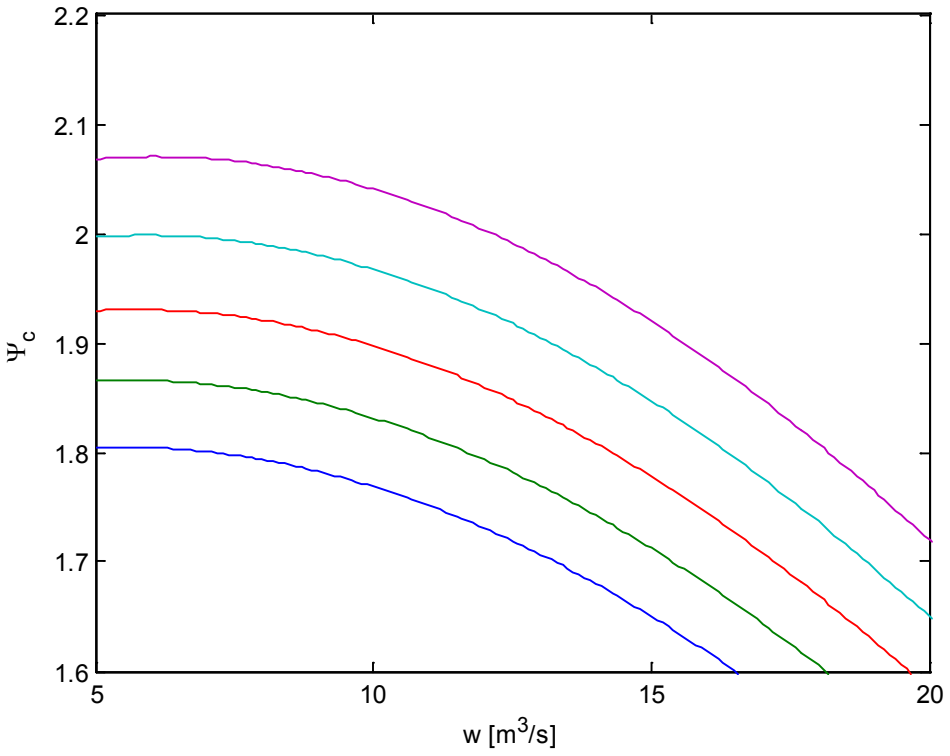

FIGURE 7.3: Compressor characteristic in this load sharing scheme

In this formulation of the load sharing problem, the goal is to try to retain the mission of having e.g. both compressors working in the highest possible area of efficiency. Fuel consumption is not considered as a goal in this project, but is considered a part of further work.

As discussed in the earlier optimization chapter, the efficiency curve for both compressors is described as equation (6.17). The optimal area is if each term is zero. This can be shown as an example. If we look at the efficiency plot in Figure 6.2, the optimal running of each compressor is at $w = w1 = 10\ [m^3/s]$ and a common plenum pressure of $P_p = 1.75$ [bar], given that each characteristic and efficiency definition are the same for both compressors.

The load sharing setup in this thesis will be as following in Figure 7.4.

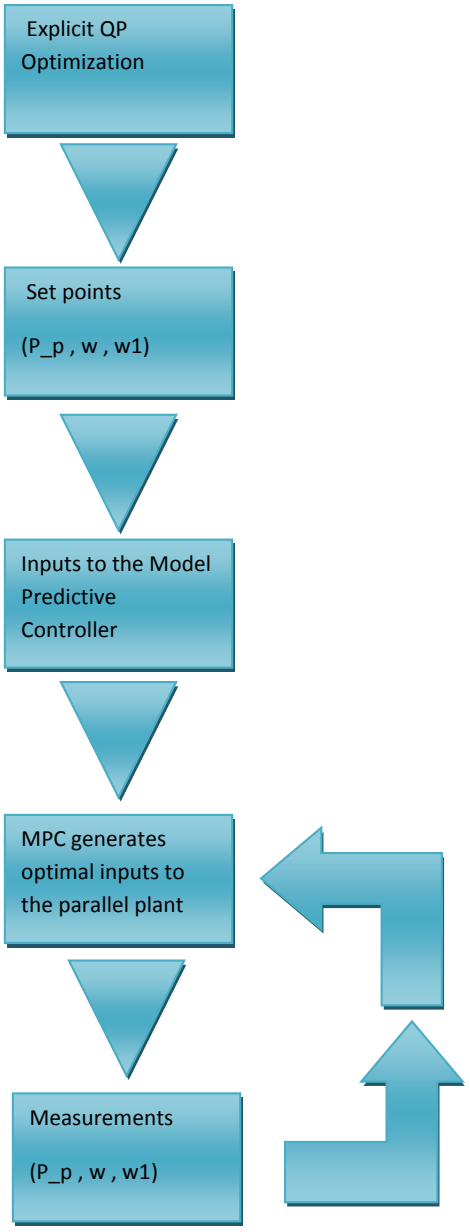

FIGURE 7.4: Compressor characteristic in this load sharing scheme

The points seen in this flow chart are described below.

1. Explicit optimization of the parallel compressor setup, using the continuous ellipse efficiency definition.
2. Gives set points for mass flow w, $w1$ and pressure ratio p_p.
3. Uses the references from point 2 as inputs to the MPC scheme.
4. The MPC gives optimal inputs to the plant.
5. Mass flow w, $w1$ and pressure ratio p_p are measured in the parallel compressor plant and are fed back to the MPC.

Using the QP optimization script given in the appendix, the optimal references for pressure and mass flow are calculated. It is assumed that the total flow through the system is given as an equality constraint for the optimization, and this will be the flow demand from the user.

When the optimized set points are generated and the model used for the simulation is linearized around a specified steady state work point, the linear model is used in the prediction of the linear MPC.

Next the MPC is tuned for a desired response and costs are set on the inputs and outputs. Using MPC toolbox in MATLAB, this is shown in Figures 11-13 in Appendix B. This represents the total setup for the MPC used in the SIMULINK diagram shown in Figure 8.

Chapter 8

Simulation

8.1 The single compressor system

This Chapter presents the results of the designed parallel model shown in the equations (4.2) - (4.4). At first the focus is set to the simple compressor system shown in Appendix and in Figure 2, with the system equations from Chapter 3 which is the differential equation of pressure (3.27) and flow (3.28) and lastly the throttle valve dynamics written in equation (3.29). This system is simulated while running at a constant speed and no disturbances in the outflow from the throttle valve.

The characteristic function is first stated in equation (6.21) and used in MATLAB as

$(1+(\text{mu*r2}^2\text{*u[1]}^2 - ((\text{r1}^2)/2)\text{*(u[1] } -\text{alpha } * \text{u[2]})^2 - \text{kf} * \text{u[2]}^2)/(cp * T01))^{\frac{kappa}{kappa-1}}$

The values of Table 8.1 are mostly found in Gravdahl et al. (2002), while some of them are discovered through testing and analyzing the compressor map.

Mathematical term	Term used in MATLAB	Value
μ	mu	0.9091
r_1	r1	0.3457 m
r_2	r2	1.1140 m
α	alpha	50
k_f	kf	5
c_p	cp	2064 J/kg K
T_{01}	T01	293 K
κ	kappa	1.3

TABLE 8.1: Table shows compressor characteristic data

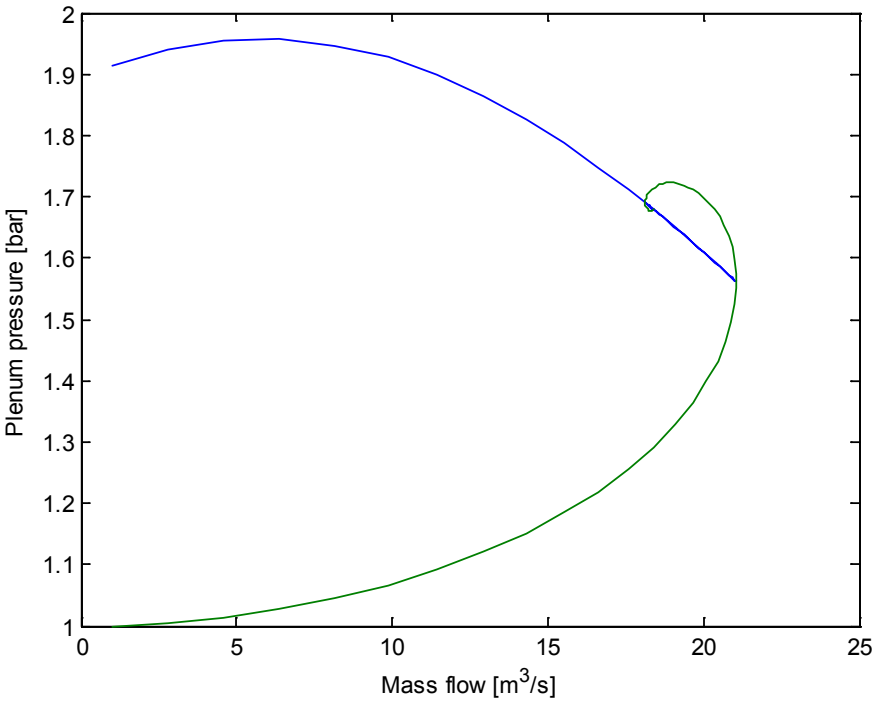

FIGURE 8.1: Pressure in relation to mass flow for one compressor

The top curve of Figure 8.1 shows the compressor pressure ratio [-] for the specified rotational speed, while the other one starting at 1 [bar] initial condition shows the final steady flow from the compressor and into the plenum while reaching a final pressure level.

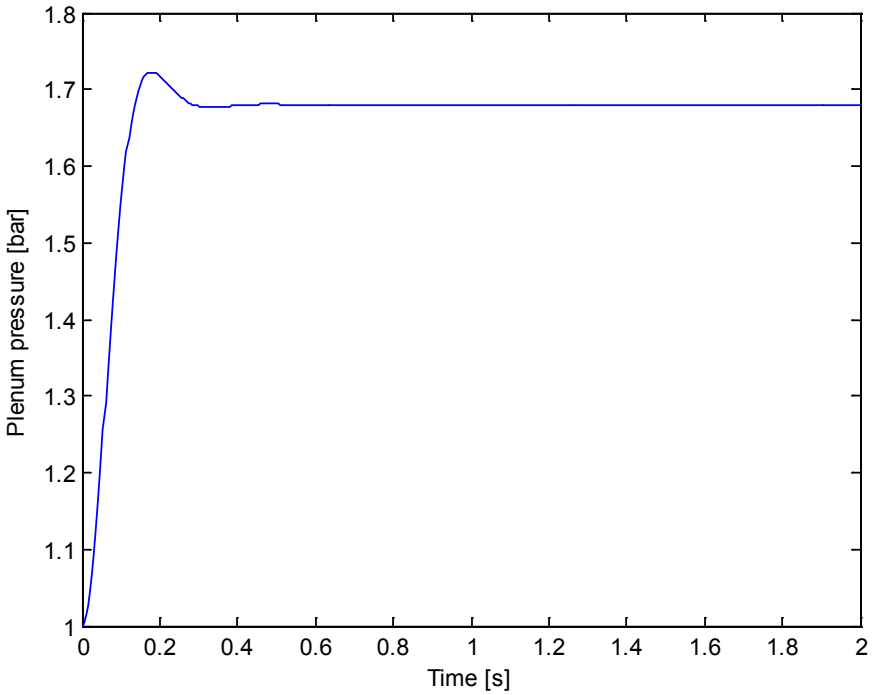

FIGURE 8.2: Pressure in the plenum

As is seen in Figure 8.2 and Figure 8.3 the pressure in the plenum and mass flow through the throttle are quickly to reach a stationary level as long as the compressor is working in the stable region. Notice here that it is not set any reference on the desired outflow or pressure, only a constant is used for throttle gain and compressor speed, which is run in open loop.

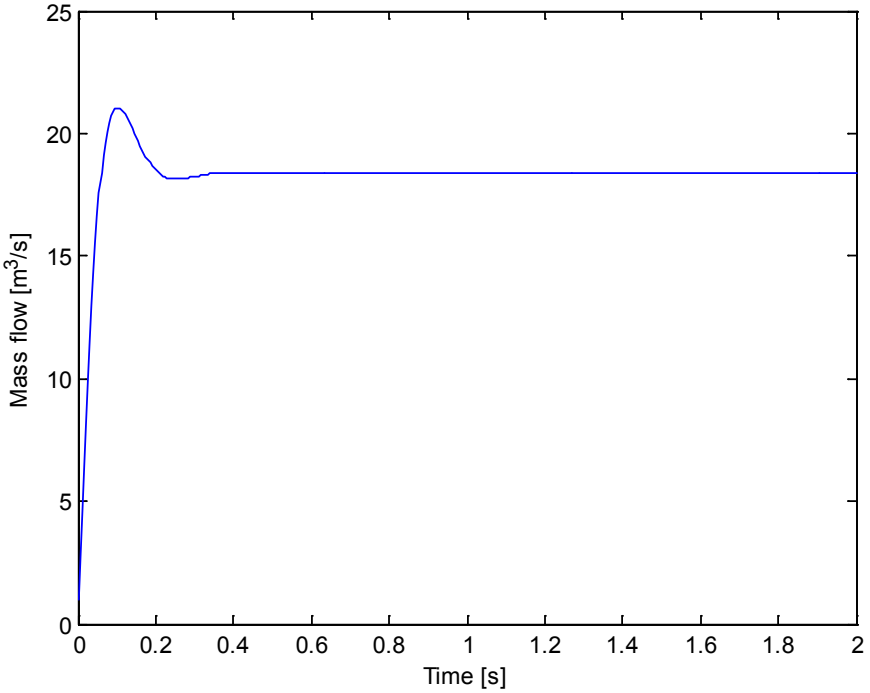

FIGURE 8.3: Mass flow for one compressor

8.2 The parallel system

In this section the focus is on the parallel model given in equations (4.2) - (4.4). To test the model, two constant impeller speeds were selected and a constant gain in the throttle valve. The result is shown in Figure 8.4. This gives a stationary flow from each compressor and a common pressure in the plenum. This can be seen from the two different characteristic curves drawn on the figure.

The plotted mass flow is shown in Figure 8.5 and the top curve shows the compressor running the highest speed. As said earlier the pressure is plotted from the common plenum and is produced in Figure 8.6. Lastly in Figure 8.7 we see the flow dynamics, running through the duct and out from the throttle valve. Both flow dynamics move to a common steady flow.

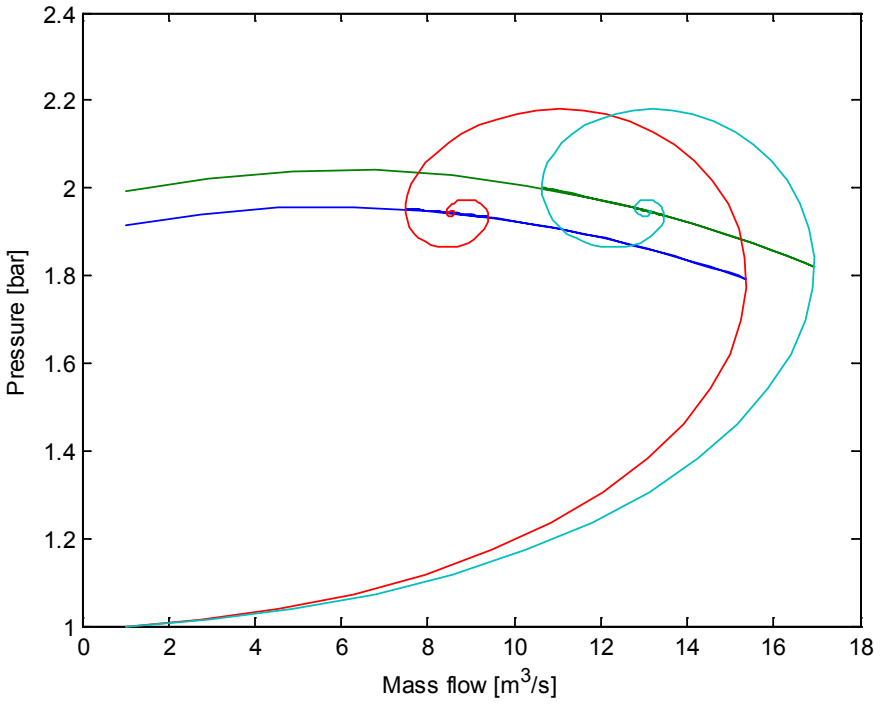

FIGURE 8.4: Compressor characteristics for each of the two compressors with different speeds

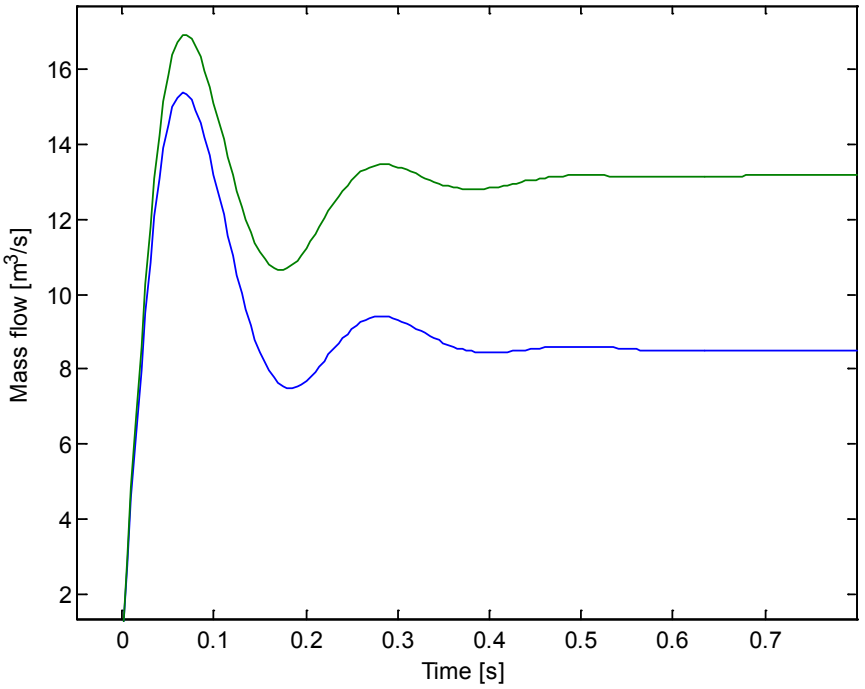

FIGURE 8.5: Mass flow for each of the two compressors

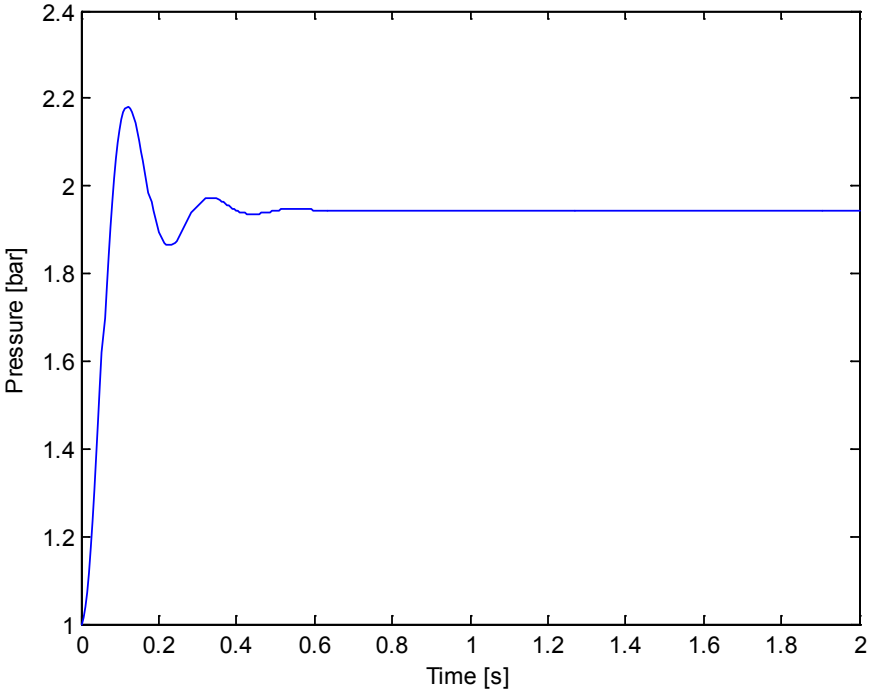

FIGURE 8.6: Pressure in the plenum for compressors connected in parallel

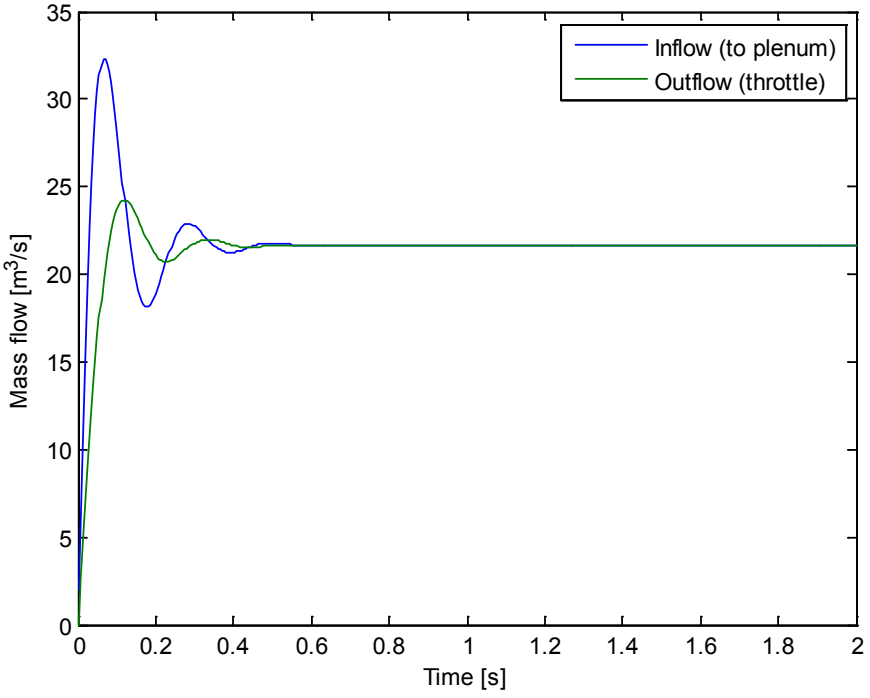

FIGURE 8.7: Total in- and outflow for the plenum

8.3 MPC implementation

In this section of the simulations, we focus on the interaction between the two parallel coupled compressors and the model predictive controller which is implemented in SIMULINK. This setup is shown in the simulation diagram of Figure 8. From the QP optimization given in previous sections, a value is given for each specified reference. The set points represent plenum pressure [bar] and desired load from each compressor $[m^3/s]$. Table describing reference points is Table 8.2.

	P_p	w	w1
r_1	1.75	10	10
r_2	1.84	10.50	10.50
r_3	1.66	9.50	9.50
r_4	1.66	9.50	9.50
r_5	1.87	10.99	14.01

TABLE 8.2: Set-point references for each simulation, computed by QP

8.3.1 Simulation one

Shown in simulation one is the optimization containing no constraints. Here the r_1 values are given as set points to the process and we see from Figure 8.8 that the pressure level almost reaches its desired level but not quite. The reason for this can be incorrectly given tuning parameters in the controller, or the linearized prediction model is not good enough and the system should be re-linearized to fit the desired point of operation.

In Figure 8.9 the total flow through the system is fast stabilized and both the flow through the duct and the flow through the throttle are the same, while still moving slowly to the desired value of 20 $[m^3/s]$. In the Figures 8.10 and 8.11, both the reference and the trajectory are drawn and it takes about 110 seconds for the compressor to reach its set point.

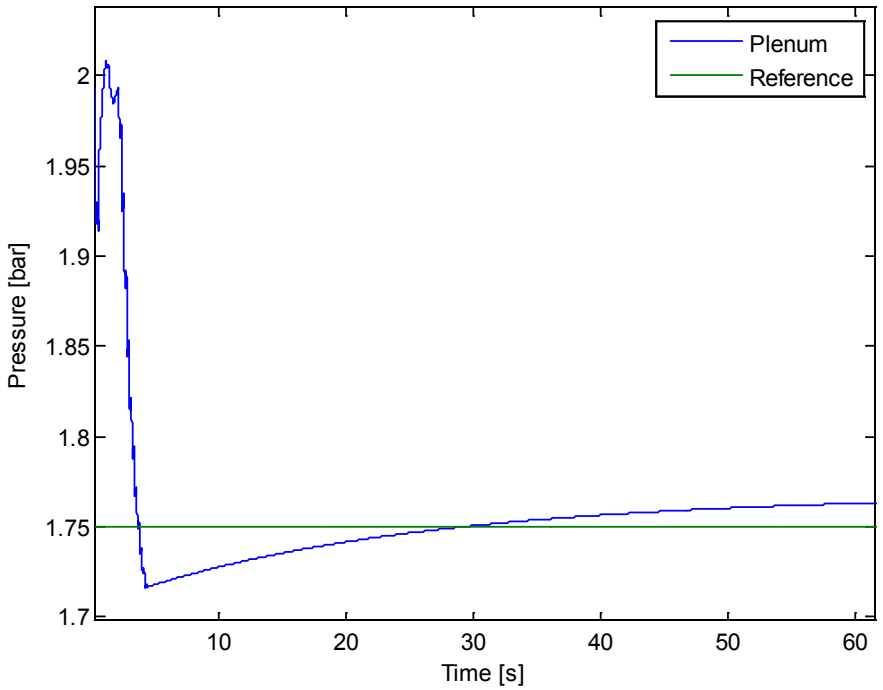

FIGURE 8.8: Pressure in the plenum

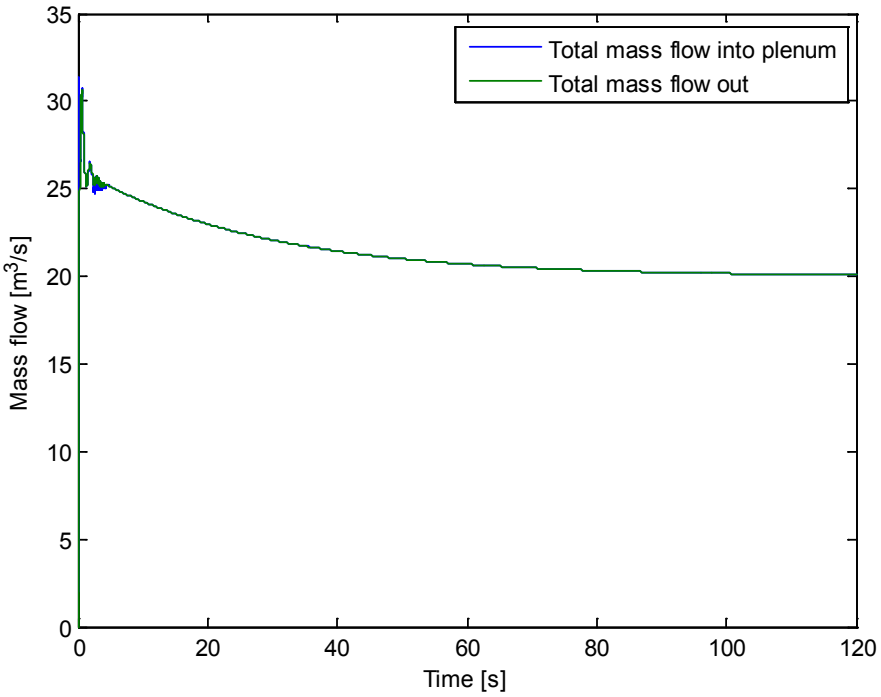

FIGURE 8.9: Total flow into and out from the system

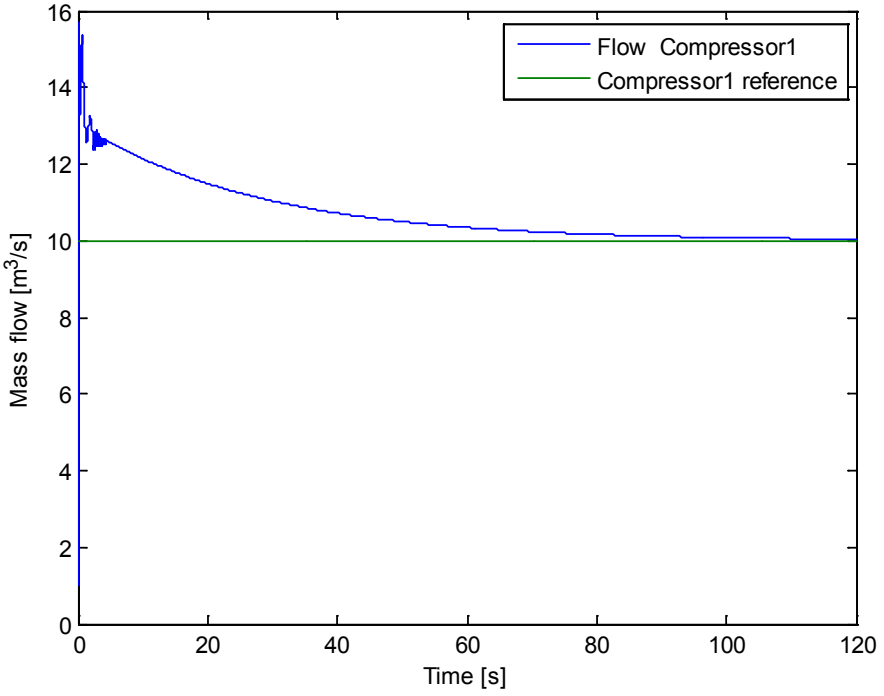

FIGURE 8.10: Flow from compressor 1 with reference

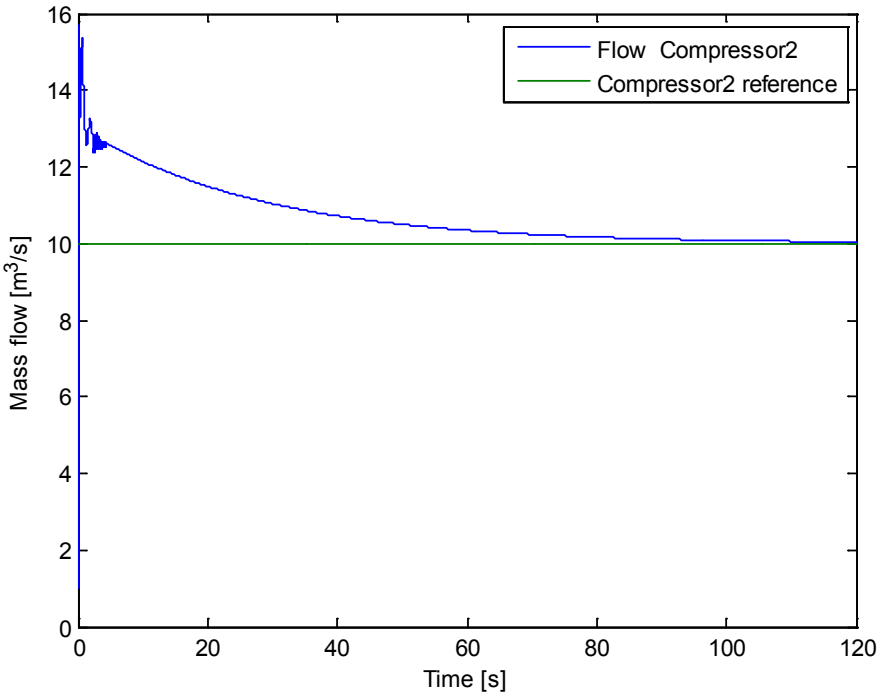

FIGURE 8.11: Flow from compressor 2 with reference

Since there were no constraints in the QP formulation of this problem, it is seen here in

Figure 8.12 that the optimal point lies in the center of the ellipses. As was explained earlier each ellipse represents an area of efficiency which in this case has its optimum in the center of the inner ellipse. Each compressor is assumed to have the same characteristic and therefor only one plot is given.

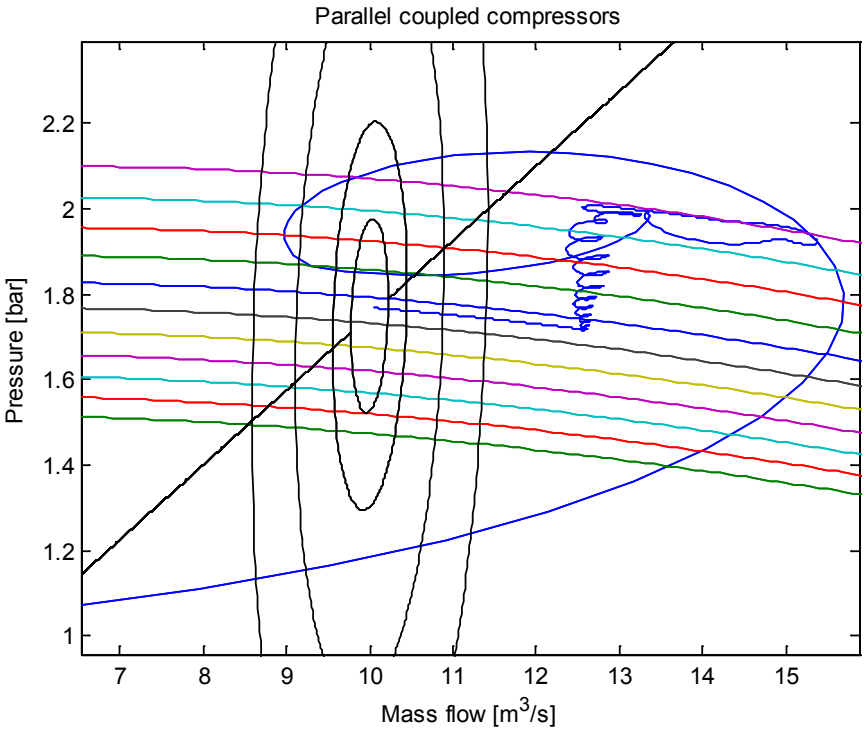

FIGURE 8.12: Plotted pressure rise in relation to mass flow

8.3.2 Simulation two

The optimization is now performed with a desired flow of 21 $[m^3/s]$ which implies that this will be an equality constraint, and each compressor will share this load. The optimal values for flow and pressure are then given as r_2 in Table 8.2.

In relation to the previous simulation, it is seen here in Figures 8.13, 8.15 and 8.16 that the calculated values are reached and does not give a offset. Same as before the plotted flow through the centrifugal compressor is represented in Figure 8.14.

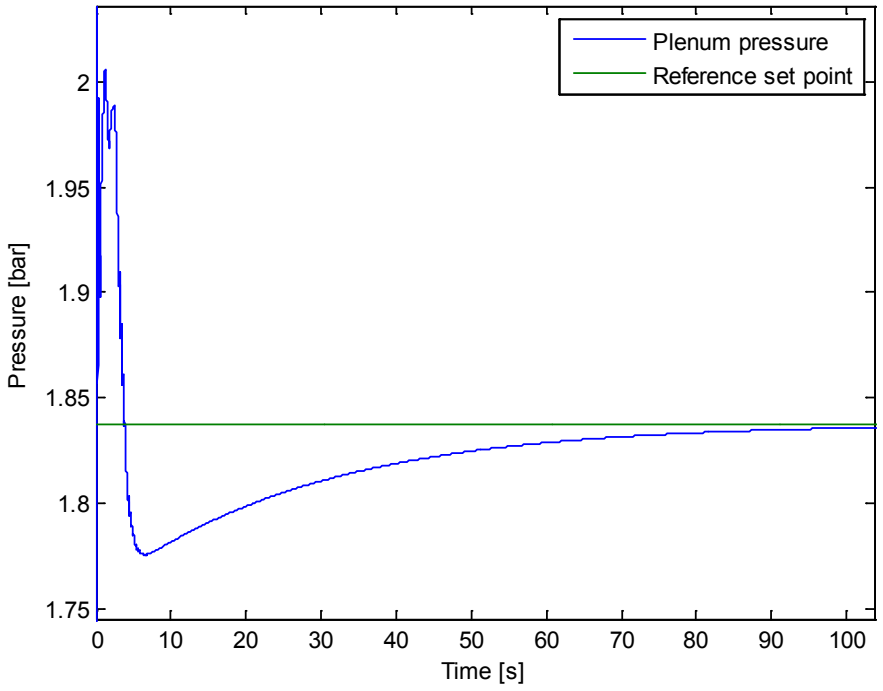

FIGURE 8.13: Pressure in plenum with reference set-point

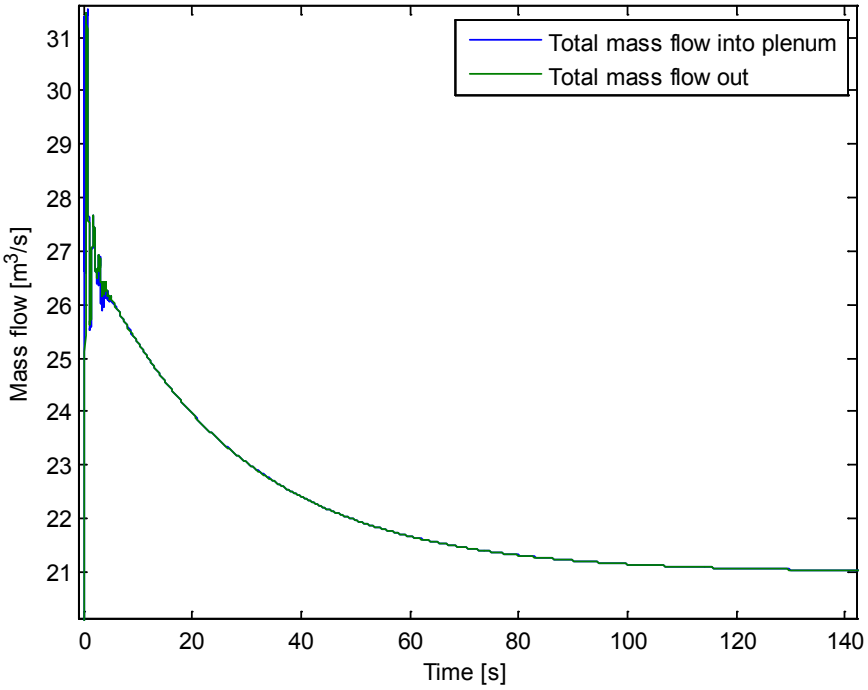

FIGURE 8.14: Plotted mass flow in and out of the system

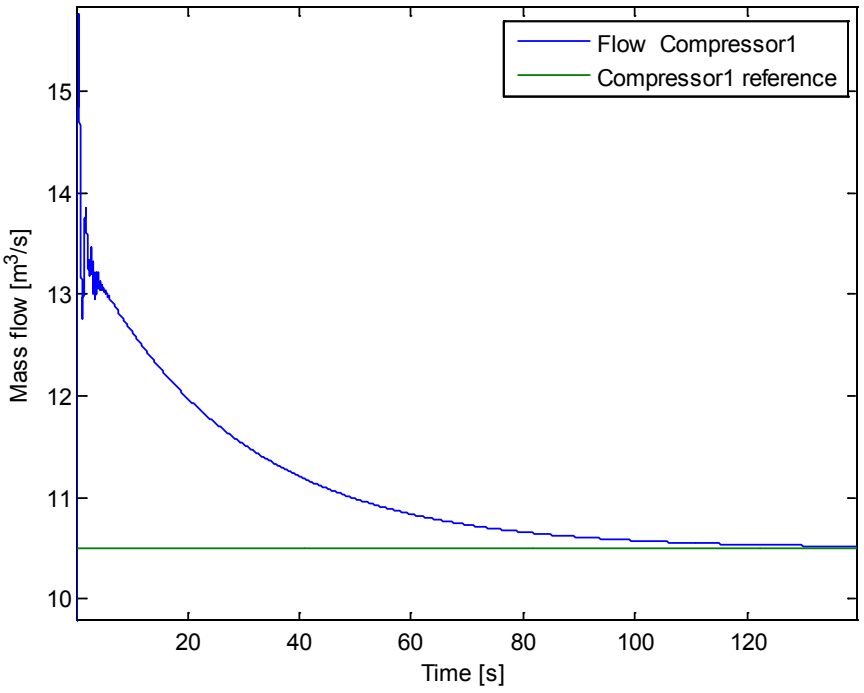

FIGURE 8.15: Flow from compressor 1 with reference plotted

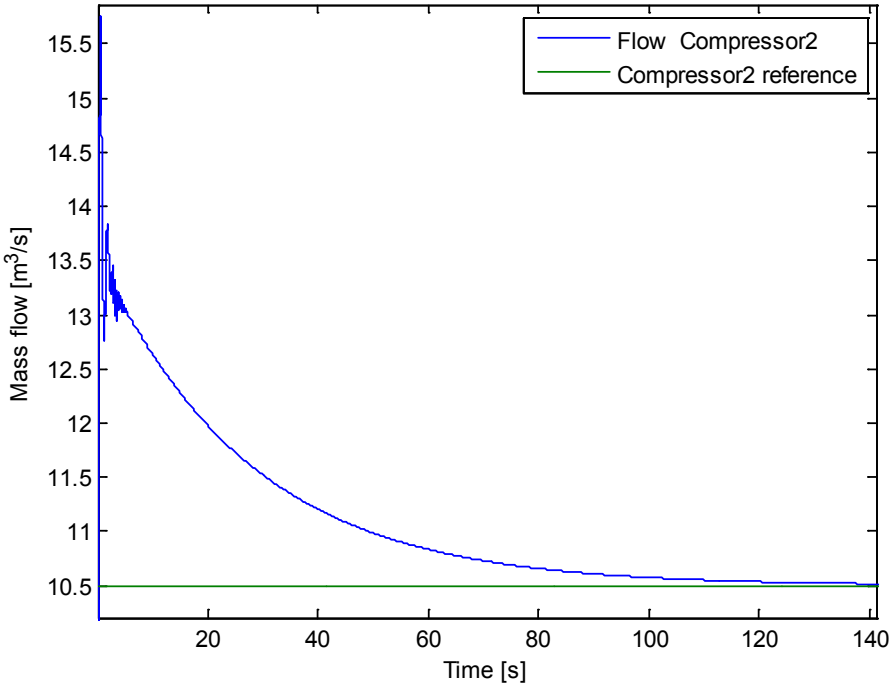

FIGURE 8.16: Flow from compressor 2 with reference plotted

The Figure 8.17 shows the plotted efficiency characteristic and the trajectory which leads

to the calculated references. The plot is given in relation to mass flow and pressure in the plenum. It is seen here that it is not possible to reach the highest efficiency, instead an optimized point is given subject to the constraints.

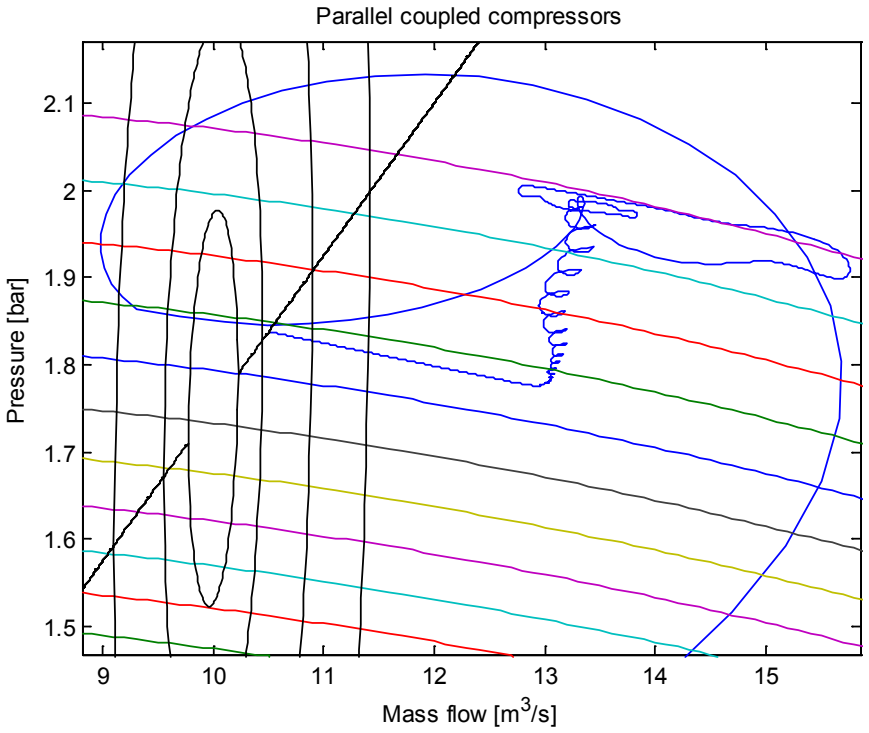

FIGURE 8.17: Plotted pressure rise in relation to mass flow

8.3.3 Simulation three

For the third simulation, a desired flow was set to 19 $[m^3/s]$ and the calculations from the QP resulted in the three set points, 1.66 [bar] and w = w1 = 9.50 $[m^3/s]$. The Figures 8.18, 8.20 and 8.21 show that the desired values does not seem to be reached, only a steady state is reached, but this is not satisfactory. The plotted flows in Figure 8.19 have the same characteristic as in the previous simulations and reaches a steady state.

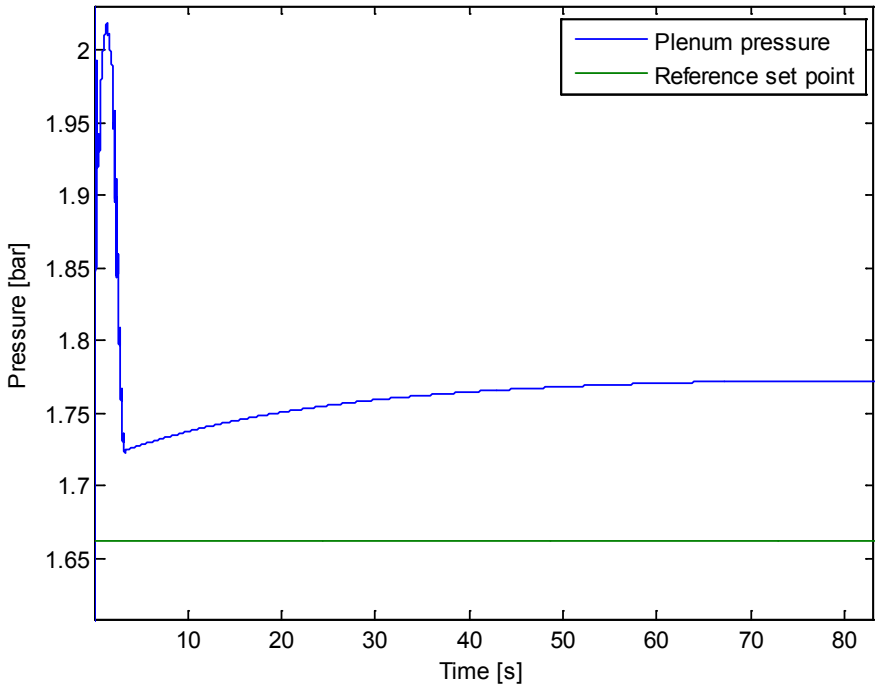

FIGURE 8.18: Pressure in plenum with reference set-point

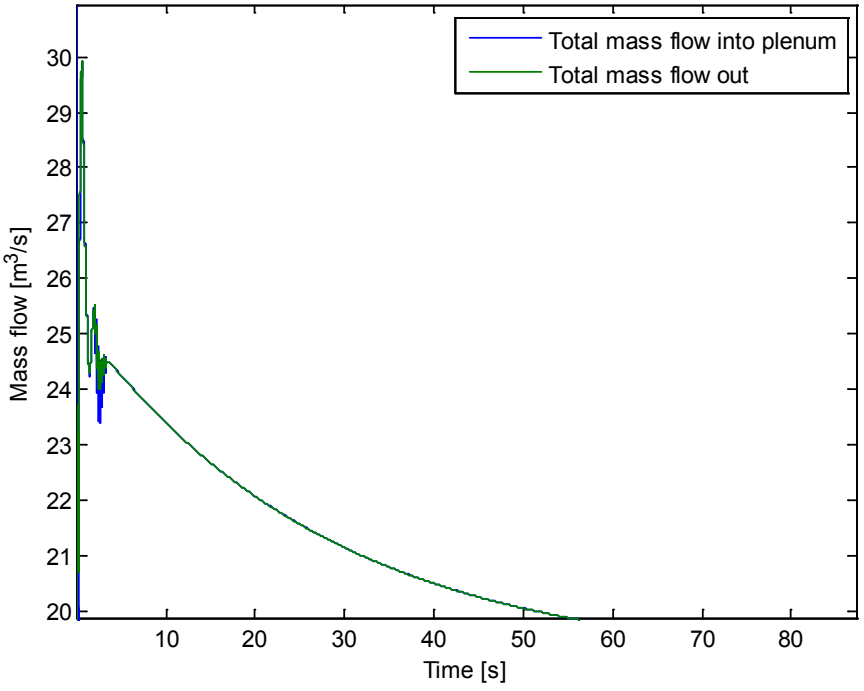

FIGURE 8.19: Plotted mass flow in and out of the system

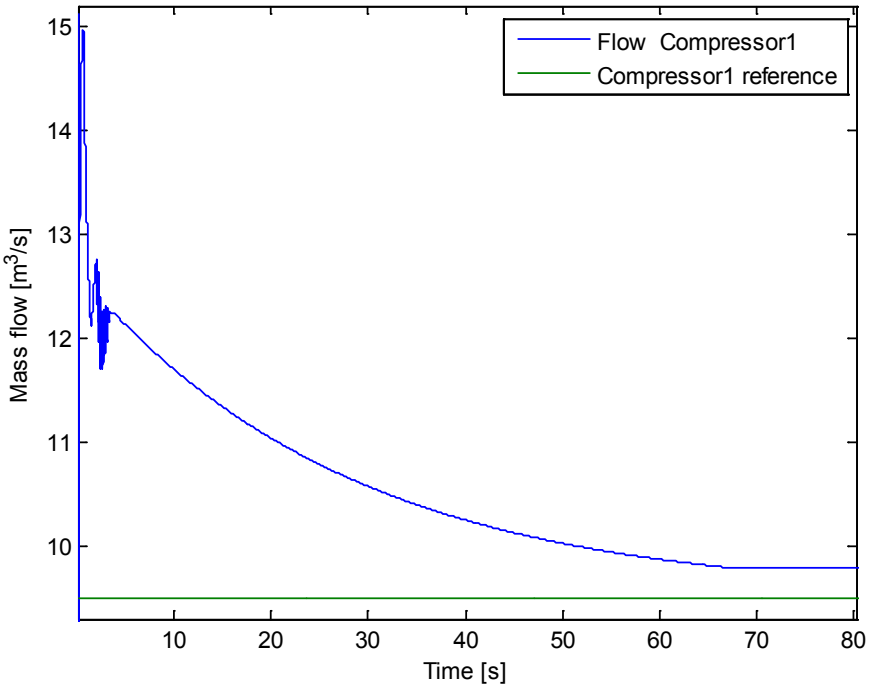

FIGURE 8.20: Flow from compressor 1 with reference plotted

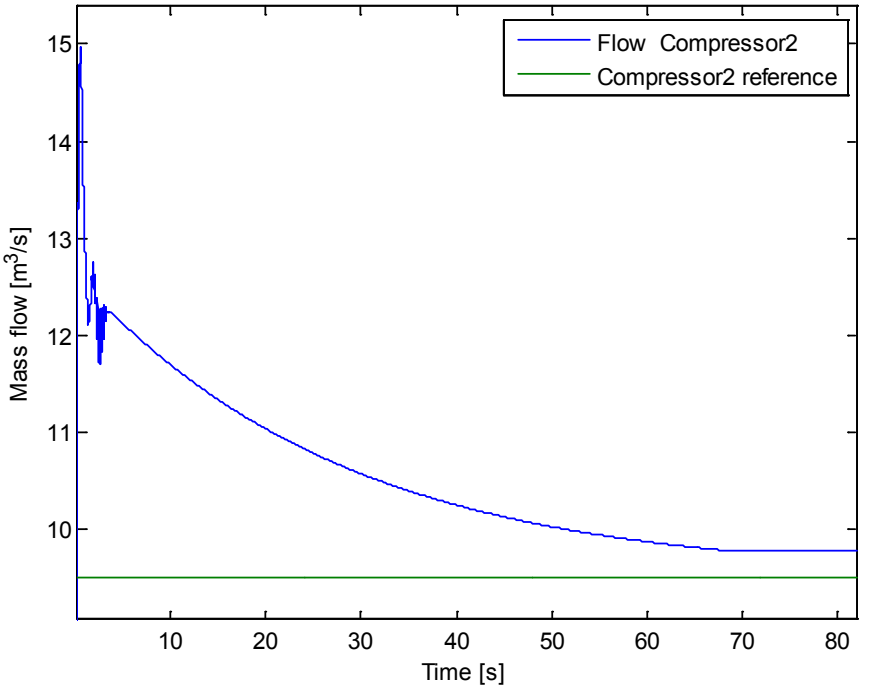

FIGURE 8.21: Flow from compressor 2 with reference plotted

The efficiency plot in Figure 8.22 reaches a good value and is also inside the smallest ellipse, but this has little to say since the wrong value for flow and pressure is reached.

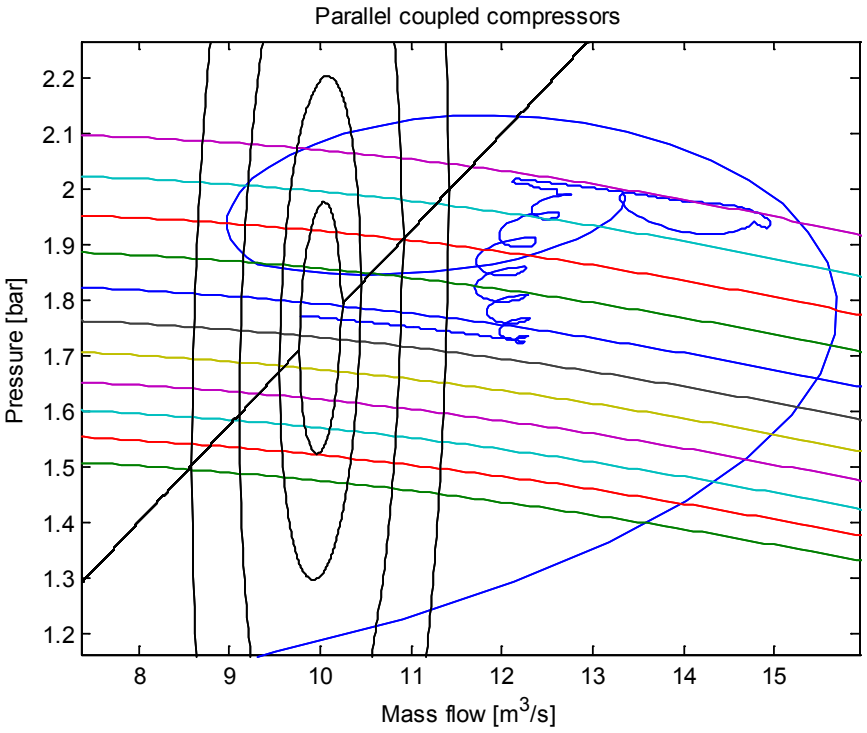

FIGURE 8.22: Plotted pressure rise in relation to mass flow

8.3.4 Simulation four

Now the same set-point is used, as was looked at in the previous subsection, but now the prediction model in the MPC scheme was re-linearized around a different operating point. With both compressors running at a speed of 280 rounds/s.

Now it seems that the desired points of operation are reached in Figures 8.23, 8.25 and 8.26. The total in- and outflow in the plant is plotted in Figure 8.24. The author performed this by testing some points of operation by setting different constant speeds and then linearizing. This might imply a need for re-linearization of the process, when the desired operating point is shifted too far off from the point which was previously linearized about.

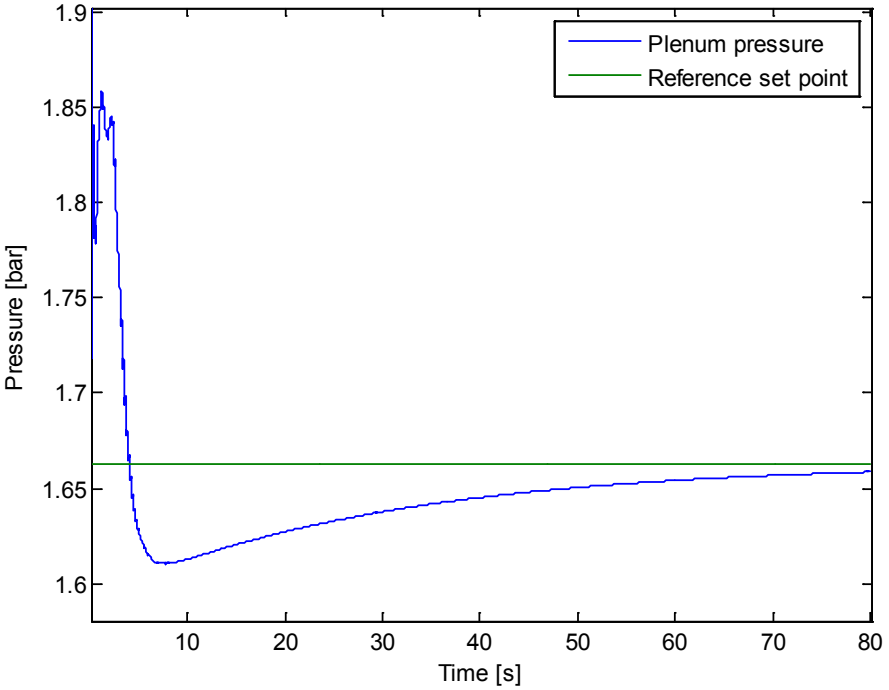

FIGURE 8.23: Pressure in plenum with reference set-point

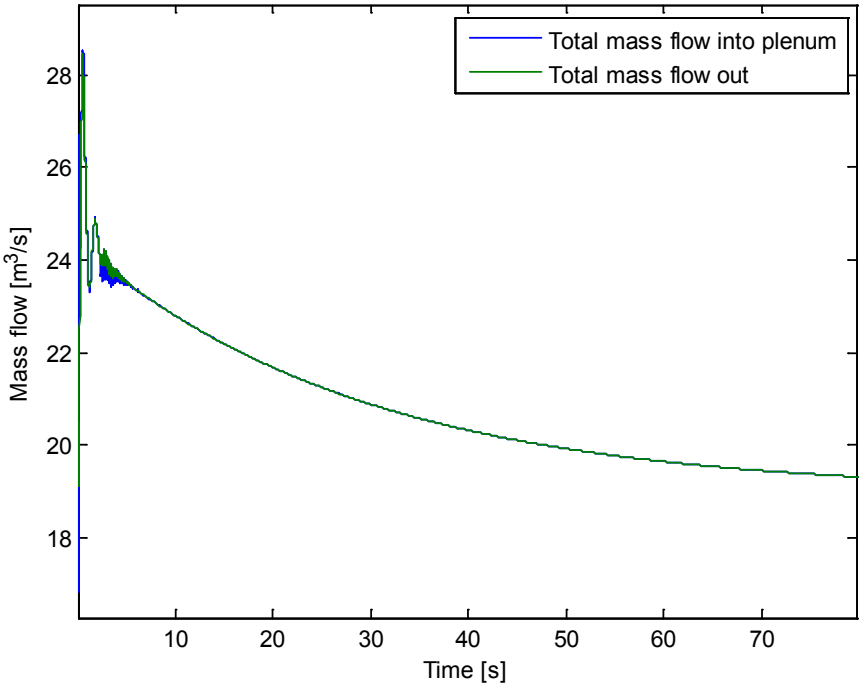

FIGURE 8.24: Plotted mass flow in and out of the system

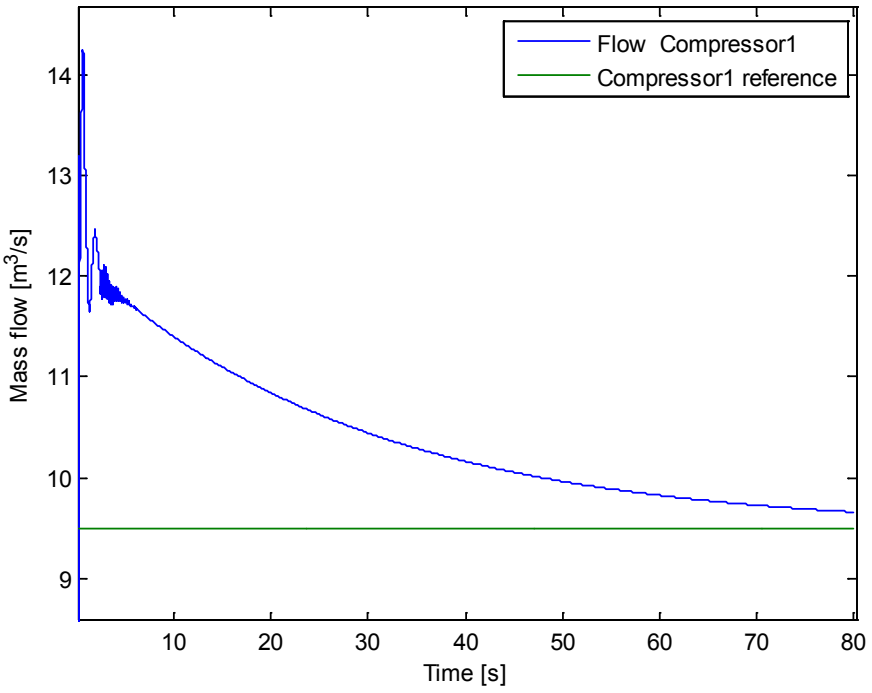

FIGURE 8.25: Flow from compressor 1 with reference plotted

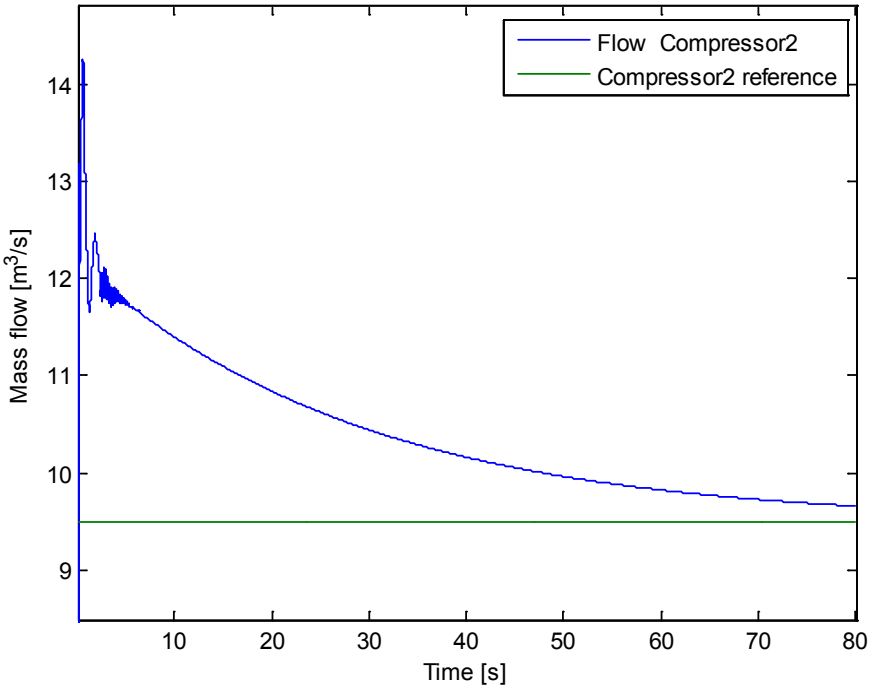

FIGURE 8.26: Flow from compressor 2 with reference plotted

The mass flow and pressure seams to have reached an optimal value in Figure 8.27. Here the trajectory is plotted starting at an initial condition of 1 [bar].

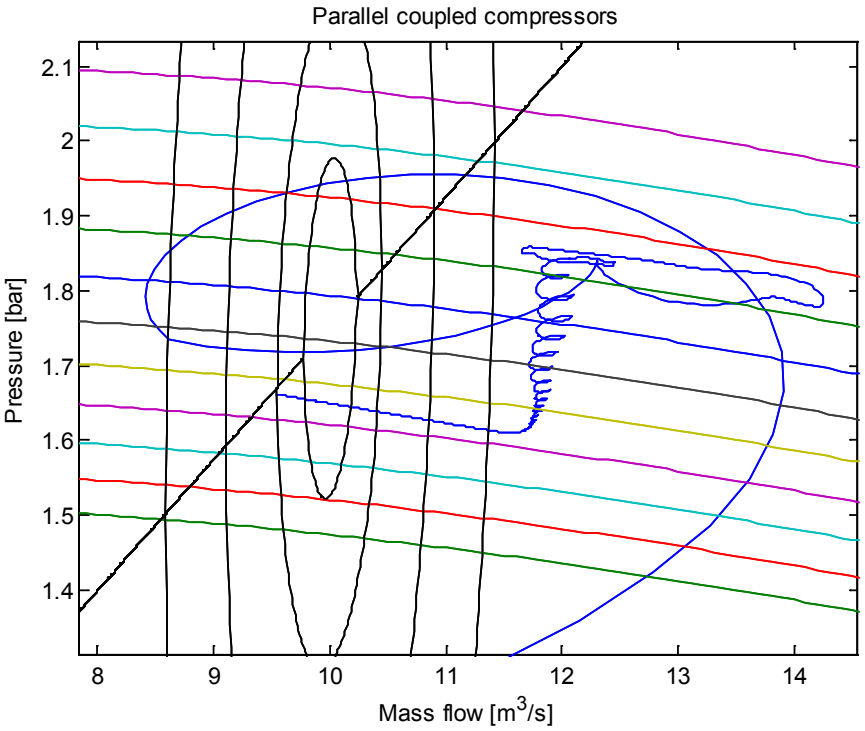

FIGURE 8.27: Plotted pressure rise in relation to mass flow

8.3.5 Simulation five

In this simulation setup two different compressor efficiency characteristics are chosen, which can be seen in the Figures 8.32 and 8.33, together with the simulated trajectory in relation to mass flow and pressure. The given reference points are found in row r_5 of Table 8.2. As is seen in the Figures 8.28 − 8.31 the reference values are reached. The trajectories of the simulation are shown in the Figures 8.32 and 8.33 and here we see that the efficiency plot of both compressors are almost equal as is also the pressure, the flow and the impeller rotational speeds are different.

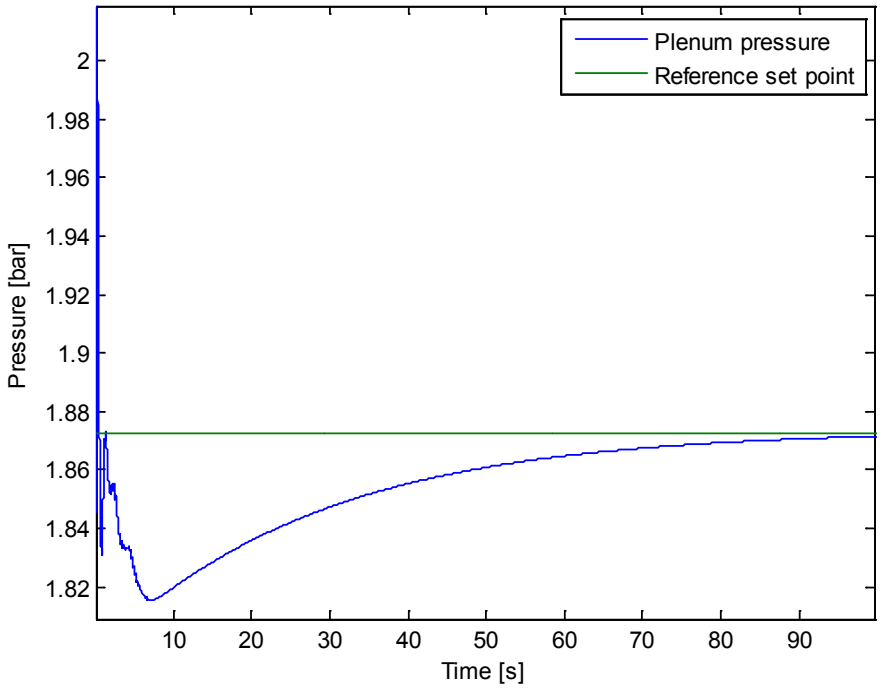

FIGURE 8.28: Pressure in plenum with reference set-point

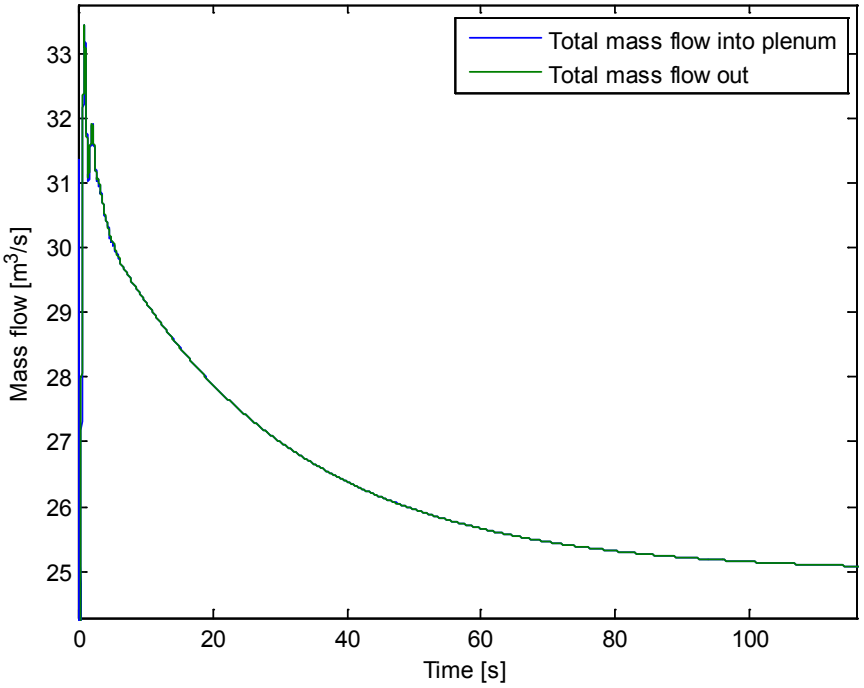

FIGURE 8.29: Plotted mass flow in and out of the system

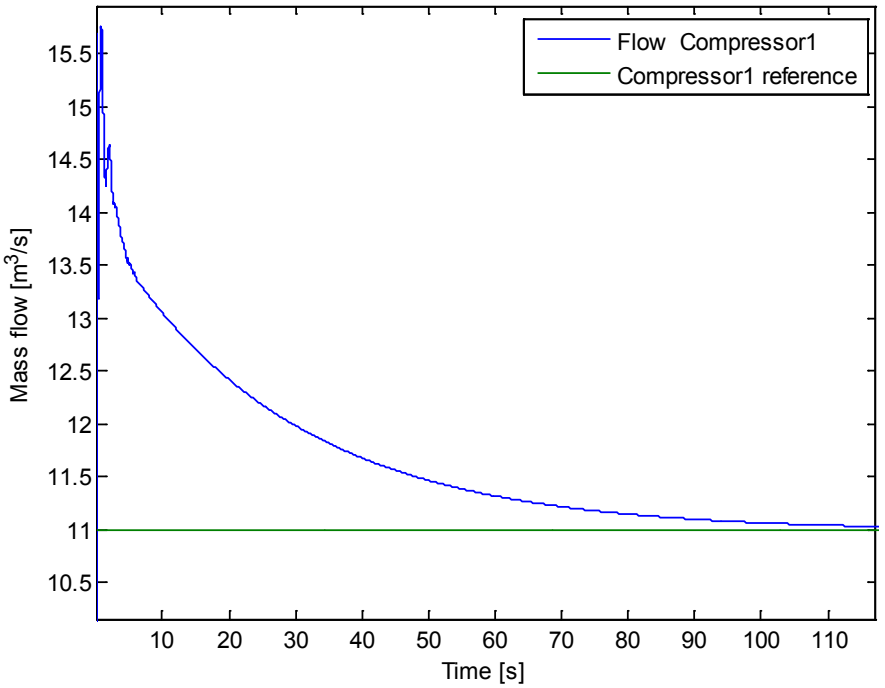

FIGURE 8.30: Flow from compressor 1 with reference plotted

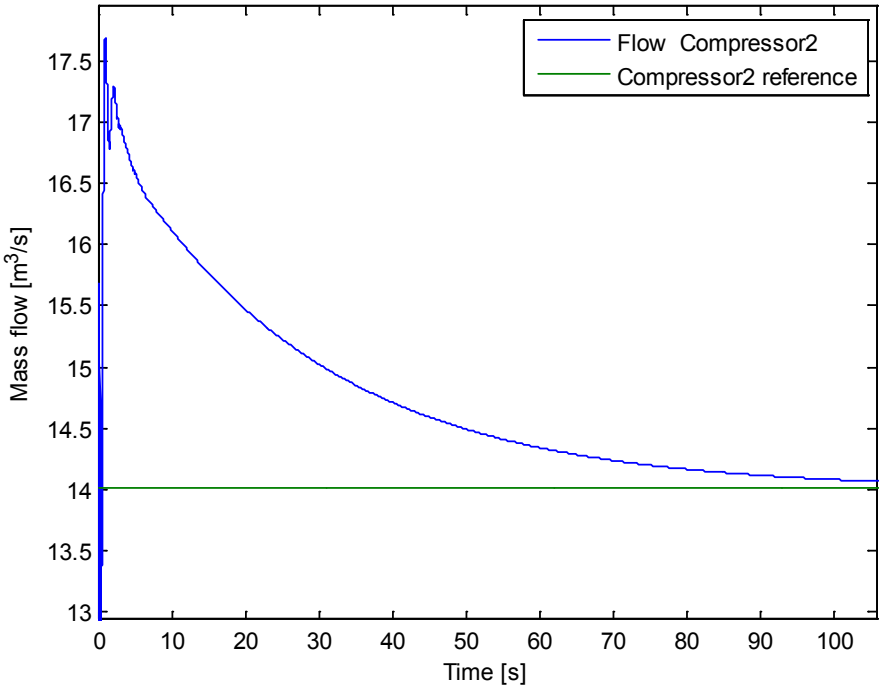

FIGURE 8.31: Flow from compressor 2 with reference plotted

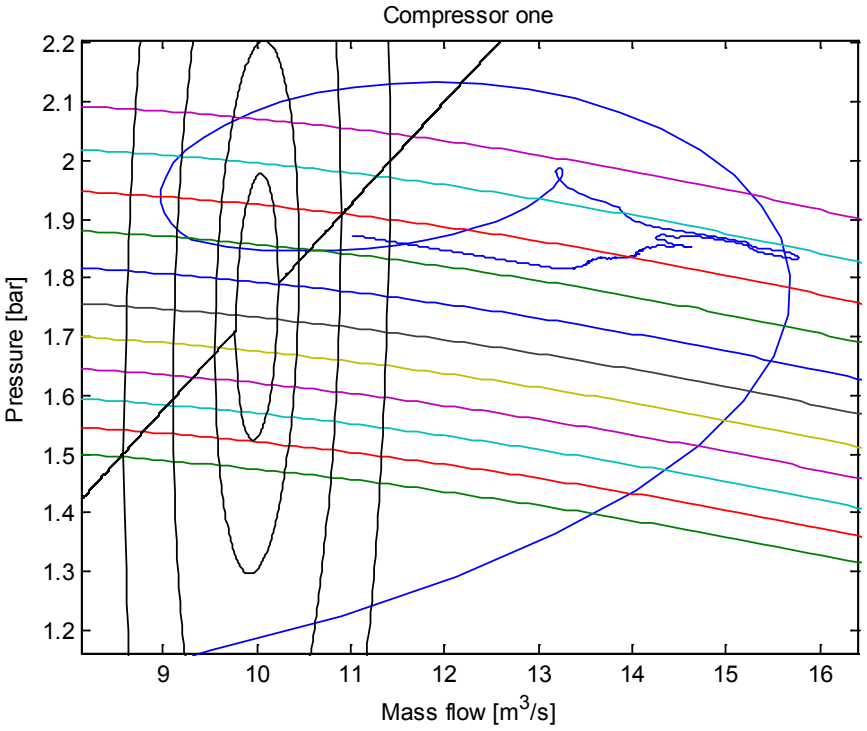

FIGURE 8.32: Plotted pressure rise in relation to mass flow for compressor one

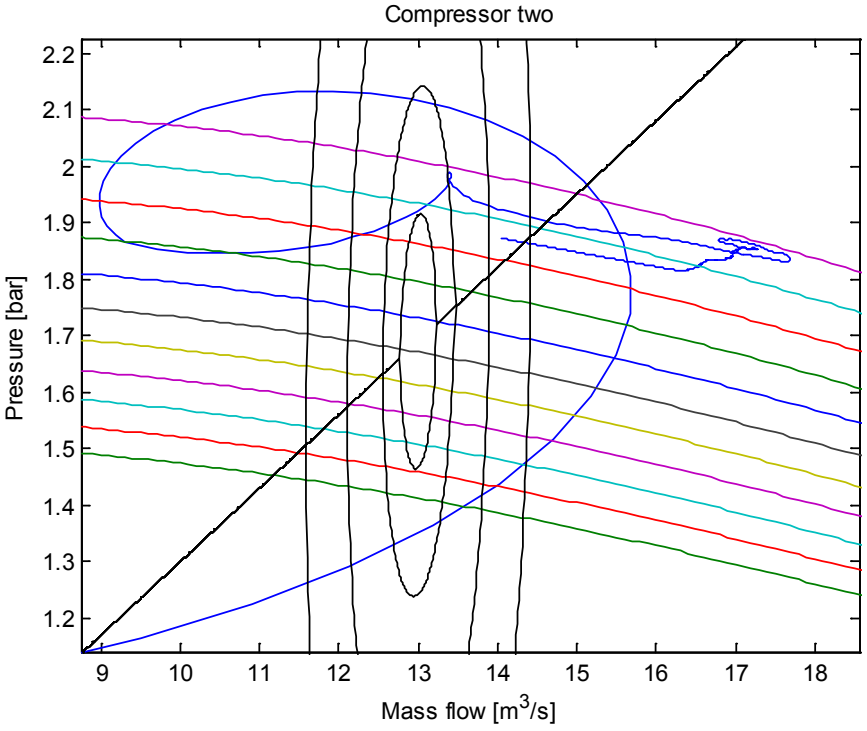

FIGURE 8.33: Plotted pressure rise in relation to mass flow for compressor two

In Figures 8.34 and 8.35, the control outputs from the MPC are shown. In Figure

8.34 the input to the throttle valve is plotted. This is assumed modeled according to a realistic valve, the signal is therefore constrained between $0 \leq u_v \leq 1$ where 1 relate to a fully open valve. This can be seen from the first control input which jumps up to maximum.

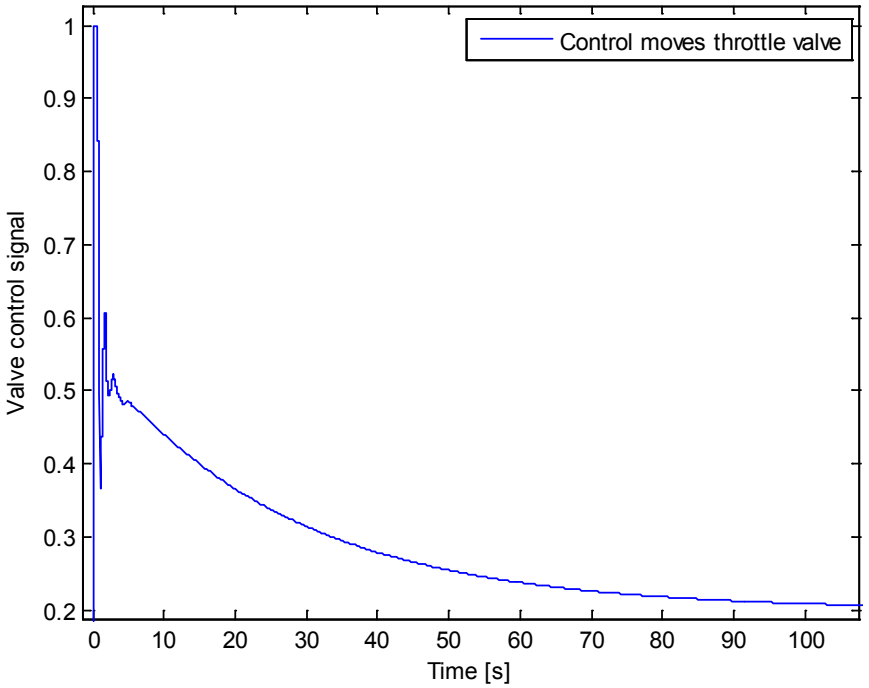

FIGURE 8.34: Plotted control moves for compressor throttle valve

Shown in Figure 8.35 are the control inputs for the impeller. The rotational speeds are given as [rps], and are constrained between $-20 \leq u\_\omega \leq 15$. Since the model is linearized around a constant input of 300 [rps], this is added to the control signal. This finally constrains the impeller for $-280 \leq \omega \leq 315$. Since the two compressors carry different loads the speeds will be different, as is shown in the same figure.

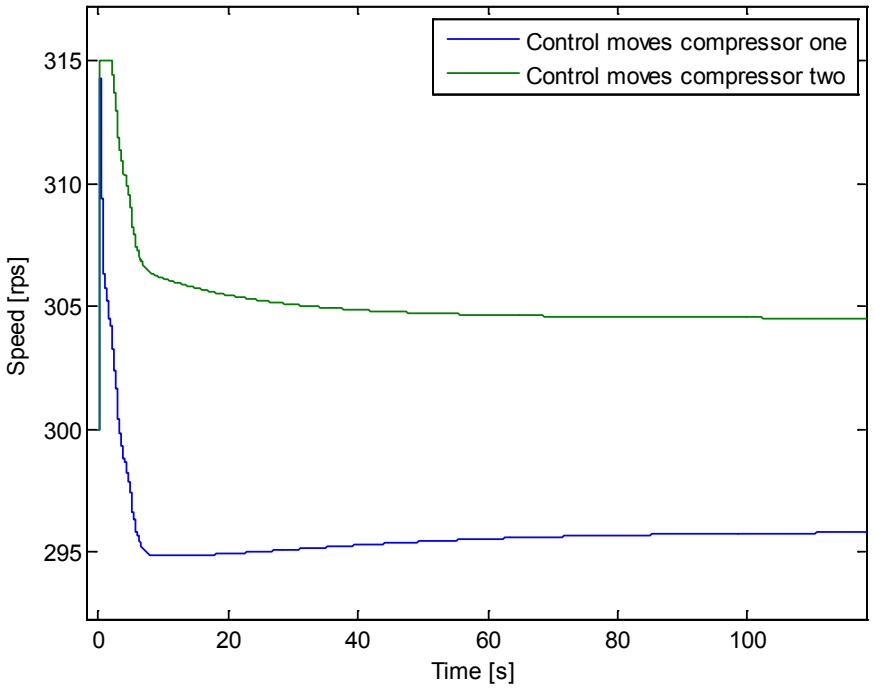

FIGURE 8.35: Plotted control moves for impeller speed on both compressors

Chapter 9

Discussion

The results of this project are presented and discussed in this chapter. Firstly the model consisting of one compressor is looked into. Further the model extension is examined. Lastly the extended model implemented with the model predictive controller is discussed together with the definition of efficiency.

9.1 The one compressor model

This model from Gravdahl and Egeland (1999) is presented in Chapter 3. Here both the dimensional and the non-dimensional model are derived. The compressor characteristic for both the models are presented, and the stability of the model is investigated. This model was tested and simulated in its extent in Oevervaag (2012), together with a surge recycle system. Since some simplifications had to be done, the recycle system was left out in the further development of the model used for load sharing.

9.2 Model extension

The model extension is based on the model of Gravdahl and Egeland (1999). The dimensional form was chosen since it would be easier for the user to recognize the elements in the model in relation to a physical compressor. The pressure in the plenum was decided to be presented in [bar] since the values given in [Pa] were not efficient to handle. To first simplify the model, each compressor map were designed equal to each other. In the last simulations in Chapter 8 the map with the efficiency characteristic was changed. This was done to have a better proof of how the load sharing optimization

would function, and to see if the model predictive controller could handle having different loads on each compressor while still reaching a desired pressure set point.

A simplification was also performed on the model of the performance map. This changed the model of the map to consider only positive values for mass flow. This made the map continuous for both mass flow and impeller rotational speed, and it made it possible to have a continuous simulation. In the load sharing scheme, surge is not included as a problem which needed to be handled. This could be stated since the load sharing is only defined for positive values of mass flow and pressure. Therefore this simplification could be done without further discussion.

To handle the problem with surge dynamics, a solution could be to have the operating point of the two compressors be of equal distance to each other. A discussion of this can be viewed in e.g. the paper of Blotenberg et al. (1984). For this situation on the other hand it would probably be complicated to give optimal points of operation when taking this constraint into consideration. This would imply that for some operating points the compressors would not function optimally.

9.3 Implementation of MPC

The main problem of implementing a functional MPC algorithm, was to understand which operating point the prediction model should be linearized for. The solution here was then to specify a steady state point for each compressor operating in the stable region of the map. This produced a linear model with negative and complex eigenvalues, which was observable and controllable. A control signal was attached to the valve, and one to the velocity control of each impeller.

The next step was to choose weights for the inputs and outputs of the controller. These were selected by trying different values and then seeing from the plots which ones gave the best response. The same was performed when setting the values for the constraints. All the values are shown in the Figures 11 - 13 in the appendices. These screens were taken from the Model Predictive Controller GUI in MATLAB, which was used for producing the MPC object used in the SIMULINK diagram. The MPC1 object can be seen in Appendix B.

No extra controllers was selected, but this could be included in the system as a backup for the MPC. This could be preferable if in a case where the MPC could loose its control input to the process. Each controller would then work according to the last working control signal. For this project on the other hand this was not considered a problem.

9.4 Simulations

As seen in Chapter 8 and the figures presented here the results from the simulations are varying. Working in one operating point close to the linearized plant, it seems easier to reach convergence. When the desired result swayed too far off in the simulation, a new prediction model was found closer to the point of operation which helped in reaching convergence. From this result a re-linearization would have to be performed when the deviation is too large from the desired set point.

9.5 Efficiency

In the beginning there was a problem with finding a useful explanation of how the efficiency islands in the compressor characteristic map was produced. The conclusion was that the map was developed from lab- or on-site tests from which the most effective region was found and calibrated. To solve this problem the idea was first to then make a look up table, with data consisting of which efficiency each mass flow and pressure ratio had. Then it would maybe be possible to input a desired flow, and then a function could choose the optimal pressure ratio. This solution was researched, but in the end this was not the preferred solution since there could be some implementation issues.

A different solution was made, since this was a convex set up and could be handled by a QP solver. The efficiency islands was found to be similar to ellipses or circles on the performance map. An assumption was made that the equation (6.10), would assume the same characteristic as the real islands in Figure 6.1. To get set points which are used in the parallel model with the controller, the equation was extended to equation (6.17). Here it is possible to choose the center points of the efficiency curves by adjusting the coordinates in the equation to fit the center point the real map. This definition of efficiency is a great simplification of the reality, and this solution can not be assumed to be overall correct.

Chapter 10

Conclusion

This thesis has mainly consisted of developing and analyzing the centrifugal compressor system and an extension to this including two compressors connected in parallel with a common discharge. This parallel model is used for designing a load sharing scheme including model predictive control.

10.1 Concluding remarks

The results of this work has has lead to the conclusion that MPC can in some cases be used for controlling a nonlinear parallel centrifugal compressor plant operating in the stable region of the compressor map, taking into consideration that the prediction model is good. This MPC scheme was constructed as a simplification for the control design of such systems.

The model created here shows the possibilities of controlling several compressors connected in parallel with a direct feed through from the model predictive controller, without the use of e.g. PI controllers. It can be stated that a certain range of operation is possible considering mass flow and pressure ratio, for each compressor in the plant with either equal or non equal compressor performance maps. It is on the other hand no conclusions that can be drawn about the specific range of which each compressor should stay inside to guarantee that the requirements are reached, before one would have to linearize the plant at a different operating point.

Further results have been presented, describing an approximated compressor map. This gives rise to a convex problem which can be solved by quadric programming. The solution to this QP algorithm giving the assumed optimal set points for the plant, which

is proved valid for problems without constraints. Adding equality constraints on the other hand the solution will not be assumed to be optimal.

10.2 Contributions

To the authors knowledge no continuous efficiency island definition has been developed to the intent of giving optimal reference set points for pressure and mass flow. The work also produced a parallel centrifugal compressor system model including model predictive control, which is used for load sharing.

10.3 Further work

The scope of this work only extended to investigating how MPC can be used for controlling a nonlinear centrifugal compressor plant. A conclusion was made stating that seemingly a re-linearization had to be performed on the plant to increase the area of operation. Further work can then consist of implementing a continuous procedure which re-linearizes the plant if it should deviate too far off from the desired reference trajectory.

Another issue which could be investigated would be to further add dynamics to the model, describing the moment of inertia of the impeller and the drive. Including the starting and stopping costs of each compressor could help to analyze how the total savings of the entire network would best be handled. In relation to this scheme presented in this thesis, checking how fuel can be saved using this load sharing algorithm would be necessary to figure out if this is a cost effective routine.

A different method of controlling a compressor network could be to use nonlinear model predictive control. With the plant being both dimensional and non-dimensional, this procedure would be an interesting field of research since this type of plant yields severe nonlinearities in different points of operation.

Regarding the efficiency islands used in this thesis, a better method could be developed to improve the accuracy of the map and how this could be related to an actual compressor performance map, used for finding the optimal area of efficiency. Also a method for finding the efficiency of a compressor when running in real time could be investigated to help adjusting the set points.

As stated in this work, surge is not considered a problem here this system stability could be analyzed using recycle- or blow out valves.

Bibliography

James Tobin. Natural gas compressor stations on the interstate pipeline network: Developments since 1996. 2007.

Forced performance turbochargers. Forced performance turbochargers @ONLINE, 2013. URL http://store.forcedperformance.net/merchant2/merchant.mvc?Screen=Info_Turbofailure.

Thomas .F. Oevervaag. *An introduction to compressor modeling and load sharing*. 2012.

E. Greitzer. Surge and rotating stall in axial flow compressors, part i: Theoretical compression system model. *Journal of Engineering for Power*, 98:190–198, 1976.

Jan T. Gravdahl and Olav Egeland. *Compressor Surge and Rotating Stall: Modeling and Control*. London: Springer Verlag, 1999.

E.S. Menon. *Gas Pipeline Hydraulics*. Taylor & Francis, 2005.

Eric Fahlgren. Not2fast @ONLINE, 2013. URL http://www.not2fast.com/turbo/maps/all.html.

W. Blotenberg, H.O. Jeske, and H. Voss. Design, control and startup features of three parallel-working propane compressors each having three stage groups. In *Proceedings of the... Turbomachinery Symposium*, volume 13, page 39. Gas Turbine Laboratories, Department of Mechanical Engineering, Texas A & M University, 1984.

JPM Smeulers, WJ Bournan, and HA Van Essen. Model predictive control of compressor installations. In *IMECHE CONFERENCE TRANSACTIONS*, volume 6, pages 555–566. MECHANICAL ENGINEERING PUBLICATIONS, 1999.

NaturalGas.org. Background, November 2012. URL http://www.naturalgas.org/overview/background.asp.

Phil Ferber, Ujjal Basu, Ganesh Venkataramanan, Mary Goodreau, and Peter Linden. Gas pipeline optimization. 1999.

PilotLight. Passing gas, 2013. URL http://www.fscc-online.com/pilotlight.html#anchor1492704.

L. Magni, D.M. Raimondo, and F. Allgöwer. *Nonlinear Model Predictive Control: Towards New Challenging Applications*. Springer, 2009.

O. Egeland and J.T. Gravdahl. *Modeling and Simulation for Automatic Control*. Sit Tapir Trondheim, 2002.

Meherwan P. Boyce. chemicalprocessing @ONLINE, 2012. URL http://www.chemicalprocessing.com/experts/answers/2008/045.html.

Albert Ruprecht, Frank Ginter, and Ralf Neubauer. Numerical simulations of unsteady flow instabilities (rotating stall) in pumps. 2005.

Frank M. White. *Fluid mechanics*. McGraw-Hill New York, 6th. edition, 2008.

E. Greitzer. Surge and rotating stall in axial flow compressors, part ii: Experimental results and comparison with theory. *Journal of Engineering for Power*, 98:199–217, 1976b.

K. Louie, H. Clark, and P. C. D. Newton. Analysis of differential equation models in biology: a case study for clover meristem populations. *New Zealand Journal of Agricultural Research*, 41:567–576, 1998.

F. K. Moore and E. M. Greitzer. A Theory of Post-Stall Transients in Axial Compression Systems: Part IDevelopment of Equations. *Journal of Engineering for Gas Turbines and Power-transactions of The Asme*, 108, 1986. doi: 10.1115/1.3239887.

N. Uddin and J.T. Gravdahl. Bond graph modeling of centrifugal compressor system. 2012.

H.K. Khalil. *Nonlinear Systems*. Prentice Hall, 2002.

C.T. Chen. *Linear System Theory and Design*. Oxford University Press, 2009.

Lars Imsland. Introduction to model predictive control. 2007.

Bjarne A. Foss. Linear quadratic control. 2007.

J. M. Maciejowski. *Predictive Control with Constraints*. Pearson Education Limited, 2002.

Mark Cannon. *C21 Model Predictive Control*. Oxford University, Oxford, United Kingdom, 2012.
Available: http://www.eng.ox.ac.uk/ conmrc/mpc/mpc1-2.pdf.

Alberto Bemporad, Manfred Morari, Vivek Dua, and Efstratios N. Pistikopoulos. The explicit linear quadratic regulator for constrained systems. *Automatica*, 38(1):3 – 20, 2002.

M.P. Boyce. *Centrifugal Compressors: A Basic Guide*. PennWell, 2003.

J. Nocedal and S.J. Wright. *Numerical optimization*. Springer series in operations research. Springer, 2006.

AE Nisenfeld and CH Cho. Parallel compressor control: What should be considered. *Hydrocarbon Processing*, pages 147–150, 1978.

Jan Tommy Gravdahl, Olav Egeland, and Svein Ove Vatland. Drive torque actuation in active surge control of centrifugal compressors. *Automatica*, 38(11):1881 – 1893, 2002.

Appendix A.
The one unit setup

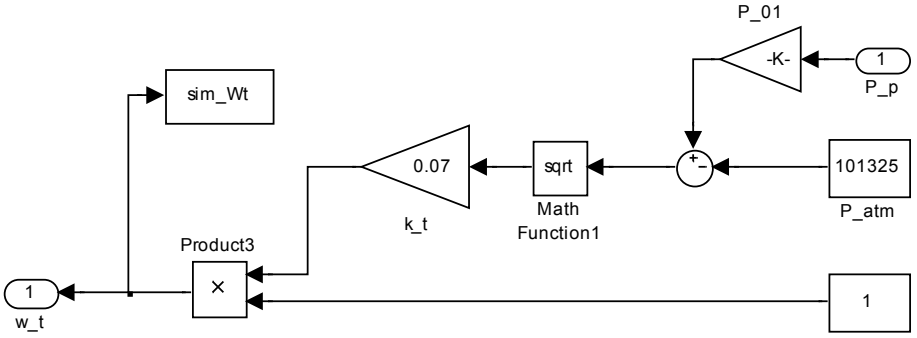

FIGURE 1: Throttle system for the single compressor, Oevervaag (2012)

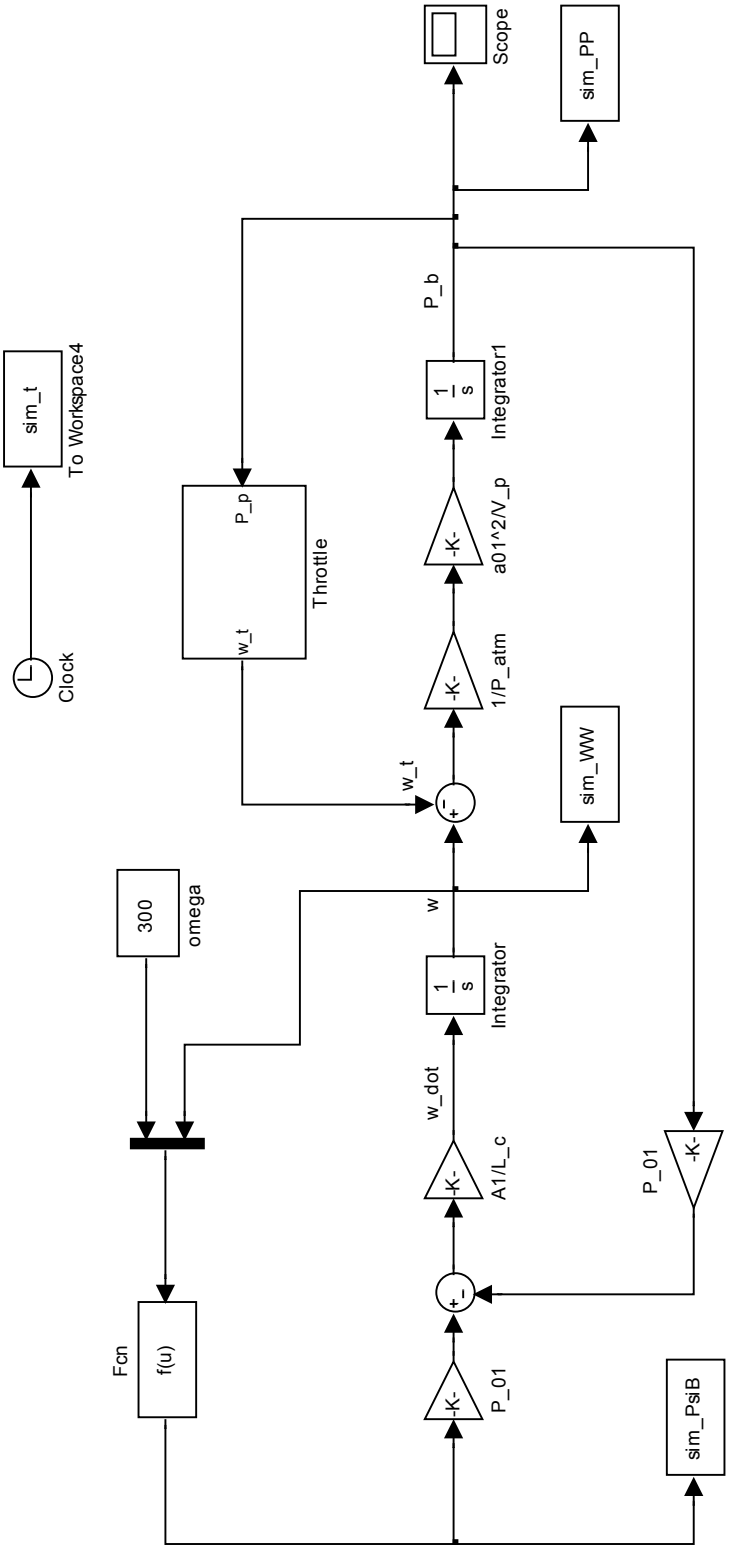

FIGURE 2: The single compressor system, Oevervaag (2012)

Appendix B.
The parallel coupled plant

```
%% Script for linearizing the parallel compressor plant
% Author Thomas F. Oevervaag

 clear all
 clc


omega1=300;
omega2=300;
omega_c1=omega1;
omega_c2=omega2;

dh1=0.095;
ds1=0.210;
d1=(dh1^2+ds1^2)^0.5;
r1=3*d1/2;
d2=0.557;
r2=4*d2/2;

rho1=1.2;
A1=0.00956;
beta1b=40*pi/180;
beta2b=90*pi/180;
nblades=22;
sigma=1-2/(nblades);
ws=10;
kf=5;
cp=2064;
kappa=1.3;
T01=293;
%alpha=(cot(beta1b)/(rho1*A1*r1));
alpha=50;
mu = 0.9091;

%=========================
a0=340;
Vp=1;
% A1=pi*(0.07/2)^2;
```

```
Lc=1;
p0=1e5;
kt=0.5;
ut=0.1;
p=1e5;
%=======================


sim('ParallelCouplingLinearize.mdl')
sys = 'ParallelCouplingLinearize';
load_system(sys);

opspec = operspec('ParallelCouplingLinearize');

op1 = findop('ParallelCouplingLinearize',opspec);

sys1 = linearize('ParallelCouplingLinearize',op1);

op2 = findop('ParallelCouplingLinearize',1);

sys2 = linearize('ParallelCouplingLinearize',op2);

op = operspec('ParallelCouplingLinearize');


Ob1 = obsv(sys1);
unob1 = length(sys1.a)-rank(Ob1)
Co1 = ctrb(sys1);
unco1 = length(sys1.a)-rank(Co1)


Ob2 = obsv(sys2);
unob2 = length(sys2.a)-rank(Ob2)
Co2 = ctrb(sys2);
unco2 = length(sys2.a)-rank(Co2)


WW=sim_WW.signals.values;
WW1=sim_WW1.signals.values;
PP=sim_PP.signals.values;
Wt=sim_Wt.signals.values;
time=sim_t.signals.values;
PSI1=sim_PsiB.signals.values;
PSI2=sim_PsiB1.signals.values;

plot(WW,PSI1,WW1,PSI2,WW,PP,WW1,PP)

E1=eig(sys1.a)

E2=eig(sys2.a)
```

```
%% MPC controller object
% Script produced from MATLAB, mpctool
%
```

```
>> MPC1

MPC object :
---------------------------------------------
Sampling time:      0.2
Prediction Horizon: 20
Control Horizon:    6
Model:
          Plant: [4x3 ss]
        Nominal: [1x1 struct]
    Disturbance: []
          Noise: []

        Output disturbance model: default method (type "getoutdist(MPC1)" for details)

Details on Plant model:
                                      --------------
      3  manipulated variable(s)   -->|  4 states  |
                                      |            |-->  4 measured output(s)
      0  measured disturbance(s)   -->|  3 inputs  |
                                      |            |-->  0 unmeasured output(s)
      0  unmeasured disturbance(s) -->|  4 outputs |
                                      --------------
Weights:
        ManipulatedVariables: [1 0 0]
    ManipulatedVariablesRate: [0.1000 0.1000 0.1000]
           OutputVariables: [10 0 2 2]
                       ECR: 1000000

Constraints:
0 <= ParallelCouplingLinearize/u_v <= 1,
ParallelCouplingLinearize/u_v/rate is unconstrained,
 -Inf <= P <= 3
-20 <= ParallelCouplingLinearize/omega <= 15,
ParallelCouplingLinearize/omega/rate is unconstrained,
ParallelCouplingLinearize/flow is unconstrained,
-20 <= ParallelCouplingLinearize/omega1 <= 15,
ParallelCouplingLinearize/omega1/rate is unconstrained,
flow1 is unconstrained,
```

```
%% Script for running the parallel compressor plant
% The object MPC1 must be included in the workspace before running
% Author Thomas F. Oevervaag

sim('ParallelCouplingLinearizeHANDINN.mdl')
WW = sim_WW.signals.values;
WW1 = sim_WW1.signals.values;
PP = sim_PP.signals.values;
Wt = sim_Wt.signals.values;
time = sim_t.signals.values;
PSI1 = sim_PsiB.signals.values;
PSI2 = sim_PsiB1.signals.values;
u_v = u_v.signals.values;
```

```
u_omega1 = u_omega1.signals.values;
u_omega2 = u_omega2.signals.values;

t=length(time);


%% ========================
% Speed and mass flow vectors

speed = 14000:500:19000; %rpm
w = (0.1:0.1:30);
w2 = 0:0.01:20;

%========================
v = length(speed);
n = length(w);
f = length(w2);

PSII = zeros(n,1);
my1 = zeros(n,1);
Psi=zeros(n,v);
w1=zeros(n,v);

%% ========================
% Building the speedlines

P_pref(1:t) = Pref;
WWref(1:t)=Wref;
WW1ref(1:t)=W1ref;
WWtot=WW+WW1;

for k=1:v
    omega = speed(k)/60;

    for i = 1:n

    my1(i) = sigma*(1-cot(beta2b)/(rho1*A1*r1)*w(i)/omega);

    PSII(i) = (1+(my1(i)*r2^2*omega^2 - ((r1^2)/2)*(omega - alpha * w(i))^2 ...
              - kf*w(i)^2)/(cp*T01))^(kappa/(kappa - 1));

    end

    Psi(:,k)=PSII;
    w1(:,k)=w;

end

for t=1:f

y1(t) = 0.175*w2(t) + sqrt(0.05-(w2(t)-10)^2);
y2(t) = 0.175*w2(t) - sqrt(0.05-(w2(t)-10)^2);

y3(t) = 0.175*w2(t) + sqrt(0.2-(w2(t)-10)^2);
y4(t) = 0.175*w2(t) - sqrt(0.2-(w2(t)-10)^2);
```

```
y5(t) = 0.175*w2(t) + sqrt(0.8-(w2(t)-10)^2);
y6(t) = 0.175*w2(t) - sqrt(0.8-(w2(t)-10)^2);

y7(t) = 0.175*w2(t) + sqrt(2-(w2(t)-10)^2);
y8(t) = 0.175*w2(t) - sqrt(2-(w2(t)-10)^2);

%----------------------------------

y11(t) = 0.13*w2(t) + sqrt(0.05-(w2(t)-13)^2);
y21(t) = 0.13*w2(t) - sqrt(0.05-(w2(t)-13)^2);

y31(t) = 0.13*w2(t) + sqrt(0.2-(w2(t)-13)^2);
y41(t) = 0.13*w2(t) - sqrt(0.2-(w2(t)-13)^2);

y51(t) = 0.13*w2(t) + sqrt(0.8-(w2(t)-13)^2);
y61(t) = 0.13*w2(t) - sqrt(0.8-(w2(t)-13)^2);

y71(t) = 0.13*w2(t) + sqrt(2-(w2(t)-13)^2);
y81(t) = 0.13*w2(t) - sqrt(2-(w2(t)-13)^2);

end

figure(1)
plot(WW,PP,w,Psi(:,:))
hold on
plot(w2,y1,'k',w2,y2,'k',w2,y3,'k',w2,y4,'k');
hold on
plot(w2,y5,'k',w2,y6,'k',w2,y7,'k',w2,y8,'k');
title('Compressor one');
xlabel('Mass flow [m^3/s]');
ylabel('Pressure [bar]');
%
figure(2)
plot(WW1,PP,w,Psi(:,:))
hold on
plot(w2,y11,'k',w2,y21,'k',w2,y31,'k',w2,y41,'k');
hold on
plot(w2,y51,'k',w2,y61,'k',w2,y71,'k',w2,y81,'k');
title('Compressor two');
xlabel('Mass flow [m^3/s]');
ylabel('Pressure [bar]');
%
figure(3)
plot(time,WW,time,WWref)
xlabel('Time [s]');
ylabel('Mass flow [m^3/s]');
legend('Flow  Compressor1','Compressor1 reference')
%
figure(4)
plot(time,WW1,time,WW1ref)
xlabel('Time [s]');
ylabel('Mass flow [m^3/s]');
legend('Flow  Compressor2','Compressor2 reference')
%
```

```
figure(5)
plot(time,PP,time,P_pref)
xlabel('Time [s]');
ylabel('Pressure [bar]');
legend('Plenum pressure','Reference set point')
%
figure(6)
plot(time,WWtot,time,Wt)
xlabel('Time [s]');
ylabel('Mass flow [m^3/s]');
legend('Total mass flow into plenum','Total mass flow out')
%
figure(7)
plot(time,u_omega1,time,u_omega2)
xlabel('Time [s]');
ylabel('Speed [rps]');
legend('Control moves compressor one','Control moves compressor two')
%
figure(8)
plot(time,u_v)
xlabel('Time [s]');
ylabel('Valve control signal');
legend('Control moves throttle valve')
%

clear WWref WW1ref P_pref
```

```
%% One compressor setup
% Script for finding operating points
% Author Thomas F. Oevervaag

syms p_p w;

x = [p_p ; w ; 1];

H=[2 -2*0.175 0 ;-2*0.175 2*(1+0.175^2) 0 ;0 0 200];

f = [0 -20 0]';

F = 0.5*x'*H*x + f'*x;


opts = optimset('Algorithm','active-set','Display','off');

lb = [0 0]; % Lower bounds
ub = [3 15]; % Upper bounds


[x,fval,exitflag,output,lambda] = ...
    quadprog(H,f,[],[],[],[],lb,ub,[],opts);

p_p = x(1);
w = x(2);
```

```
%% Parallel connected compressors
% Script for finding operating points
% Author Thomas F. Oevervaag
syms  P_p w w1;

x = [P_p; w; w1; 1]

opts = optimset('Algorithm','active-set','Display','off');

lb = zeros(3,1); % Lower bounds
ub = [2.1 15 15]; % Upper bounds


H2 = [4 -2*0.175 -2*0.175 0; -2*0.175 2*(1+0.175^2) 0 0;...
    -2*0.175 0 2*(1+0.175^2) 0; 0 0 0 200]
f2 = [0;-20;-20;0]

Aeq = [0 1 1 0];
beq = [20];


[x,fval,exitflag,output,lambda] = ...
    quadprog(H2,f2,[],[],Aeq,beq,lb,ub,[],opts);


Pref=x(1);
Wref=x(2);
W1ref=x(3);
```

```
%% Script for displaying efficiency curves
% on the compresssor characteristic
% Author Thomas F. Oevervaag


%% ========================
% Speed and mass flow vectors

speed = 14000:500:19000;
w = (0.1:0.1:30);
w2 = 0:0.01:20;

%========================
v = length(speed);
n = length(w);
f = length(w2);

PSII = zeros(n,1);
my1 = zeros(n,1);
Psi=zeros(n,v);
w1=zeros(n,v);

%% ========================
```

```
% Building the speedlines

for k=1:v
    omega = speed(k)/60;

    for i = 1:n

    my1(i) = sigma*(1-cot(beta2b)/(rho1*A1*r1)*w(i)/omega);

    PSII(i) = (1+(my1(i)*r2^2*omega^2 - ((r1^2)/2)*(omega - alpha * w(i))^2 ...
              - kf*w(i)^2)/(cp*T01))^(kappa/(kappa - 1));

    end

    Psi(:,k)=PSII;
    w1(:,k)=w;

end

%% ========================
% Making the vectors for displaying efficiency

for t=1:f

y1(t) = 0.175*w2(t) + sqrt(0.05-(w2(t)-10)^2);
y2(t) = 0.175*w2(t) - sqrt(0.05-(w2(t)-10)^2);

y3(t) = 0.175*w2(t) + sqrt(0.2-(w2(t)-10)^2);
y4(t) = 0.175*w2(t) - sqrt(0.2-(w2(t)-10)^2);

y5(t) = 0.175*w2(t) + sqrt(0.8-(w2(t)-10)^2);
y6(t) = 0.175*w2(t) - sqrt(0.8-(w2(t)-10)^2);

y7(t) = 0.175*w2(t) + sqrt(2-(w2(t)-10)^2);
y8(t) = 0.175*w2(t) - sqrt(2-(w2(t)-10)^2);

end


figure(1)
plot(w,Psi(:,:));
hold on
plot(w2,y1,'k',w2,y2,'k',w2,y3,'k',w2,y4,'k');
hold on
plot(w2,y5,'k',w2,y6,'k',w2,y7,'k',w2,y8,'k');
axis([5 20 1 2.5])
title('Efficiency Plot');
xlabel('w [m^3/s]');
ylabel('\Psi_c');
```

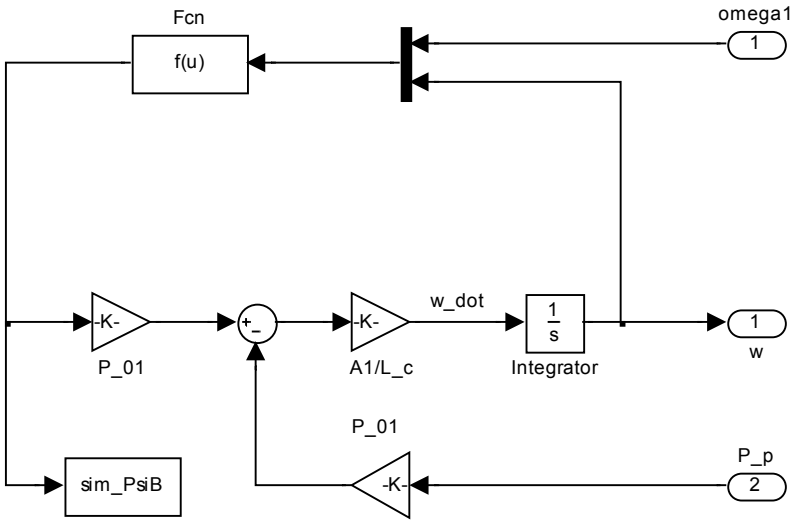

FIGURE 3: Compressor one in the parallel system

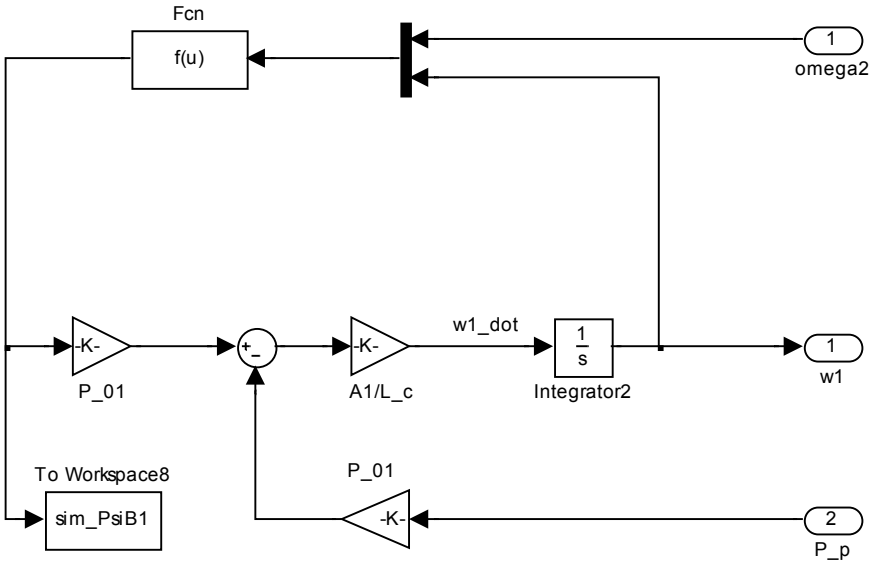

FIGURE 4: Compressor two in the parallel system

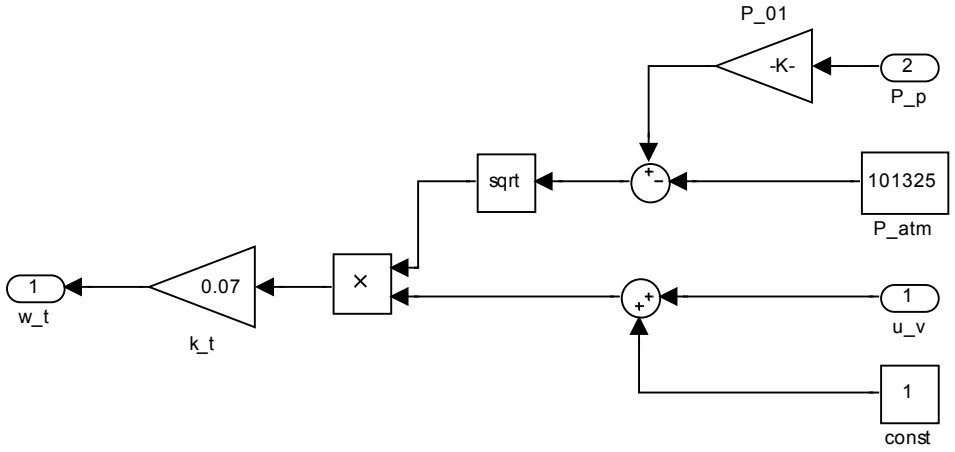

FIGURE 5: Throttle system for the parallel model

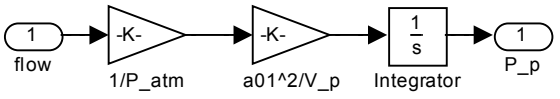

FIGURE 6: Plenum modeled for the parallel system

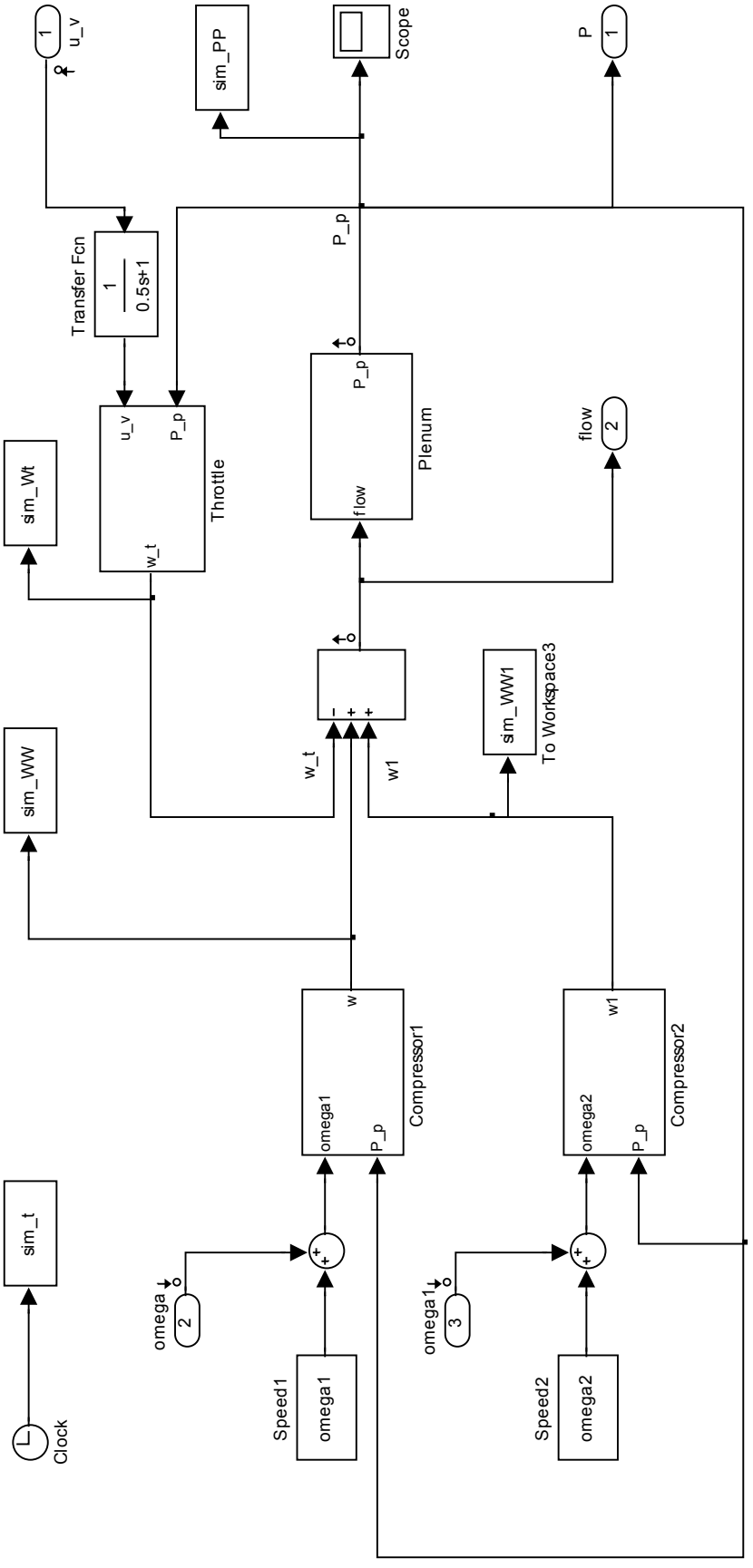

FIGURE 7: The complete setup with linearization points

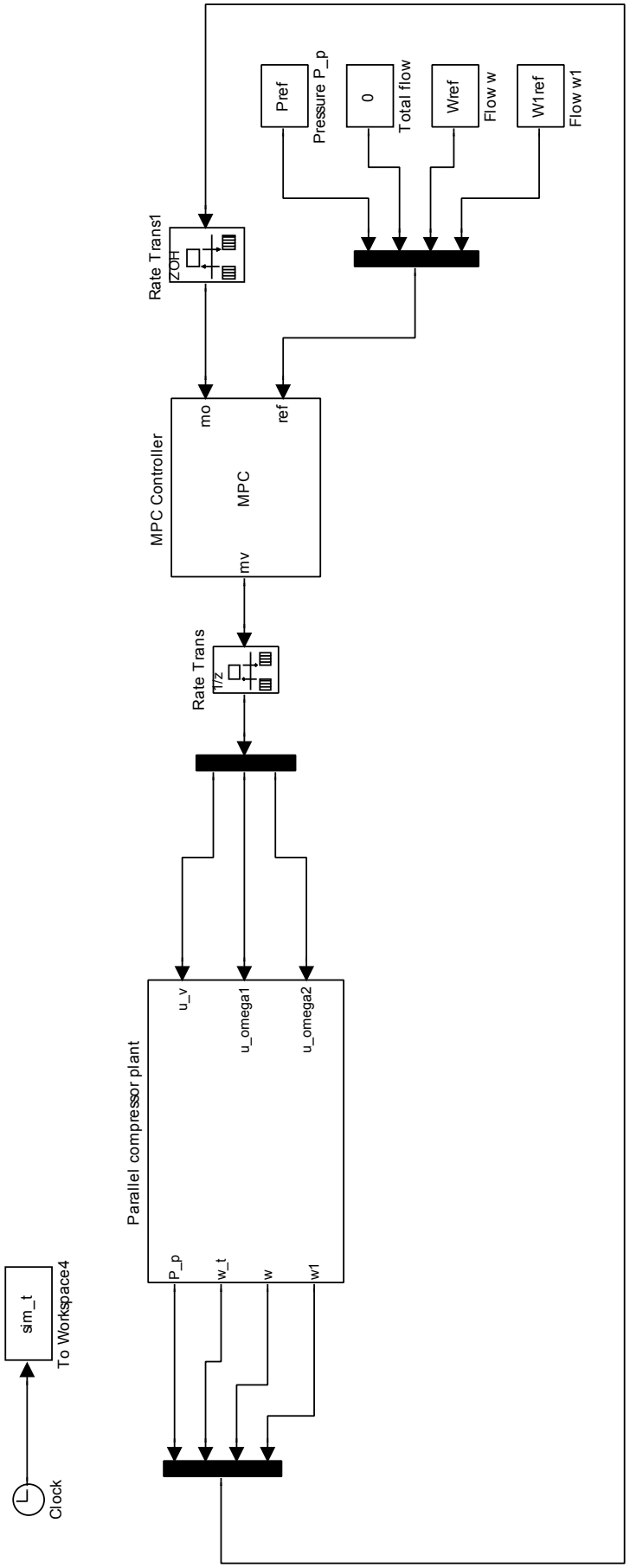

FIGURE 8: Overview of the total parallel compressor plant with the Model Predictive Controller

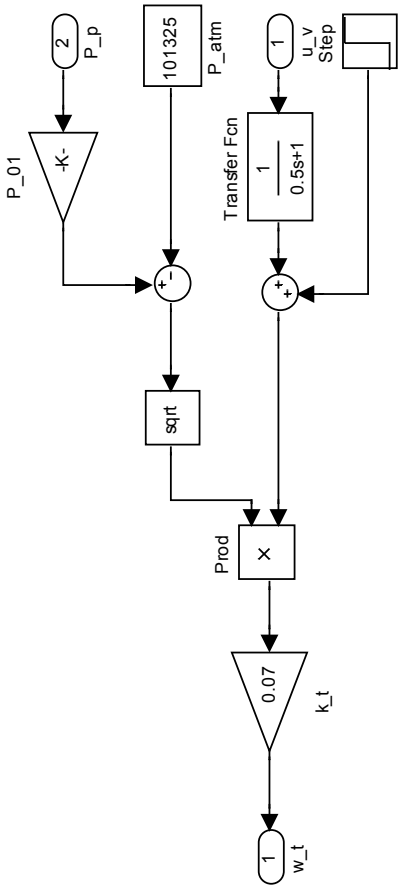

FIGURE 9: Throttle system used in the SIMULINK diagram setup of Figure 8.

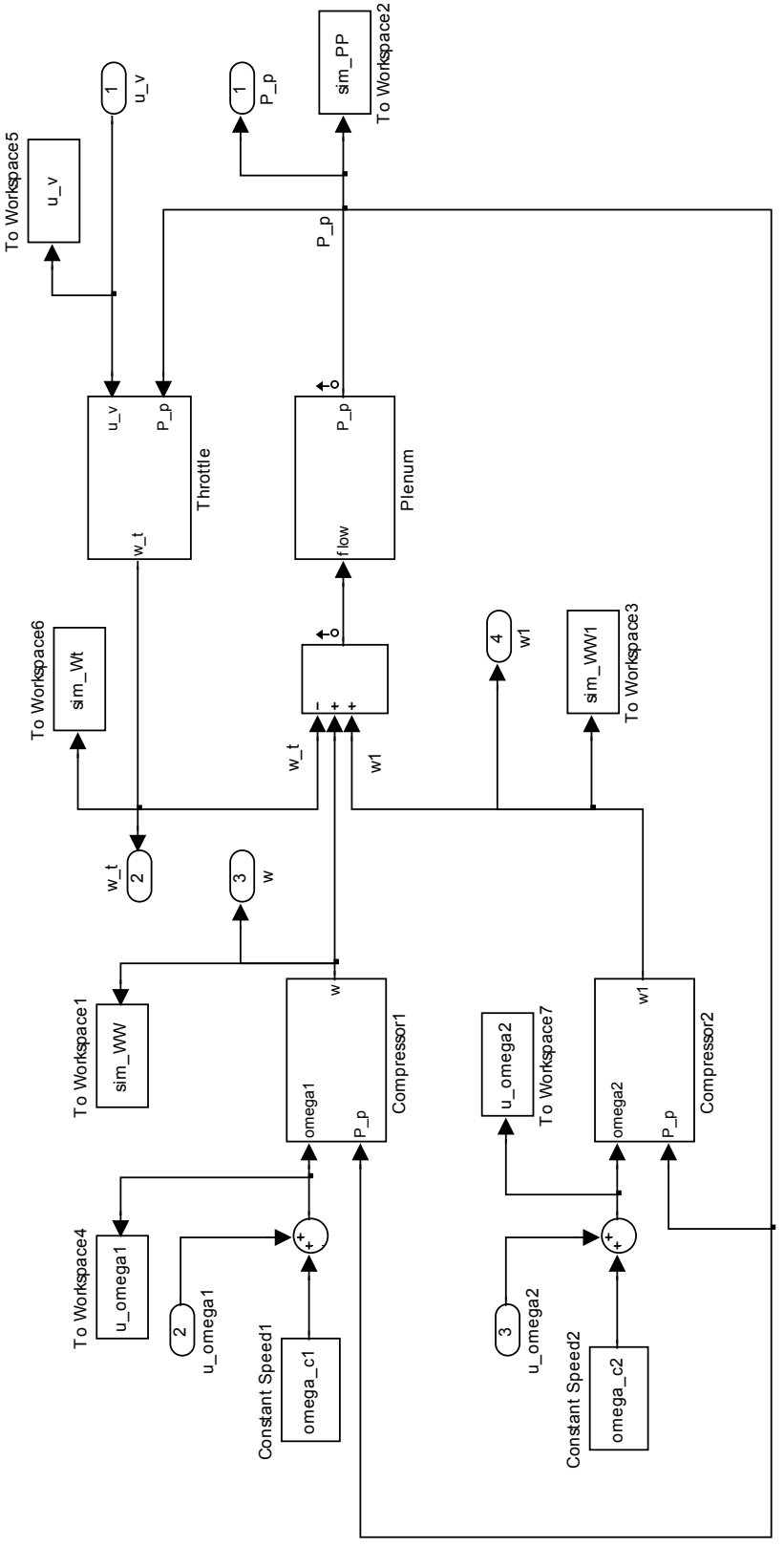

FIGURE 10: Overview of the parallel compressor system with plenum and throttle

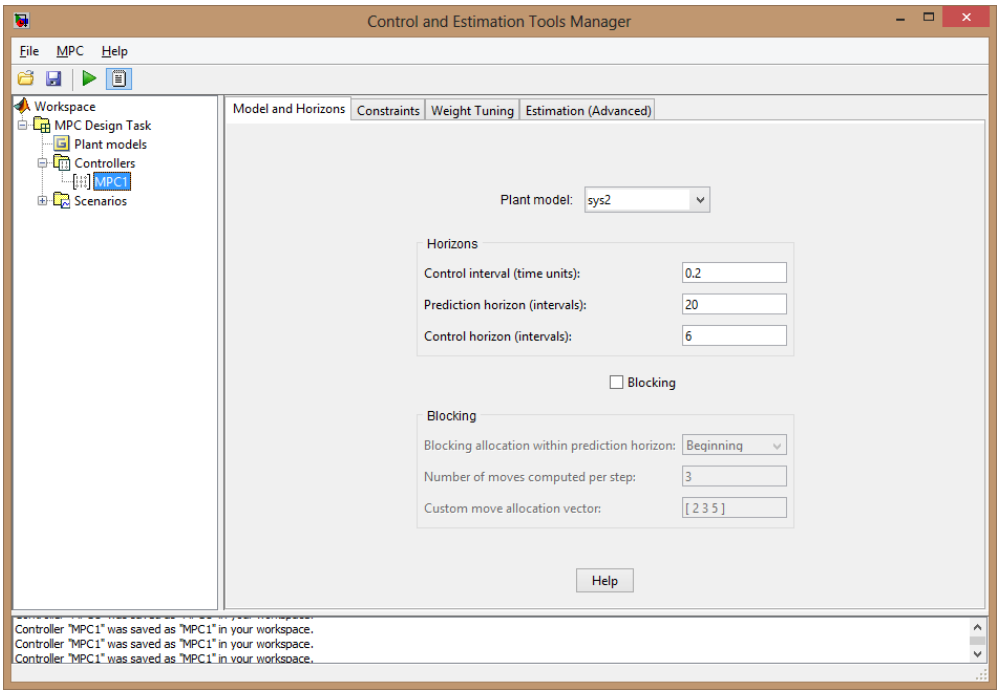

FIGURE 11: Window for choosing prediction model, prediction horizon and control horizon, Control and Estimation Tools Manager

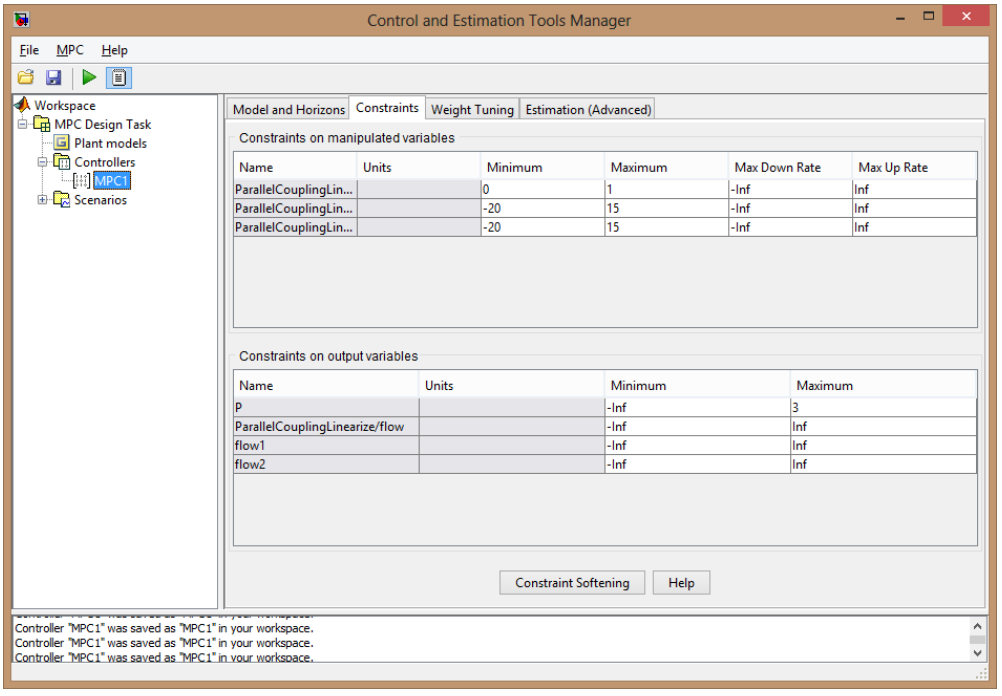

FIGURE 12: Window for setting constraints on output- and manipulated variables, Control and Estimation Tools Manager

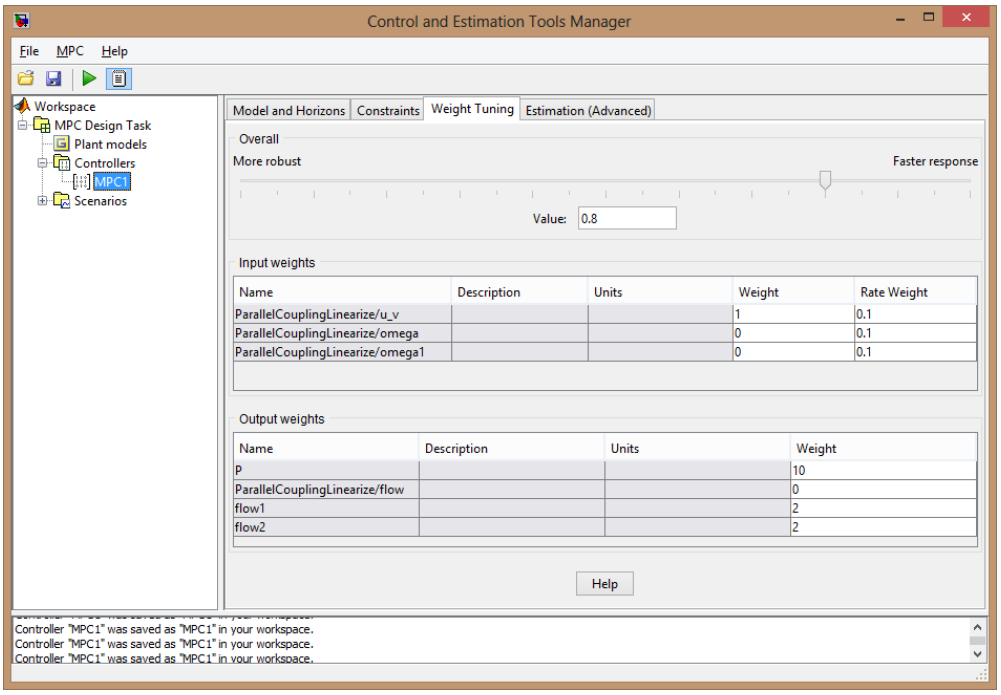

FIGURE 13: Window for setting weights on input and output parameters, Control and Estimation Tools Manager